UNIVERSIDAD AUTÓNOMA DE BAJA CALIFORNIA

FACULTAD DE CIENCIAS QUIMICAS E INGENIERÍA

MAESTRÍA Y DOCTORADO EN CIENCIAS E INGENIERÍA

"Estrategias farmacológicas para el aislamiento e identificación de potenciales receptores membranales de la (-)-epicatequina"

TESIS

QUE PARA OBTENER EL GRADO DE:

DOCTOR EN CIENCIAS

PRESENTA

EVA VIVIANA SARMIENTO GUTIÉRREZ

DIRECTOR DE TESIS
DIEGO ROMERO PÉREZ

CO-DIRECTOR DE TESIS
ISRAEL RAMÍREZ SÁNCHEZ

Tijuana, B. C. ***MARZO DEL 2018***

Universidad Autónoma de Baja California

FACULTAD DE CIENCIAS QUÍMICAS E INGENIERÍA

COORDINACIÓN DE POSGRADO E INVESTIGACIÓN

FOLIO No. 237

Tijuana, B. C., a 20 de febrero de 2018

C. Eva Viviana Sarmiento Gutiérrez
Pasante de: Doctor en Ciencias
Presente

El tema de trabajo y/o tesis para su examen profesional, en la Opción TESIS

Es propuesto, por los C. Dres. Diego Romero Pérez e Israel Ramírez Sánchez

Quienes serán las responsables de la calidad de trabajo que usted presente, referido al tema "Estrategias farmacológicas para el aislamiento e identificación de los potenciales receptores membranales de la (-)-epicatequina"

el cual deberá usted desarrollar, de acuerdo con el siguiente orden:

I.- INTRODUCCIÓN
II.- MATERIALES Y MÉTODOS
III.- RESULTADOS Y DISCUSIÓN
IV.- CONCLUSIONES

UNIVERSIDAD AUTÓNOMA DE BAJA CALIFORNIA
FACULTAD DE CIENCIAS QUÍMICAS E INGENIERÍA

Dr. Diego Romero Pérez
Director de Tesis

Dr. José Luis González Vázquez
Sub-Director Secretario

Dr. Israel Ramírez Sánchez
Co-Director de Tesis

Dr. Luis Enrique Palafox Maestre
Director

“Resumen de la tesis que presenta Eva Viviana Sarmiento Gutiérrez, como requisito parcial para la obtención del grado de Doctor en Ciencias “

“ESTRATEGIAS FARMACOLÓGICAS PARA EL AISLAMIENTO E IDENTIFICACIÓN DE LOS POTENCIALES RECEPTORES MEMBRANALES DE LA (-)-EPICATEQUINA”

Las enfermedades cardiovasculares (ECV) constituyen actualmente una de las principales preocupaciones para las autoridades de salud a nivel mundial ya que representan la principal causa de muerte alrededor del mundo [1]. Se ha demostrado que el cacao, posee propiedades cardioprotectoras [Schroeter *et al.* 2005; Ellinger *et al.* 2012] y las más recientes evidencias experimentales sugieren que su flavanol más abundante la (-)-epicatequina (Epi), es el responsable de tales beneficios [Schroeter *et al.* 2005, Ottaviani *et al.* 2011]. Los mecanismos propuestos mediante los cuales la Epi ejerce sus efectos incluyen un aumento en la biodisponibilidad/producción de óxido nítrico (NO) por la activación de la óxido nítrico sintasa endotelial (eNOS) asociada a la inducción de las vías PI3K/AKT y calcio (Ca^{2+}) [Ramirez-Sanchez *et al.* 2010]. La activación de la eNOS y sus vías relacionadas está asociado a la estimulación de varias proteínas de membrana, tales como los receptores de tirosín-cinasa y los receptores acoplados a proteínas G (GPCR) (Dudzinski and Michel; 2007, Manning BD, Cantley, 2007). Con la finalidad de identificar los posibles receptores de la Epi, diseñamos una estrategia que se desarrolló en varias etapas: 1) síntesis de diversos derivados de la Epi, 2) seguido por un análisis *in silico* de los nuevos derivados sintetizados y 3) evaluación biológica de los mismos en la producción de NO y su capacidad antioxidante, 4) elaboración de una columna inmovilizando el derivado de Epi mediante química de click, y finalmente 5) utilización de la columna para aislar proteínas que se unan a la Epi utilizando extractos de células endoteliales. Para la síntesis de los derivados, los grupos hidroxilo de la Epi fueron modificados usando bromuro de propargilo y cloruro de mesilo, posteriormente se realizó un ensayo *in silico* de las moléculas recién sintetizadas, éste análisis reveló que la unión entre los derivados de la Epi con el receptor de estrógenos acoplado a proteínas G (GPER) es termodinámicamente favorable. La incubación de células de arteria coronaria de bovino (BCAEC) con los derivados estimuló la producción de NO y la activación de la eNOS, estos efectos fueron atenuados por el uso de G15, un inhibidor del GPER. Adicionalmente, la actividad antioxidante de los derivados de la Epi se evaluó mediante métodos químicos (análisis electroquímico y ABTS/trolox) y biológicos. Los derivados de la Epi fueron incapaces de prevenir el daño oxidativo en las BCAEC tratadas con H_2O. Usando la columna de afinidad elaborada con el derivado de la Epi, se logró aislar varias proteínas, las cuales fueron separadas posteriormente mediante electroforesis. El análisis de estas proteínas mediante inmunoblot reveló al GPER como una proteína de unión a la Epi. En conjunto, estos resultados validan la estrategia propuesta para aislar e identificar nuevos receptores de la Epi que puedan explicar su actividad biológica.

.

Abstract from the thesis presented by Eva Viviana Sarmiento Gutiérrez as a partial requirement for the degree of Doctor of Philosophy in Science.

PHARMACOLOGICAL STRATEGIES FOR THE ISOLATION AND ELUCIDATION OF POTENTIAL CELL MEMBRANE RECEPTORS FOR (-)-EPICATECHIN

The consumption of flavonol-rich foods as cacao is associated with reduced risk of cardiovascular diseases (CVDs) [Schroeter *et al.* 2005; Ellinger *et al.* 2012]. (-)-epicatechin (**Epi**) is the main flavonoid found in cacao seeds and its oral intake mimics beneficial effects as cocoa flavonols, particularly improving the endothelium-dependent vasodilation [Schroeter *et al.* 2005, Ottaviani *et al.* 2011]. Proposed mechanisms by which (-)-epicatechin mediate its vascular effects include an increase in nitric oxide (NO)-bioavailability/synthesis by activation of the endothelial NO synthase (eNOS) through the induction of the PI3K/AKT and calcium (Ca^{2+}) pathways (Ramirez-Sanchez *et al.* 2010). The eNOS activation and its related pathways involve stimulation of several membrane proteins as tyrosine kinase receptors, and G-protein-coupled receptors (GPCRs) (Dudzinski and Michel; 2007, Manning BD, Cantley, 2007). To potentially identify receptors that mediate Epi responses we implemented the following strategy: 1) synthesis of novel Epi derivatives amenable to affinity column use, 2) *in silico* molecular docking studies of the novel derivatives on GPER, 3) biological assessment of the derivatives on NO production and antioxidant activity, 4) implementation of an inmobilized Epi derivative affinity column and, 5) affinity column based isolation of Epi interacting proteins from extracts of endothelial cells. In order to implement our strategy, the Epi phenol and C3 hydroxyl groups were chemically modified with propargyl or mesyl groups. Docking studies of the novel Epi derivatives on GPER conformers at 14 ns and 70 ns demonstrated favorable thermodynamic interactions reaching the binding site. Cultures of bovine coronary artery endothelial cells (BCAEC) treated with Epi derivatives stimulated NO production via Ser1179 phosphorylation of eNOS; these effects were attenuated by the use of the GPER blocker, G15. The antioxidant activity of Epi derivatives was assessed using chemical methods with an *in vitro assay* (ABTS/trolox scavenging activity and voltammetry analysis) and biologically assessed using BCAEC. Epi derivatives displayed no antioxidant activity suggesting that the alkyne derivatization attenuates antioxidant activity. Epi derivative affinity columns yielded multiple proteins from BCAEC. Proteins were separated by electrophoresis, and immunoblotting analysis revealed GPER as an Epi derivative binding protein. Altogether, these results validate the proposed strategy to potentially isolate and identify novel Epi receptors that may account for its biological activity.

TABLA DE CONTENIDO

TABLE OF CONTENTS

LIST OF ABBREVIATIONS

ABTS	2,2'-azino-bis(3-ethylbenzothiazoline-6-sulphonic acid)
AKT	Serine/threonine kinase
ATP	Adenosine triphosphate
CVD	Cardiovascular Disease
EDTA	Ethylenediaminetetraacetic acid
ERK ½	Extracellular signal–regulated kinases
H-donating	Hydrogen donating
LDL	Low-density lipoprotein
MTT	3-(4, 5-dimethylthiazol-2-yl)-2,5-diphenyltetrazolium bromide
NMR	Nuclear magnetic resonance
PI3K	Phosphoinositide 3-kinase
ROS	Reactive oxygen species
TEAC	Trolox equivalent antioxidant capacity
β	Beta
ΔG	Gibbs free energy

- AMINOACID RESIDUES -

A (Ala)	Alanine
C (Cys)	Cysteine
F (Phe)	Phenylalanine
H (Hys)	Histidine
L (Leu)	Leucine
M (Met)	Methionine
N (Asn)	Asparagine
P (Pro)	Proline
Q (Gln)	Glutamine
S (Ser)	Serine
T (Thr)	Threonine
V (Val)	Valine
W (Trp)	Tryptophan
Y (Tyr)	Tyrosine

LIST OF FIGURES

LIST OF TABLES

BACKGROUND

Cardiovascular diseases (CVDs) are the primary chronic disease afflicting industrialized societies today [WHO; 2011]. Development of atherosclerosis and thrombosis is a multifactorial process in which endothelial dysfunction, inflammatory response, modified lipids and lipoproteins and activated platelets all play significant roles in the process [Widlansky *et al*. 2003, WHO; 2011].

CVDs are the leading cause of global death, an estimated 17.5 million people die annually [WHO; 2011]. In México it was estimated that 7 million people are at high cardiovascular risk, due to the presence of one or more risk factors (Figure i) such as tobacco use, obesity, age, hypertension, hyperlipidemia, physical inactivity, and poor dietary habits. [Rosas-Peralta *et al*; 2007].

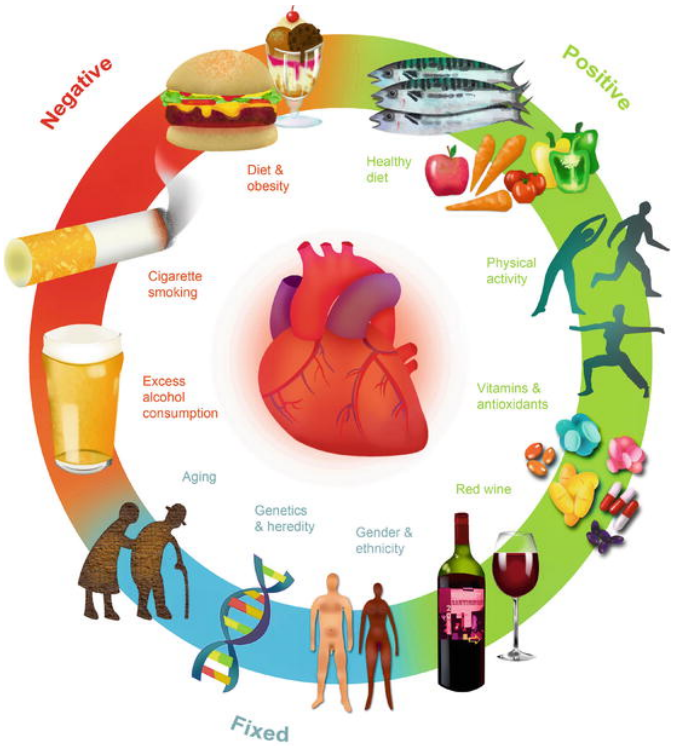

Figure i. Multiple cardiovascular risk factors. Modifiable risk factors (negative) and non-modifiable risk factors (fixed). (From https://www.creative-diagnostics.com)

One of the the most important lifestyle factors, diet (Figure i) can strongly influence the incidence of CVDs [Eyre *et al.* 2004; Bhupathiraju *et al.* 2013]. Concurrently, accumulating data from epidemiological investigations indicate an association of an improved cardiovascular prognosis with flavanol-rich diets [Lichtenstein *et al.* 2006]

Flavonoids are plant secondary metabolites (Figure ii) that are found in fruit, vegetables, grains, bark, roots, stems, flowers, tea, and wine [Arts *et al;* 2000. Min-Hsiung *et al;* 2010].

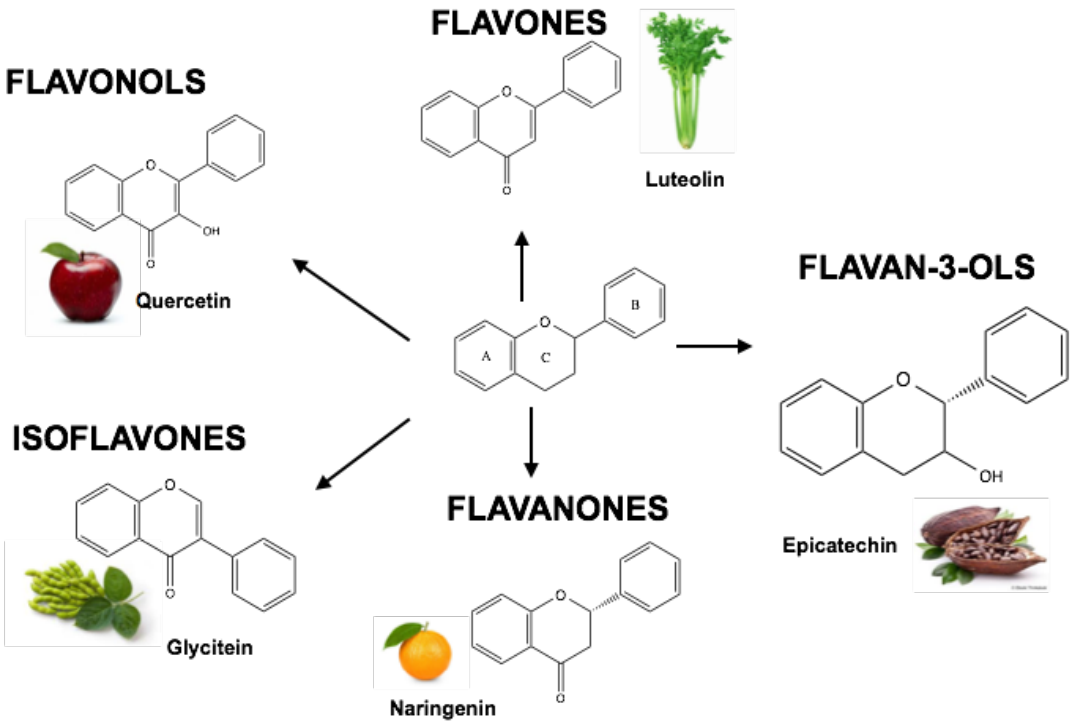

Figure ii. Representative natural flavonoids and their dietary sources. Flavones, flavonols, flavan-3-ols, flavanones and isoflavones. [Min-Hsiung Pan *et al.,* 2010].

Recent dietary interventions in humans using flavanol-containing foods (as cacao) have substantiated epidemiological data on an inverse relationship between flavanol intake and the risk of CVD [Schroeter *et al;* 2005, Ostertag *et al.* 2010; Flammer *et al;* 2012], indicating various potential flavanol-mediated bioactivities

including the improvement of vasodilation in healthy subjects [Schroeter *et al;* 2005] and endothelial function [Zubaida *et al.* 2008], blood pressure [Min *et al.* 2010], and insulin resistance and glucose tolerance [Hooper *et al.* 2012], as well as the attenuation of platelet reactivity [Ostertag *et al.* 2010; Flammer *et al;* 2012].

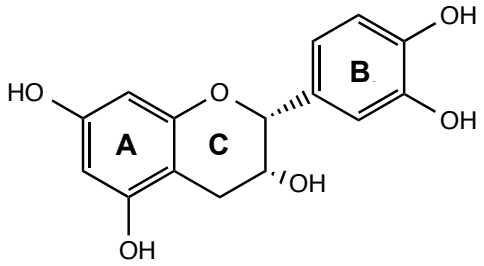

Figure iii. Structure of (-)-epicatechin (**Epi**).

(-)-epicatechin (**Epi**) is the main flavanol found in cacao seeds and its oral intake mimics the beneficial effects of cocoa products, particularly improving endothelium-dependent vasodilation [Schroeter *et al.* 2005, Ottaviani *et al.* 2011].

Structurally, **Epi** is comprised of two aromatic rings (A and B) linked by an oxygenated heterocycle (c) with a 4-hydroxyl group (Figure iii).

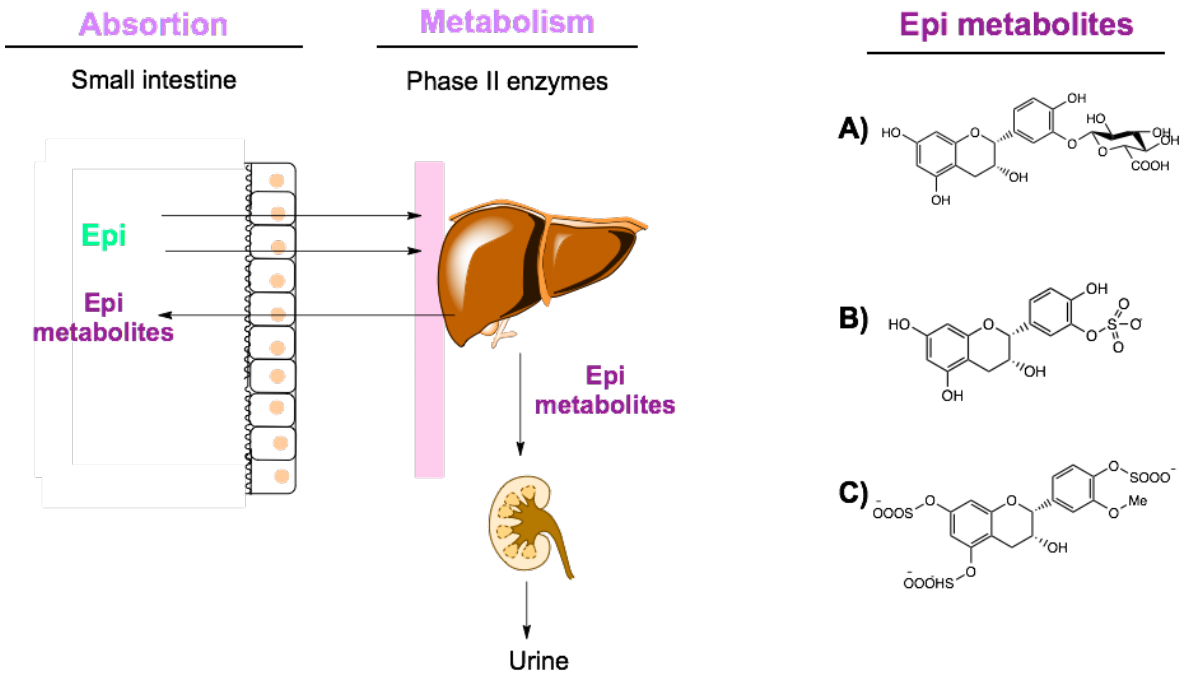

Figure iv. Epi metabolism and structure of several Epi metabolites. Once it reaches the small intestine Epi is extensively metabolized to A) glucuronide derivatives, B) sulfated conjugates and C) O-methylated sulfated-conjugates. After intake of flavanol rich foods, Epi and several of these metabolites are found in plasma [Schroeter *et al.,* 2006; Barnett *et al.,* 2015; Spencer *et al.,* 2001].

Epi is metabolized into a wide range of metabolites by methylation, glucuronidation or sulfation (Figure iv), retaining an intact flavanol ring [Schroeter *et al.,* 2006; Moreno-Ulloa *et al.,* 2015]. **Epi** metabolites may exert further biological effects [Schroeter *et al.,* 2006, Loke *et al.,* 2008], therefore, it is essential to elucidate the actual molecules eliciting the effects observed after **Epi** consumption.

The proposed mechanisms, by which **Epi** may mediate the observed vascular effects include: increased nitric oxide (NO)-bioavailability/synthesis by activation of endothelial NO synthases (eNOS) through the induction of the PI3K/AKT and calcium (Ca^{2+}) pathways [Ramírez-Sánchez *et al,.* 2010] (Figure v).

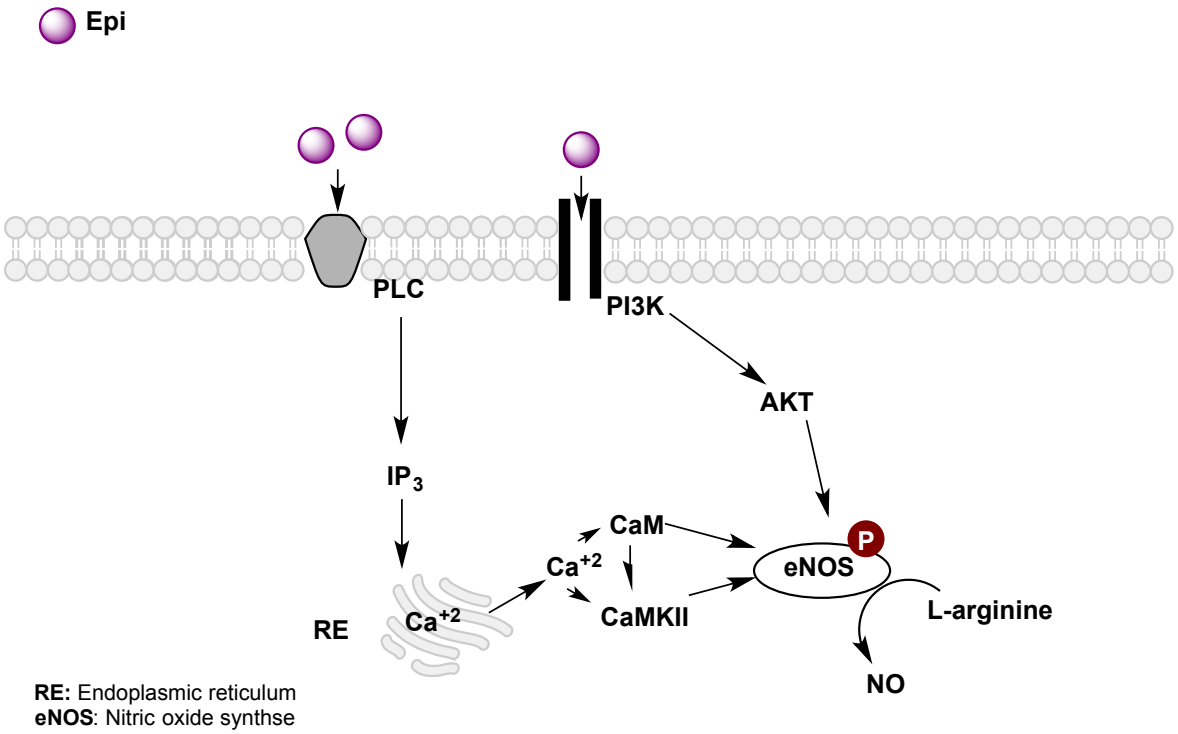

Figure v. **Epi** vascular effects. Proposed mechanisms by which **Epi** mediates its vascular effects include: increased nitric oxide (NO)-bioavailability/synthesis by activation of the endothelial NO synthase (eNOS) through the induction of the PI3K/AKT and calcium (Ca^{2+}) pathways. [Ramírez-Sánchez *et al.,* 2010]

The eNOS activation and its related pathways involve stimulation of several membrane proteins such as tyrosine kinase receptors, and G-protein-coupled receptors (GPCRs) [Dudzinski and Michel; 2007, Manning BD, Cantley, 2007].

There has been an increasing interest in elucidating the mechanisms by which **Epi** mediates the receptor related effects [Panneerselvam *et al.,* 2010, Moreno-Ulloa, 2015]. To this end, a recent study explored the use of a cell-surface impermeable (-)-epicatechin-dextran conjugate (Figure vi).

The main findings from this study showed that treatment with both 100 nM **Epi** and 100 nM (−)-epicatechin-dextran for 10 minutes induced PI3K/AKT, and activated eNOS in human coronary artery endothelial cells (HCAEC). Interestingly, (-)-epicatechin-dextran exerted a significantly higher activation than the native

compound, suggesting the existence of an **Epi** cell membrane receptor [Moreno *et al.,* 2014].

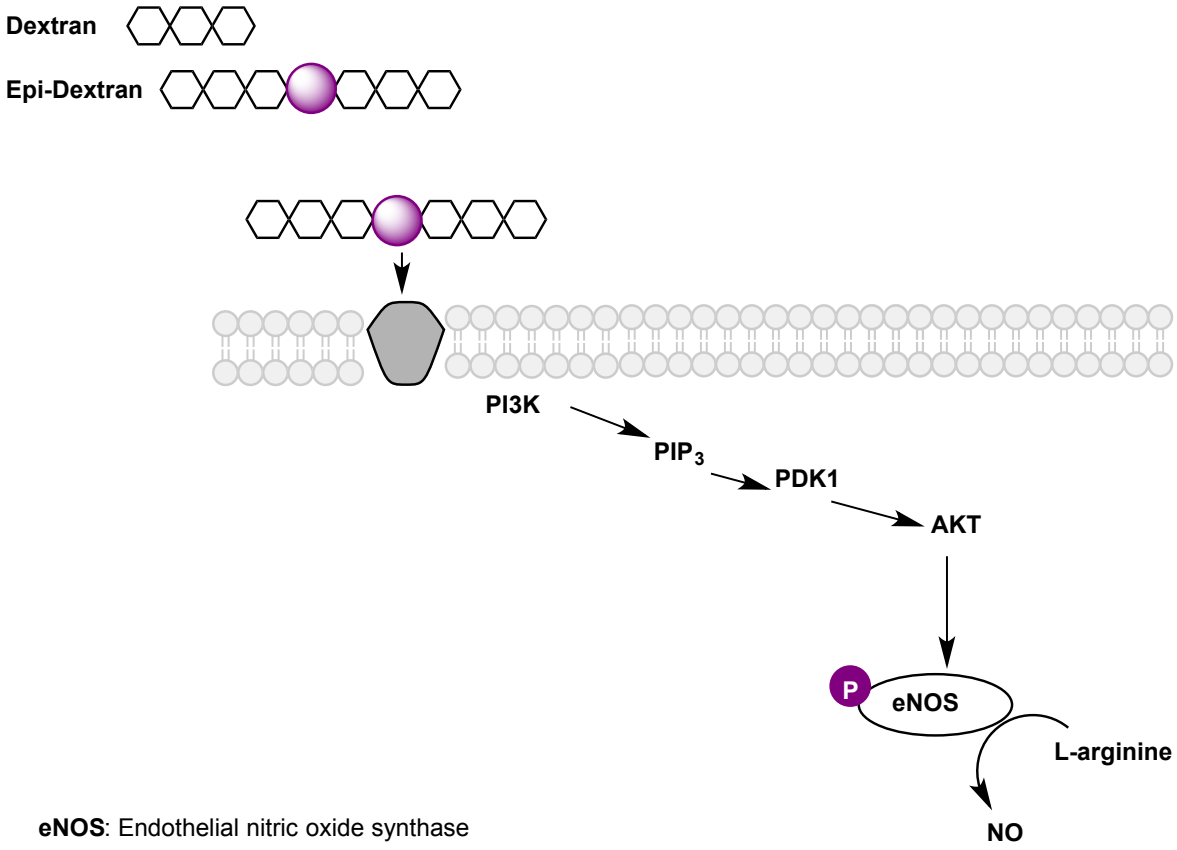

Figure vi. A cell-surface impermeable Epi-Dextran ((-)-epicatechin-dextran conjugate). The treatment with 100 nM Epi-Dextran ((−)-epicatechin-dextran) for 10 minutes induced PI3K/AKT, and activted eNOS in HCAEC. [Moreno *et al.,* 2014].

Similarly, Moreno-Ulloa *et al.,* demonstrated that **Epi**, mediates NO production at least partially through the activation of the G protein-coupled estrogen receptor (GPER) via ERK 1/2 and calmodulin-dependent kinase II (CaMKII) in cultured bovine endothelial cells, and induced vasodilation in isolated rat aortas. Identification of **Epi** binding targets is essential to elucidate the molecular mechanisms underlying its action. Several studies have suggested that the beneficial properties of flavonoids are dependent on the availability of hydroxyl groups [Vaya *et al.,* 2003, Garg *et al.,* 2001], therefore **Epi** might exerts its biological effects by interacting with its protein targets via the phenolic hydroxyl

groups. Thus a partial or total chemical modification of these groups may modify its ability to bind its target proteins and facilitate their identification. However, there is still insufficient structural data on the formation of complexes between the target proteins and **Epi** and its specific targets on vascular endothelium remain to be determined.

.

AIM OF THE THESIS AND STUDY OBJECTIVES

The main focus of this dissertation tested the hypothesis that Epi exerts its biological effects by interacting with membrane proteins via phenolic hydroxyl groups. To identify proteins candidates through which **Epi** exerts its beneficial effects, we designed a strategy comprising several distinct stages. **Specific aim 1: Design and synthesis of Epi derivatives**. First, we describe the rational design and synthesis of novel Epi derivatives. For the synthesis of these compounds, native Epi was used as starting material. The phenolic hydroxyl and C3 hydroxyl groups were modified with propargyl or mesyl groups which may be optimal for the generation of affinity columns for the purification of Epi binding proteins.

Specific aim 2: Biological assessment of the Epi derivatives in cultured cells, by measuring Nitric oxide (NO) production, endothelial Nitric oxide synthase (eNOS) activation and antioxidant activity. Chapter 2 describes the biological effects of these novel Epi derivatives on endothelial cells. In these studies we analyzed the influence of alkyne derivatization on protein-Epi derivative interactions (docking studies), antioxidant activity and NO production by eNOS activation. 1) Epi derivatives were docked into the active site of GPER using 14 and 70 ns conformers in molecular dynamics (MD) simulations. Results suggest that interactions between all derivatives and GPER are energetically favorable. 2) Epi derivatives were tested for their *in vitro* capability to induce the activation of the eNOS/NO pathway in BCAEC. For GPER blocking assays, cells were pre-incubated with G15, a GPER inhibitor**.** Our results demonstrated that all derivatives were able to stimulate NO production (through eNOS activation measured as Ser1179 phosphorylation [p-eNOS]), meanwhile the GPER inhibitor, G15 abrogated the Epi and Epi derivatives effects. 3) Finally, the antioxidant activity of the Epi derivatives was chemically assessed by an *in vitro assay* (ABTS/trolox scavenging activity and voltammetry analysis) and biologically assessed using BCAEC (protection against oxidative damage). Epi derivatives had no significant

antioxidant effect suggesting that the alkyne derivatization attenuates the antioxidant activity.

Specific aim 3. Covalent immobilization of an Epi derivative onto a chromatography column, using click chemistry (EPI-COLUMN). (Calculating the yield of the coupling reactions by chemical and electrochemical methods). In order to capture and isolate putative Epi-binding proteins, we developed an affinity chromatography method (EPI-COLUMN) by using an Epi derivative immobilized onto agarose-azide beads. The presence of the Epi derivative at the ends of the agarose-azide beads was investigated by quantitation of the compound recovered using concentration dependent fluorescence experiments and zeta potential measurements. The results showed that 86.6% of the Epi derivative was attached to the agarosa-azide beads

Specific aim 4. Assessment and optimization of the interaction between the column with attached Epi and proteins extracts from cultured endothelial cells. Cell lysates from BCAEC were subjected to affinity chromatography using the EPI-COLUMN. Experimental conditions were optimized to obtain a reproducible pattern of protein bands by SDS-PAGE stained with Coomassie-Blue. Immunoblotting analysis of the fractions eluted from the EPI-COLUMN, revealed GPER as an Epi derivative binding protein. Altogether, these results validate the proposed strategy to potentially isolate and identify novel Epi receptors that may account for its biological activity.

CHAPTER 1

CHAPTER 1: INTRODUCTION

1.1 Synthesis of derivatives of flavonoids

Flavonoids represent a well-known family of compounds and their synthesis has been the object of a great number of studies. In general, procedures for laboratory synthesis of flavonoids are still based on the approaches originally developed by Robinson [Allan and Robinson, 1924], with other methods including the Baker–Venkataraman rearrangement [Mahal and Venkataraman, 1933; Wheeler, 1976], synthesis via chalcones [Linuma *et al.,* 1984], and synthesis via an intramolecular Wittig reaction [Hercouet *et al.,* 1982].

Despite the number of steps often involved in these methods, they constitute the most popular methodologies used nowadays for the preparation of flavonoids.

The synthesis of flavonoid derivatives is also an area of significant interest and many synthetic routes have been used to add moieties to the natural flavonoid nucleus. Using the Mannich reaction, it is possible to produce alkylamine derivatives. And the reaction of dihydroquercetin with formaldehyde and amines has as its main products mono and diaminomethyl derivatives [Kukhareva *et al.,* 2004].

Another frequently used method is alkylation. Using aldol condensation, alkyl and benzyl substituents can be added to the flavonoid molecule [van Aardt *et al.,* 1998]. Other feasible possibilities are provided by the Williams synthesis of ethers or alcoholysis of epoxides.

Alkylation is often performed with alkyl halogenides. In nature, some alkylated flavonoid derivatives can also be found, mainly derivatives with lower alcohols [Materska *et al.,* 2008]. Simple ethers can be prepared from alkylene oxides. Penta and tetrahydroxyethyl quercetin were obtained via alkylation with an excess of ethylene oxide in water, using potassium hydroxide as catalyst [Bridson *et al.,* 2007].

In chemical synthesis, one of the most frequently used methods is esterification, particularly acetylation. With this approach, some reactive or all hydroxyl groups can be modified. Some of the most commonly used reaction substrates include acetyl chloride or acetic anhydride in pyridine or dimethyl formamide (DMF).

However, selective esterification is often required to maintain especific properties of initial flavonoids. Therefore, the modificaction of these molecules with non-polar groups is an efficient solution in order to confer antioxidant effects in this hydrophobic environment [Bridson *et al.,* 2007].

To obtain mono-derivatives, it is necessary to use blocking groups for the rest of the hydroxyl groups, and remove them afterwards. For example, in the synthesis of 4'-*O*-methylquercetin (yield 63 %), selective blocking of the catechol group is performed with dichloro diphenyl methane at 175 °C in diphenyl ether. Chloromethyl ether is a suitable blocking agent for the hydroxyl groups in positions 3 and 7 [Li *et al.,* 2009].

In this area of organic synthesis, most synthetic research has focused on protocols to obtain catechin derivatives [Park *et al.,* 2004; Banerjee *et al.,* 2014]. In such research, phenolic hydroxyl groups have been commonly blocked by benzyl groups in order to obtain specific catechin mono-derivatives. Multiple alternative benzylation protocols of catechins have been described in the literature [Tuckmantel *et al.,* 1999]. The original protocol for catechin benzylation was reported in 1968 by Weings [Weings *et al.,* 1968], he employed BnBr/NaH in dimethylformamide (DMF) to obtain 3-glucosyl and 3-galloyl cathechin.

Several methods for benzylation have been developed which involved the use of bases such as K_2CO_3, DBU, Et_3N, Cs_2CO_3, $NaHCO_3$ and Na_2CO_3, in solvents such as DMF, acetone, ethyl acetate (EtOAc), water, and EtOAc/water with and without a phase transfer catalyst (nBu_4NI) at RT, at moderate temperature (40-45 °C), or at reflux.

The selective reduction at the C-3 position of catechins has been reported after hydroxyl phenolic protection. Fatty acid ester derivatives of catechins are described as having antitumorigenesis as well as antibacterial activity [Fukami *et al.,* 2007]. A different catechin derivative, 3-O-octanoyl-(þ)-catechin, was synthesized by Aoshima *et al.,* in 2005, by incorporation of an octanoyl chain into (þ)-catechin.

Moreover 3-O-acyl and alkyl-(-)-epicatechin derivatives were synthesized, to be screened as anticancer agents, using acyl chloride and triethylamine (TEA) [Park *et al.,* 2004]. Protection of the free phenolic functionalities before C-3 transformations, followed by the deprotection step, proved to be the most fruitful and selective in the synthesis of the catechin derivatives.

Several one-step deprotective methods have been reported, of which Pd-catalyzed deprotection was one of the most interesting [Green *et al.,* 1999]. In fact, combinations of $Pd(PPh_3)_4$ and reducing agents such as $NaBH_4$, $LiBH_4$,Bu_3SnH, $PhSiH_3$, morphorine, $ZnCl_2$-polymethylhydrosiloxane, or $TolSO_2H$ were reported [Beugelmans *et al.,* 1994; Bois-Choussy *et al.,* 1996; Four and Guibe, 1982; Dessolin *et al.,* 1995; Eicher *et al.,* 1996; Chandrasekhar *et al.,* 2001; Honda *et al.,* 1997].

Electrochemical cleavage using $PdCl_2$ was also investigated [Franco *et al.,* 1999]. As an alternative catalyst, Boss and Scheffold reported a reaction using 10% Pd/C with p-TsOH under reflux conditions [Boss *et al.,* 1976].

Ishizaki *et a.l,* reported a new methodology for the deprotection of O-allylphenols under mild and basic conditions. Using 10% Pd/C in 10% KOH/ Methanol at room temperature they cleaved the allyl aryl ethers. A growing interest for flavonoid transformation by specific synthesis has emerged. It has now been established that regioselective modification of the flavonoid skeleton may increase certain biological activities or confer novel properties. [Nanjo *et al.,* 1999; Ishihara *et al.,* 2003; Uesato *et al.,* 2003].

1.2 Vascular effects of Epi

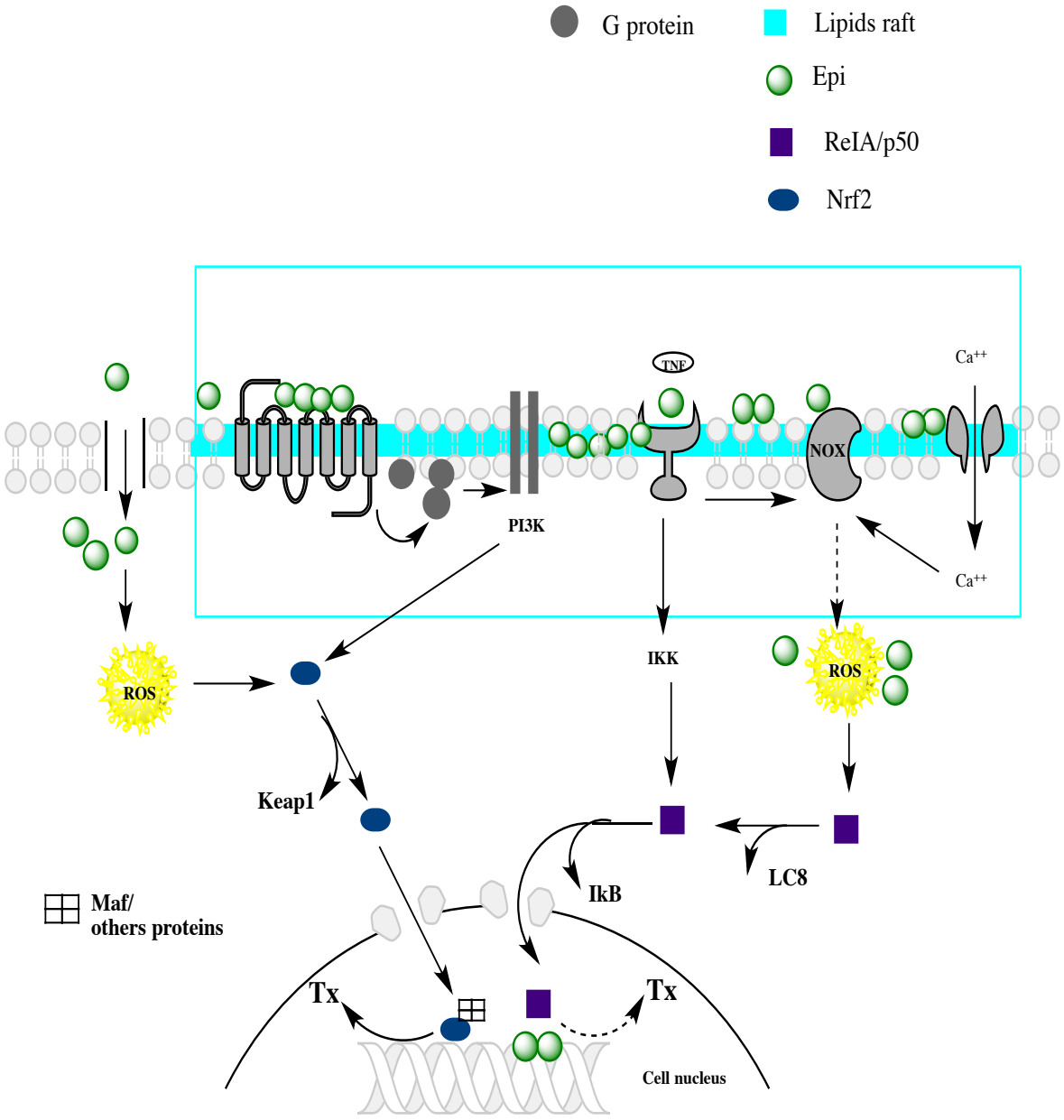

Figure 1.1 Epi antioxidant activity. Proposed mechanisms include: direct scavenging of ROS, or indirect scavenging of ROS by modulating pathways that regulate ROS scavenging compounds and enzymes, respectively.Tx: transcription, ReLA/p50/LC8/IkB: transcription heterodimer complex, IKK: IκB kinase, Maf: transcription factor Maf, Keap 1: Kelch-like ECH-associated protein 1, NOX: NADPH oxidase, TNF: Tumor necrosis factor receptor. [Heim *et al.,* 2002; Fujimura *et al.,* 2008; Patra *et al.,* 2008; Steffen *et al.,* 2008; Monagas *et al.,* 2009; Martin *et al.,* 2010; Nakayama *et al.,* 2012].

(-)-Epicatechin (**Epi)** has a wide array of biological actions related directly to its chemical structure. The main proposed mechanisms through which **Epi** mediates its vascular effects include: increases in nitric oxide (NO)-bioavailability/synthesis by activation of the endothelial NO synthase (eNOS) through the induction of the PI3K/AKT and calcium (Ca^{2+}) pathways [Ramírez-Sánchez *et al.,* 2010].

Likewise, **Epi** displays antioxidant activity by directly scavenging ROS, or indirectly by modulating pathways that regulate ROS scavenging compounds and enzymes (Figure 1.1). These antioxidant properties are structure-dependent, and directly related to electronic delocalization on the aromatic nucleus. [Heim *et al.,* 2002; Martin *et al.,* 2010; Monagas *et al.,* 2009; Steffen *et al.,* 2008].

During oxidative stress, free radicals decrease membrane fluidity by modifying lipids *via* lipid peroxidation, which may significantly alter membrane properties and possibly disrupt the function of membrane-associated proteins [Beckman and Ames, 1998]. Several studies have revealed that the ability of catechins to interact directly with membrane lipids presumably plays an essential role in the mechanisms of the observed biological effects [Fujimura *et al.,* 2008; Patra *et al.,* 2008; Nakayama *et al.,* 2012], therefore membrane-active flavonoids are believed to cause antioxidant activity by reducing the rigidity of membranes cooperatively, with an effect on reactive oxygen species [Sato *et al.,* 1999]. Thus, increasing lipophilicity increases the probability that lipid molecules will interact with membrane-associated proteins, likely improving its effects.

It has been proposed that selective flavonoid lipophilization with acyl and alkyl substituents by organic synthesis may modify propierties such as penetration through the cell membrane and enhance its effects. [Nanjo *et al.,* 1999; Uesato *et al.* 2003; Park *et al.,* 2004].

1.3 Identification of targets for Epi

Due to the healthy effects trigered by **Epi**, there is an increasing interest in elucidating the mechanisms by which this flavanol mediates its cardiometabolic protective effects [Panneerselvam *et al.,* 2010, Moreno-Ulloa, 2015]. Previous studies have provided crucial evidence that the stimulatory effects of **Epi** on endothelial cells nitric oxide (NO) production may involve the participation of a GPER [Moreno-Ulloa *et al.,* 2015]. Current evidence indicates that the eNOS activation occurs after the stimulation of cell surface receptors including those from the tyrosine kinase and G-protein-coupled receptor (GPCRs) families [Dudzinski and Michel; 2007, Manning BD, Cantley, 2007]. However, knowledge about how these beneficial effects are mediated at the cellular level at this moment is still very limited. Elucidation of the molecular targets of **Epi** at the cellular level is essential for the improvement of the specificity of human studies and for an understanding of their mode of action.

We recently demonstrated that **Epi** seems to stimulate NO production through the involvement of the G-protein coupled estrogen receptor (GPER) and epidermal growth factor receptors (EGFR) [Moreno-Ulloa, 2015]. However, the use of selective blockers or receptor gene silencing approaches resulted only in an incomplete blockade of **Epi** stimulated NO production. Thus, other cell membrane receptors are likely involved in mediating the effects of Epi and there is little knowledge about the identity of such chemical structures. Interestingly, several studies have suggested that the biological properties of flavonoids are largely dependent on the availability of “free” phenol groups on their structure [Vaya *et al.,* 2003, Garg *et al.,* 2001].

Several strategies for target identification have been developed that rely on genetic, computational [Strausberg and Schreiber, 2003; Lambe *et al.,* 2006] and biochemical studies [Cuatrecasas *et al.,* 1968] principles. Although several key molecular targets have been identified through affinity chromatography [Harding *et al.,* 1989; Bach *et al.,* 2005].

Chromatography is a highly selective separation technique commonly used for the isolation and purification of biological macromolecules [Jones *et al.,* 1995; Sofer, 1995]. A wide range of chromatographic techniques has been used for large-scale biopurifications: size-exclusion chromatography, ion-exchange, hydroxyapatite, hydrophobic interaction chromatography, reversed-phase chromatography, and affinity chromatography [Lyddiatt, 2003].

Affinity, in the chemical setting, is the attractive force of varying strength for individual elements or compounds that causes atoms and molecules to combine and stay combined [Johnston, 2001]. These binding interactions are used by affinity chromatography for the purposes of purification.

For small molecules such as **Epi**, the affinity chromatography involves several steps. Synthesis and design of a ligand with intact bioactivity, selective immobilization, and finally, optimization and application of the adsorbent for the purification of the target protein. Morever there is insufficient structural data on the formation of complexes between target proteins and **Epi.** Studies have suggested that the extent of biological activity of **Epi** depends on its chemical structure, mainly on the availability of hydroxyl groups (Vaya *et al.,* 2003, Garg *et al.,* 2001).

Thus, we hypothesized that **Epi** exerts its biological effects by interacting with its proteins targets via phenolic hydroxyl. To test this, we implemented a rational strategy comprising the following steps: 1) synthesis of novel Epi derivatives (which relied on the introduction of mesyl or propargyl groups) that may be optimal for the generation of affinity columns and purification of **Epi** binding proteins, 2) *in silico* molecular docking of the novel Epi derivatives on a previously validated GPER platform, 3) *in vitro* analysis of the novel Epi derivatives on NO production and, 4) implementation of an inmobilized Epi derivative affinity column to isolate Epi binding proteins from protein extracts of endotelial cells.

CHAPTER 2

CHAPTER 2: METHODS AND MATERIALS

2.1 Synthesis of Epi derivatives

*General***.** Solvents and reagents were obtained from comercial sources and were used as received. NMR spectra were recorded at 400 MHz with a Bruker Avance III spectrometer at 30 °C. ^{1}H and ^{13}C NMR chemical shifts are reported in ppm referenced to TMS. Coupling constants *J* are given in Hertz (Hz). High Resolution Mass Spectrometry (HRMS) data were obtained in a micrOTOF-Q III MS instrument with electrospray ionization using sodium formate as calibrant. Analytical thin-layer chromatography (TLC) was done on Merck silica gel 60 F_{254} plates.

2.1.1 *5,7,3',4'-tetra-O-benzyl-(-)-epicatechin (Epi-benzyl)*

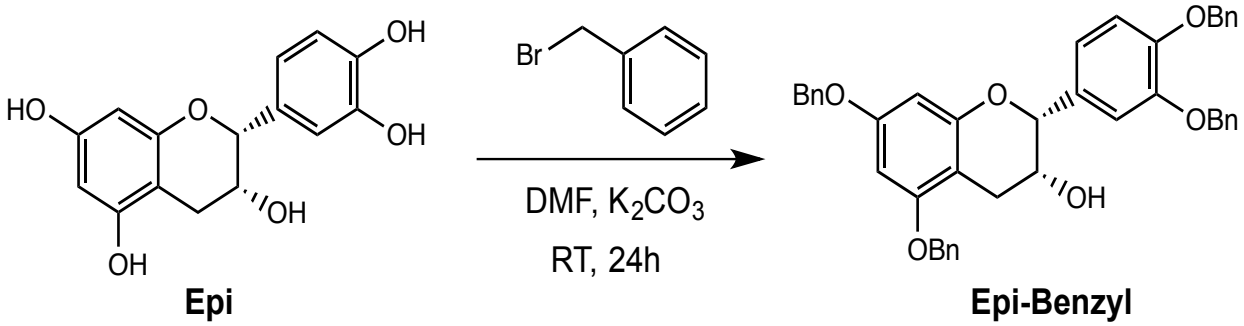

Figure 2.1. Synthetic strategy of **Epi-Benzyl**.

A solution of 0.5 g (1.72 mmol, 1eq) of **Epi,** 8 mL *N,N*-dimethylformamide (DMF) and 1.8 g of K_2CO_3 (12.9 mmol, 7.5 eq), were added to a 250 mL two-necked round-bottom flask and continuously stirred for 30 min at 0°C. Then 0.92 mL of Benzyl bromide was slowly added (dropwise) with a funnel. Finally, the reaction mixture was stirred at RT for an additional 24h, and filtered through a celite pad using CH_2Cl_2 (200 mL). The filtrate was washed with cold 10% HCl (2 x 300 mL), H_2O (2 x 300 mL) and brine (2 x 300 mL). The organic layer was dried over anhydrous $MgSO_4$ and the solvent removed under vacuum. The pasty residue was crushed with pentane (200 mL) then washed with ethyl ether (3 x 200 mL).

The resulting solid was filtered and washed with ethyl ether (3 x 100 mL) and petroleum ether (200 mL), and finally dried under vacuum for 24 h to produce ***5,7,3',4'-tetra-O-benzyl-(-)-epicatechin*** as a white solid. Yield= 79%.

^{1}H NMR [$CDCl_3$, 400 MHz]: δ 7.46-7.29 (m, 20 H, Ar-H), 7.14 (d, *J* = 1.4 Hz, 1H, H-2'), 7.00 (dd, *J* = 8.3, 1.4 Hz, 1H, H-6'), 6.96 (d, *J* = 8.3 Hz, 1H, H-5'), 6.27 (d, *J* = 2.1 Hz, 1H, H-8), 6.26 (d, *J* = 2.1 Hz, 1H, H-6), 5.18 (s, 2H, C$\underline{H}_2$Ph), 5.16 (s, 2H, C$\underline{H}_2$Ph), 5.01 (s, 2H, C$\underline{H}_2$Ph), 5.00 (s, 2H, C$\underline{H}_2$Ph), 4.90 (brs, 1H, H-2), 4.21 (brs, 1H, H-3), 2.99 (dd, *J* = 17.3, 2.0 Hz, 1H, H-4a) 2.92 (dd, *J* = 17.3, 4.2 Hz, 1H, H-4b). (See supplementary data**,** Figure 6.1).

^{13}C NMR [$CDCl_3$, 100 MHz]: *δ* 158.8, 158.4, 155.3, 149.1, 148.9, 137.3, 137.2, 137.0, 136.0, 131.6, 128.6 (2C), 128.54 (2C), 128.50 (2C), 128.48 (2C), 128.0, 127.88, 127.86, 127.82, 127.5 (4C), 127.3 (2C), 127.2 (2C), 119.6, 115.2, 113.7, 101.1, 94.8, 94.1, 78.4, 71.5, 71.4, 70.2, 70.0, 66.4, 28.3. (See supplementary data, Figure 6.2).

HRMS (ESITOF) *m*/*z*: $[M+Na]^+$, Calculated for $C_{43}H_{38}O_6Na$ 673.2561; Found 673.2541.

2.1.2 *5,7,3',4'-tetra-O-benzyl-3-O-mesyl-(-)-epicatechin (Epi-Benzyl-ms)*

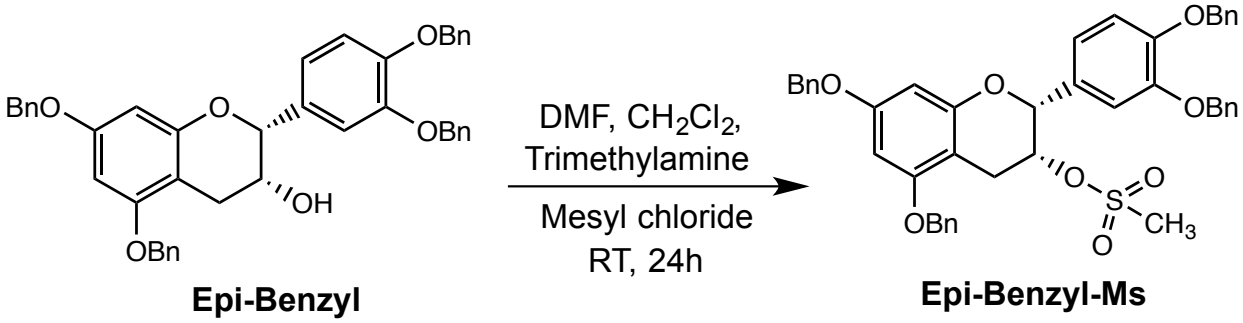

Epi-Benzyl **Epi-Benzyl-Ms**

Figure 2.2. Synthetic strategy of **Epi-Benzyl-Ms**.

A solution of 20 mL of *N,N*-dimethyformamide (DMF), 20 mL of dry CH_2Cl_2, 6 mL of trimethylamine and 0.5 g of ***5,7,3',4'-tetra-O-benzyl-(-)-epicatechin*** were added to a dry 250 mL round-bottom flask. Additionally, 0.150 mL of Mesyl chloride (1.2 mmol), previously dissolved in 5 ml of CH_2Cl_2 was dropwise to the reaction mixture, the reaction proceeded at RT for 24 h under anhydrous conditions, when it was finally quenched with $NaHCO_3$ (100 mL) and brine (50 mL). The organic layer was dried over anhydrous $MgSO_4$ and the solvent removed under vacuum. The solid was washed with a mixture of ethyl ether: methanol (2:1, 3 x 100 mL) and then dried under vacuum for 24 h to produce ***5,7,3',4'-tetra-O-benzyl-3-O-mesyl-(-)-epicatechin*** as a pale orange solid. Yield=90%

^{1}H NMR [$CDCl_3$, 400 MHz]: δ 7.47-7.28 (m, 20 H, Ar-H), 7.14 (d, *J* = 1.5 Hz, 1H, H-2'), 6.98 (dd, *J* = 8.4, 1.5 Hz, 1H, H-6'), 6.95 (d, *J* = 8.4 Hz, 1H, H-5'), 6.28 (d, *J* = 2.2 Hz, 1H, H-8), 6.26 (d, *J* = 2.2 Hz, 1H, H-6), 5.20 (s, 2H, C$\underline{H}_2$Ph), 5.18 (s, 2H, C$\underline{H}_2$Ph), 5.04 (brs, 1H, H-3), 5.01 (s, 4H, 2C$\underline{H}_2$Ph), 4.98 (brs, 1H, H-2), 3.24 (brd, *J* = 17.4 Hz, 1H, H-4a), 3.06 (dd, *J* = 17.4, 4.4 Hz, 1H, H-4b), 2.10 (s, 3H, C$\underline{H}_3$-S). (See supplementary data, Figure 6.6).

^{13}C NMR [$CDCl_3$, 100 MHz]: *δ* 159.1, 158.0, 155.0, 149.0, 148.9, 137.04, 137.00, 136.9, 136.8, 130.6, 128.63 (2C), 128.60 (4C), 128.5 (2C), 128.03, 128.01, 128.00, 127.9, 127.5 (4C), 127.4 (2C), 127.3 (2C), 119.4, 115.2, 113.5, 99.7, 94.8, 94.3, 76.9, 76.6, 71.4, 71.3, 70.2, 70.1, 37.4, 27.5. (See supplementary data, Figure 6.7).

HRMS (ESITOF) *m*/*z*: $[M+Na]^+$, Calculated for $C_{44}H_{40}O_8SNa$ 751.2336; Found 751.2323.

2.1.3 *5,7,3',4'-tetra-O-propargyl-(-)-epicatechin (Epi-4-prop)*

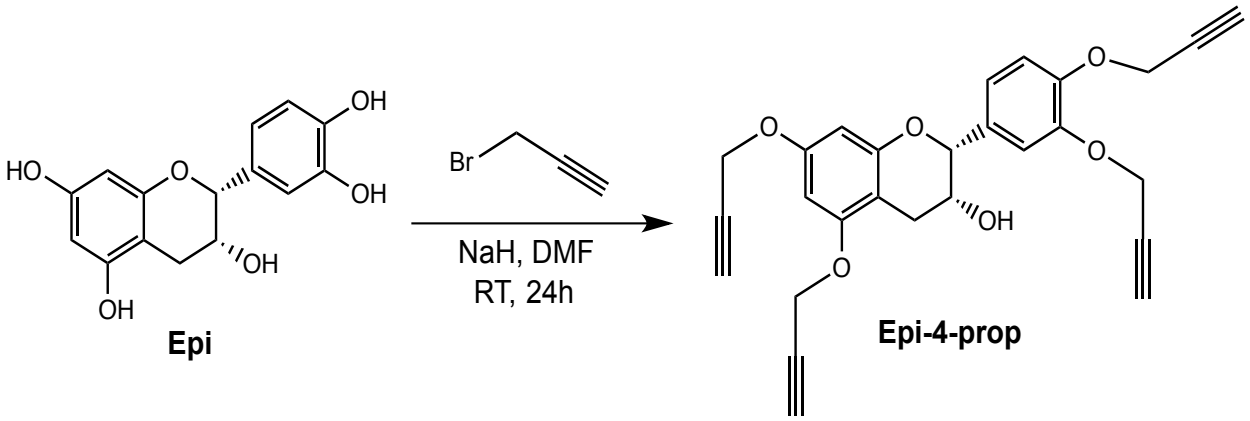

Figure 2.3. Synthetic strategy of **Epi-4-prop.**

0.37g (15.5 mmol, 9 Eq) of NaH was added slowly to 50 mL of a solution of **Epi** (0.5 g, 1.72 mmol) in *N,N*-dimethylformamide (with continuous stirring), the reaction was allowed to proceed for 30 min at 0°C, at which point 1.1 mL (13.8 mmol, 8 Eq) of propargyl bromide was added dropwise by means of a syringe. Then, the reaction mixture was stirred for 24 h at RT, and finally quenched with brine(150 mL), and extracted with CH_2Cl_2(300 mL). The organic layer was washed with water (2 x 200 mL) and dried over anhydrous $MgSO_4$. The solvent was evaporated, and the pasty residue was crushed in 100 mL of pentane and washed with a mixture of ethyl ether: methanol (2:1, 3 x 100 mL). The resulting solids were filtered and washed with petroleum ether and dried under vacuum for 24 h to produce ***5,7,3',4'-tetra-O-propargyl-(-)-epicatechin*** as a yellow solid. Yield= 87%

^{1}H NMR [$CDCl_3$, 400 MHz]: δ 7.23 (brs, 1H, H-2'), 7.11 (brs, 2H, H-5', H-6'), 6.30 (brs, 2H, H-6, H-8), 4.97 (brs, 1H, H-2), 4.79 (d, *J* = 2.4 Hz, 2H, C$\underline{H_2}$-C≡), 4.77 (d, *J* = 2.4 Hz, 2H, C$\underline{H_2}$-C≡), 4.68 (d, *J* = 2.4 Hz, 2H, C$\underline{H_2}$-C≡), 4.65 (d, *J* = 2.4 Hz, 2H, C$\underline{H_2}$-C≡), 4.28 (m, 1H, H-3), 2.94 (m, 2H, H-4ab), 2.52 (m, 4H, $\underline{H}$-C≡). (See supplementary data, Figure 6.8).

^{13}C NMR [$CDCl_3$, 100 MHz]: *δ* 157.5, 157.3, 155.3, 147.6, 147.5, 132.1, 120.1, 115.1, 113.6, 101.8, 95.5, 94.2, 78.51, 78.49, 78.47, 78.46, 78.3, 76.0, 75.9, 75.64, 75.62, 66.2, 57.1, 57.0, 56.1, 56.0, 28.0. (See supplementary data, Figure

6.9).

2.1.4 *3,5,7,3',4'-Penta-O-propargyl-(-)-epicatechin* (Epi-5-prop)

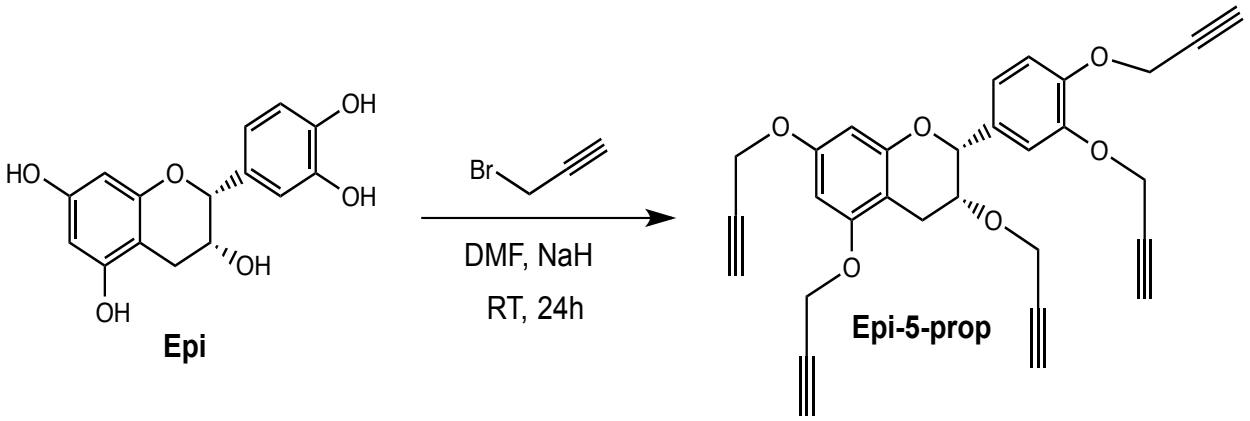

Figure 2.4. Synthetic strategy of **Epi-5-prop.**

0.98 g of NaH (40 mmol, 12 Eq) was slowly added to a solution of **Epi** (1 g, 3.4 mmol) in *N,N*-dimethylformamide, and the reaction proceeded for 30 min at 0°C. Then, 2.15 mL of Propargyl bromide (27.5 mmol, 7 Eq) was added dropwise to the reaction mixture, and the reaction was allowed to continue for 36 h at RT, with continuous stirring. After complete consumption of the starting material, monitoried by TLC (40% petroleum ether/ CH_2Cl_2, v/v), the reaction mixture was quenched with brine (150 mL) and extracted with CH_2Cl_2 (400 mL). The organic layer was washed with H_2O (2 x 200 mL) and dried over anhydrous $MgSO_4$. The solvent was evaporated, and the pasty residue was triturated in 100 mL of pentane and washed with ethyl ether (3 x 200 mL) followed by methanol (2 x 200 mL). The solids obtained were filtered and washed with petroleum ether (1 x 200 mL) and dried under vacuum for 24 h to produce ***3,5,7,3',4'-Penta-O-propargyl-(-)-epicatechin*** as a pale yellow solid. Yield= 81%.

^{1}H NMR [$CDCl_3$, 400 MHz]: δ 7.28 (d, *J* = 1.8 Hz, 1H, H-2'), 7.10 (dd, *J* = 8.3, 1.8 Hz, 1H, H-6'), 7.05 (d, *J* = 8.3 Hz, 2H, H-5'), 6.28 (d, *J* = 2.3 Hz, 1H, H-8), 6.27 (d, *J* = 2.3 Hz, 1H, H-6), 5.02 (brs, 1H, H-2), 4.78 (d, *J* = 2.4 Hz, 2H, C$\underline{H_2}$-C≡), 4.77 (d, *J* = 2.4 Hz, 2H, C$\underline{H_2}$-C≡), 4.67 (d, *J* = 2.4 Hz, 2H, C$\underline{H_2}$-C≡), 4.64 (d, *J* = 2.4

Hz, 2H, C$\underline{H}_2$-C≡), 4.22 (m, 1H, H-3), 4.10 (dd, *J* = 16.2, 2.4 Hz, 1H, C$\underline{H}_2$-C≡), 4.00 (dd, *J* = 16.2, 2.4 Hz, 1H, C$\underline{H}_2$-C≡), 2.98 (dd, *J* = 16.9, 3.2 Hz, 1H, H-4a), 2.84 (dd, *J* = 16.9, 4.5 Hz, 1H, H-4b), 2.52 (t, *J* = 2.4 Hz, 2H, $\underline{H}$-C≡), 2.50 (t, *J* = 2.4 Hz, 4H, $\underline{H}$-C≡), 2.30 (t, *J* = 2.4 Hz, 1H, $\underline{H}$-C≡). (See supplementary data, Figure 6.10).

^{13}C NMR [$CDCl_3$, 100 MHz]: *δ* 157.5, 157.0, 155.5, 147.4, 147.3, 132.3, 120.7, 114.7, 114.1, 102.1, 95.5, 93.9, 79.6, 78.60, 78.58, 78.52, 77.8, 76.7 (2C), 75.7, 75.54, 74.5, 72.2, 66.2, 57.0 (2C), 56.2, 56.0, 53.4, 29.7. (See supplementary data, Figure 6.11).

2.1.5 *Deprotection reactions*

Deprotection reactions were carried out in a hydrogenation glass apparatus. Solutions of compounds ***5,7,3',4'-tetra-O-benzyl-3-O-mesyl-(-)-epicatechin*** and ***3,5,7,3',4'-Penta-O-propargyl-(-)-epicatechin*** in ethyl acetate: methanol (25 mL) were added to a suspension of 20% Pd(OH)/C (60 wt % wet, 4.5 eq) in methanol (25 mL) at RT with stirring. The reactions vessels were purgated with N_2 followed by H_2 and were allowed to stir at RT in presence of H_2 for 48 h. After the reaction mixtures were filtered through a celite pad using CH_2Cl_2: methanol (1:1, 300mL) and concentrated. The solids were dissolved in a few milliliters of methanol and precipitation was carried out by adding a mixture of petroleum ether and CH_2Cl_2 (1:1, 100 mL). The compounds were purified by repeated precipitation with diethyl ether. Evaporation under vaccum for 24h-48 h resulted in gummy solids.

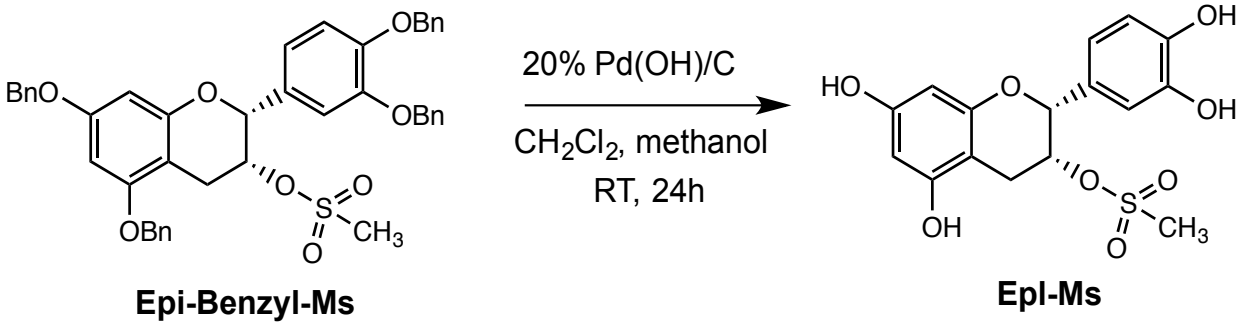

Epi-Benzyl-Ms **Epl-Ms**

Figure 2.5. Synthetic strategy of **Epi-Ms**.

3-O-Mesyl-(-)-epicatechin (Epi-Ms). Crushing with petroleum ether resulted in an orange solid. Yield= 98%. ^{1}H NMR [DMSO-d_6, 400 MHz]: δ 6.99 (d, *J* = 1.8 Hz, 1H, H-2'), 6.84 (dd, *J* = 8.2, 1.8 Hz, 1H, H-6'), 6.81 (d, *J* = 8.2 Hz, 1H, H-5'), 5.98 (d, *J* = 2.2 Hz, 1H, H-8), 5.94 (d, *J* = 2.2 Hz, 1H, H-6), 5.08 (brs, 1H, H-3), 4.99 (brs, 1H, H-2), 3.09 (dd, *J* = 17.6, 1.6 Hz, 1H, H-4a), 3.02 (dd, *J* = 17.6, 4.1 Hz, 1H, H-4b), 2.41 (s, 3H, C<u>H</u>$_3$-S). (See supplementary data, Figure 6.12).

^{13}C NMR [DMSO-d_6, 100 MHz]: *δ* 156.7, 156.5, 154.4, 145.1, 145.0, 129.5, 117.8, 114.8, 113.7, 96.9, 95.4, 94.4, 77.7, 76.4, 36.0, 26.6. (See supplementary data, Figure 6.13).

HRMS (ESITOF) *m*/*z*: $[M+Na]^+$, Calculated for $C_{16}H_{16}O_8SNa$ 391.0464; Found 391.0464.

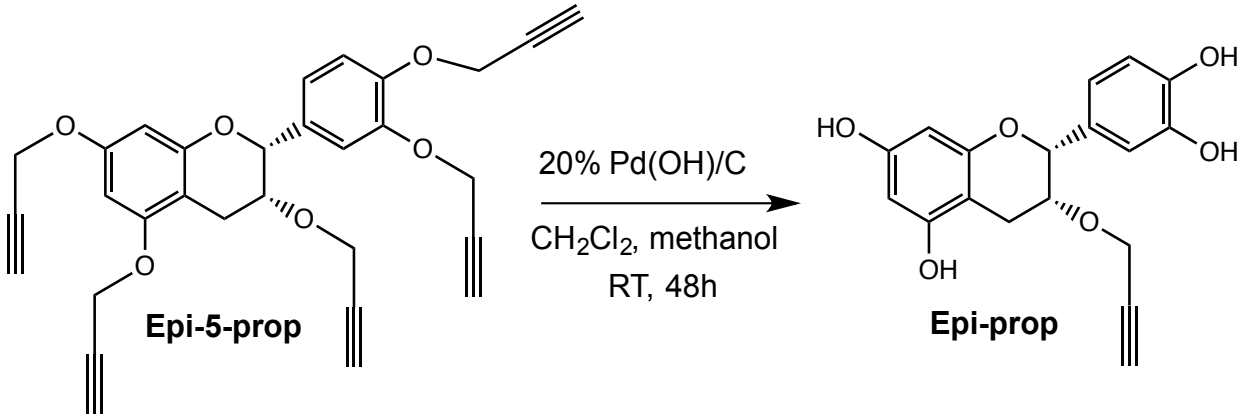

Figure 2.6. Synthetic strategy of **Epi-prop.**

***3-O-propargyl-(-)-epicatechin (Epi-prop)*.** A Pale yellow gummy solid. Yield= 89%.^{1}H NMR [$CDCl_3$, 400 MHz]: δ 7.07 (d, *J* = 1.7 Hz, 1H, H-2'), 6.88 (dd, *J* = 8.3, 1.7 Hz, 1H, H-6'), 6.78 (d, *J* = 8.3 Hz, 1H, H-5'), 6.08 (d, *J* = 2.2 Hz, 1H, H-8), 6.00 (d, *J* = 2.2 Hz, 1H, H-6), 4.89 (brs, 1H, H-3), 4.69 (brs, 1H, H-2), 2.78 (dd, *J* = 17.1, 3.7 Hz, 1H, H-4a), 2.69 (dd, *J* = 17.1, 4.5 Hz, 1H, H-4b), 2.30 (t, *J* = 2.4 Hz, 1H, <u>H</u>-C≡). (See supplementary data, Figure 6.14).

^{13}C NMR [$CDCl_3$, 100 MHz]: *δ* 157.9, 157.3, 154.6, 147.8, 147.6, 130.9,

118.6, 112.6, 112.5, 100.2, 92.8, 92.0, 77.2, 76.2, 73.0, 70.7, 54.1, 28.7. (See supplementary data, Figure 6.15).

2.2 Biological effects of Epi and Epi derivatives

2.2.1 Molecular modeling and molecular dynamic (MD) simulations

We used as a target the tridimensional (3-D) model of GPER previously developed, refined by molecular dynamics (MD) simulations and validated by docking studies [*Méndez-Luna et al.,* 2015]. This 3-D model of GPER was built using the GPCR I-Tasser web site [Zhang and Zhang, 2003] (a specialized server for building 3-D models of GPCRs). The 3-D model was evaluated by both the ERRAT (http://nihserver.mbi.ucla.edu/ERRAT/) and PROCHECK (https://www.ebi.ac.uk/thornton-srv/software/PROCHECK/) servers. The NAMD 2.9 program was used to perform the GPER refinement by MD simulations. The 14 and 70 ns snapshots derived from MD were used for docking studies, as these snapshots appeared to evidence key molecular recognitions of a G1 (agonist) and a G15 (antagonist) in the binding site of GPER [*Méndez-Luna et al.,* 2015].

2.2.2 Molecular docking studies

Docking studies were performed as previously described [*Méndez-Luna et al.,* 2015], with slight modifications. Docking parameters employed here consisted on a grid box of 60 × 60 × 60 A^3 centered at the C*α* of F208, as this residue has been suggested by us and others [Lappano *et al.,* 2012] to be the protein active site center, other parameters were kept the same.

All analyzed ligands were drawn with ACD/CHEMSKETCH (http://www.acdlabs.com/resources/freeware/chemsketch/) and converted into 3-D structures (Z-matrix) with the Gauss view 5.0 program. Ligands were energetically and geometrically optimized at the AM1 semi-empirical level using the Gaussian 03 package. The prediction and description of GPER binding site with all ligands were carried out on the AutoDock 4.2 software using the graphic interface AutoDock

Tools 1.5.2.

2.2.3 Reagents

Epi, protease inhibitor cocktail and dimethyl sulfoxide (DMSO), gallic acid (Gal), sodium ascobate (NaLAC), trypan blue solution and 0.2% trypan blue were purchased from Sigma Aldrich (St. Louis, MO, USA). Bovine Coronary Artery Endothelial Cells (BCAECs) were purchased from Cell Applications, Inc. (San Diego, CA, USA). Fetal bovine serum (FBS) and Dulbecco's Modified Eagle's Media (DMEM) with phenol red were from Life Technologies (Carlsbad, CA, USA). Bovine serum albumin (BSA) was from Tissue Culture Biologicals (Long Beach, CA, USA). Hank's Balanced Salt Solution (HBSS) phenol red free was from Mediatech Cellgro, Inc. (Herndon, VA, USA). The PVDF transfer membranes were from EMD Millipore (Bedford, MA, USA). Enhanced chemiluminescence (ECL) Plus Western Blot detection kit was from Amersham Biosciences (Piscataway, NJ, USA). G15 was from Cayman Chemical (Ann Harbor, MI, USA). Diferents dilutions of 5,7,3′,4′-Tetra-*O*-propargyl-(-)-epicatechin (Epi-4-prop), 3,5,7,3′,4′-Penta-*O*-propargyl-(-)-epicatechin (Epi-5-prop), 3-*O*-propargyl-(-)-epicatechin (Epi-prop), and 3-*O*-Mesyl-(-)-epicatechin (Epi-Ms) were prepared in water (5% DMSO, v/v). The dilutions of each derivative were prepared immediately prior to experimental use.

2.2.4 Cell culture

BCAECs were cultured in DMEM supplemented with fetal bovine serum (FBS), with 1% antibiotic and antimicotic solution and maintained at 37°C in an incubator with a humidified atmosphere of 5% CO_2. Six hours prior to experiments, BCAECs were washed with phenol red free Hank's salt solution and kept in phenol red free M-199 supplemented with 200 mmol/L of L-glutamine and 1% antibiotic mix. For eNOS activation and NO production assessment (-)-epicatechin derivatives solutions and G15 were added at 1 μM for 10 min. For antioxidant assessment (-)-epicatechin derivatives solutions and gallic acid (Gal) and sodium ascorbate (NaLAC) were added at 1 μM for previously to 200 μM H_2O_2 solution. As

a positive control, 1 µM (-)-epicatechin was used in DMSO (5%, v/v).

2.2.5 eNOS activation and NO production

2.2.5.1 Total protein extraction

Immediately after the Epi-derivative treatment of BCAECs, cells were washed three times with cold HBSS (5 ml/well), then we added 500 µl of lysis buffer (1% Triton X-100, 20 mmol/l Tris, 140 mmol/l NaCl, 2 mmol/l EDTA, and 0.1% SDS), that had been supplemented with protease and phosphatase inhibitor cocktails,1 mmol/l PMSF, with 2 mmol/l Na_3VO_4, and 1 mmol/l NaF. The cell homogenates were sonicated for 10 min at 4°C, and centrifuged (12,000x *g*) for 10 min to remove cell debris, then we transfered the supernatant to a clean tube. The total protein concentration was measured in the supernatant using the Bradford assay (for Bradford assay see supplementary data 6.8.1).

2.2.5.2 NO measurements

NO levels were measured in growth media and normalized to protein content (determined by the Bradford method). NO levels were measured in growth media and normalized to protein content (determined by the Bradford method) following the instructions provided in the commercial “Nitrite/Nitrate Fluorometric Assay Kit” (Cayman Chemical Company, Ann Arbor, MI, United States). Standard curves were plotted. For nitrate, 10 µL of each sample was diluted in 70 µL of assay buffer. Aliquots of 10 µL of enzyme cofactor and 10 µL of nitrate reductase mixture were added to the buffered sample. After 30 min of incubation at room temperature, 10 µL of DAN (2,3-diaminonaphtalene) was added and incubated for another 10 min. For nitrite, 10 µL of each sample was diluted with 90 µL of assay buffer, and 10 µL of DAN was added. Both the nitrate and nitrite samples were then incubated for 10 min, and 20 µL of NaOH was added. All samples were read in triplicate with fluorometry using an excitation wavelength of 355 nm and an emission wavelength of 430 nm using a fluorometer (FLx800, BioTek Instruments Inc).

2.2.5.3 SDS-PAGE analysis, Western Blot detection

Electrophoretic separation of proteins was carried out under denaturing conditions (i.e., in the presence of SDS) in a discontinuous gel system [Laemmli, 1970]. Electrophoresis was performed with the Mini-PROTEAN® Systemvertical gel electrophoresis system. Bio-Rad's TGX (Tris/Glycine eXtended) Electrophoresis Gels were used in all experiments. Protein extracts prepared as described in section 2.2.5.1 were mixed with 1/5 volume of 6x sample buffer and heated at 95°C for 5 min prior to electrophoresis. A total of 40 µg of protein was loaded onto a 4–15% SDS-PAGE. The electrophoresis was performed at at a constant current of 25-30 mA for 2-3 h.

Proteins separated in the SDS-polyacrylamide gels were transferred to a membrane to enable immunodetection. Immobilon P (Millipore) PVDF membranes were used in this work. Protein transfer was performed using semidry blotting. Prior to blotting, the membrane was immersed in methanol for 1 min, rinsed with distilled water and then equilibrated in transfer buffer for 15 min. The stacking gel was removed from the separating gel and discarded. The separating gel was also equilibrated in transfer buffer for 15 min. Then, the gel and membrane were placed between buffer-saturated blotting paper in the blotting apparatus. The PantherTM semidry electroblotter HEP-1 (PeqLab) was used in this work. Blotting proceded for 2h. The membrane was stained with 1x Ponceau S solution for 5 min and destained in water for the next 2 min to visualize protein bands. Finally, the membrane was left in blocking buffer (see chapter 2.7.5) overnight.

Following the transfer of proteins from gel to membrane, the membrane was incubated in blocking buffer (5% nonfat dry milk [NFM] in TBS [tris-buffered saline solution] plus 0.1% Tween 20 [TBS-T]), at 4°C overnight. Then it was washed briefly with washing buffer (TBS-T, 3 X 5 min) and incubated for 1 h with primary antibodies diluted in blocking buffer (Primary antibodies were typically diluted 1:1000 or 1:2000 in TBS-T plus 5% bovine serum albumin) Next, the membrane was washed three times with TBS-T and incubated 1h at room temperature in the

presence of HRP-conjugated secondary antibodies diluted 1:5,000 in blocking solution. The membrane was again washed three times with TBS-T and the immunoblots developed using the ECL detection kit. The band intensities were digitally quantified and phospho-proteins normalized against the total protein loaded.

2.2.6 Antioxidant activity

2.2.6.1 MTT assay

Cells were seeded (10^6/mL) into 96 well microtitre plates and allowed to adhere for 24 h. The plates, previously washed three times with phenol red free Hank's salt solution, were incubated with Epi derivatives (1 µM of Epi derivative in phenol red free M-199 supplemented with 200 mmol/L of L-glutamine and 1% antibiotic mix) for 24 h. Then, Epi derivatives were removed, and the cells were washed with sterile three times with 1X PBS before H_2O_2 exposition. Following exposure to 200 µM H_2O_2 the cells were washed twice with 1X PBS and a MTT solution (0.5 mg/mL in clear medium without serum and phenol red) was added to all wells overnight at 37°C. The MTT solution was removed with 1X PBS (three times) and the formazan crystals were solubilized in 100 µL of dimethylsulfoxide (DMSO) for 2 h at 37°C. The absorbance was measured at 435 nm in a microplate reader. Results were expressed as the percentage of cell viability against the decline in MTT reduction. Cell viability was used to estimate the cytoprotection effect conferred by **Epi** and Epi derivatives. Gallic acid (Gal) and sodium ascorbate (NaLAC) were used as antioxidant standards. (Supplementary data 6.8.2)

2.2.6.2 Trypan blue exclusion method

Cell death induced by H_2O_2 was determined using a method similar to the MTT assay. Cells were seeded (10^6/mL) into 96 well microtitre plates and allowed to adhere for 24 h in in phenol red free M-199 supplemented with 200 mmol/L of L-glutamine and 1% antibiotic mix. The plates, previously washed three times with 1X PBS, were incubated with H_2O_2 exposition. After incubation with 200 µM H_2O_2

for 4 h cells were washed three times with 1X PBS and dispersed with 0.025% trypsin-EDTA. Ten µl of BCAECs suspension was mixed with 10 µl of trypan blue solution (0.4% in 0.81% sodium chloride; 0.06% potassium phosphate, dibasic), and incubated at room temperature for 5 min. Triplicate wells were counted using a haemocytometer and the experiment was repeated at least two times. Results were expressed as the percentage of trypan blue stained cells. (Supplementary data 6.8.3).

2.2.6.3 Crystal violet assay

Cell death induced by H_2O_2 was also determined using another method similar to the MTT assay. BCAECs were seeded (10^6/mL) into 96 well microtitre plates and allowed to adhere for 24 h in phenol red free M-199 supplemented with 200 mmol/L of L-glutamine and 1% antibiotic mix. Then they were washed twice with sterile 1X PBS. Epi derivatives (1 µM of Epi derivative in phenol red free M-199 supplemented with 200 mmol/L of L-glutamine and 1% antibiotic mix) were added for 24 h overnight. Then, Epi derivatives were removed, and the cells were washed with sterile three times with 1X PBS. Followed, BCAECs were exposed to 200 µM H_2O_2 for 2 h, then washed with 1X PBS and subsequently stained with a 0.5% crystal violet solution in 20% ethanol. After removing excess stain with 1X PBS, the crystal violet stained cells were dissolved by adding 100µl of methanol, incubated for 30 minutes with shaking at room temperarure. The optical density at 590 nm from each well was measured on a microplate reader. Methanol was used as the blank. Results were expressed as the percentage of cell viability. The absorbance of untreated cells represents 100%. The absorbance was measured at 435 nm in a microplate reader. Results were expressed as the percentage of cell viability against the decline in stained cells. Cell viability was used to estimate the cytoprotection effect conferred by **Epi** and Epi derivatives. Gallic acid (Gal) and sodium ascorbate (NaLAC) were used as antioxidant standards. (Supplemetary data 6.8.4).

2.2.6.4 Resazurin assay

Finally, Cell death induced by H_2O_2 was determined using another method similar to the MTT assay. Cells were seeded (10^6/mL) into 96 well microtitre plates and allowed to adhere for 24 h in phenol red free M-199 supplemented with 200 mmol/L of L-glutamine and 1% antibiotic mix. The plates, previously washed three times with phenol red free Hank's salt solution, were incubated with Epi derivatives (1 µM of Epi derivative in phenol red free M-199 supplemented with 200 mmol/L of L-glutamine and 1% antibiotic mix) for 24 h. Then, Epi derivatives were removed, and the cells were washed with sterile three times with 1X PBS before H_2O_2 exposition. Following exposure to 200 µM H_2O_2 the cells were washed twice with 1X PBS and 100 µl of resazurin solution (0.15 mg/mL in PBS) was added to each well and the plate was incubated at 37°C for 3h. Fluorescence was recorded using a 560 nm excitation/590 nm emission filter set. Cell viability was used to estimate the cytoprotection effect conferred by **Epi** and Epi derivatives. Gallic acid (Gal) and sodium ascorbate (NaLAC) were used as antioxidant standards. (Supplementary data 6.8.5).

2.2.6.5 Trolox curve

The Trolox equivalent antioxidant capacity (TEAC) assay was performed to determine the H-donating potential of Epi and Epi derivatives. The $ABTS^{\bullet+}$ radical was produced by the oxidation of 7 mM ABTS (38.41 mg) with 2.45 mM potassium persulphate (13.38 mg) in 10 mL of water. The solution was allowed to stand for 16 h at room temperature to generate the ABTS radical cation ($ABTS^{\bullet+}$). For the experiment the ABTS stock solution was diluted with PBS (pH 7.4) to give an absorbance of 0.7 ± 0.02 at 734 nm. Then, 5 uL of each derivative in 50% aqueous methanol was mixed with 200 uL of the $ABTS^{\bullet+}$solution into 96 well microtitre plates. The absorbance was measured after 10 min of incubation at room temperature. Six diferents dilutions were performed for each derivative. All determinations were carried out in triplicate, on each occasion and at each separate concentration of the standard and samples. Gal and NaLAs were used as

a standart. The results were estimated by interpolating the absorbance on a Trolox (10–150 μM) calibration curve and expressed as TEAC values, the ability of Epi derivatives to scavenge 50% of free radical and TEAC (Trolox equivalent antioxidant capacity).

2.2.6.6 Cyclic and differential voltammetry

Electrochemical experiments were done using an Autolab PGSTAT 302N (Metrohm Autolab) version 1.11 software (NOVA). Voltammetric curves were recorded at room temperature using a three-electrode system in a small-volume electrochemical cell (25 mL capacity). The working electrode was a glassy carbon; Ag/AgCl (saturated KCl) was used as a reference electrode and a platinum wire as counter electrode. In this work, all potentials were reported using the Ag/AgCl (sat) electrode as reference. The glassy carbon working electrode was polished with Methanol. Voltammetric scans were carried out in the potential range −1.0 to +1.2V versus Ag/AgCl. Gal, NaLAC, **Epi** and Epi derivatives were used at 1mM. PBS (1X, pH 7.4) was used as the supporting electrolyte. Briefly, first we cleaned the electrodes in an effort to ensure good electron transfer. Thus we placed the glassy carbon electrode (WE), the Ag/AgCl reference electrode (RE), and the platinum wire counter electrode (CE) in a solution of 0.1 M $HClO_4$. Next, we cycled the electrode between 0.2 and 1.5 V for 10 minutes at 20 mV/sec and stoped the cyclic voltammograms after 10 min. Once we cleaned the electrodes, we started the electrochemical experiments running a voltammogram in PBS 1X without adding Epi or Epi derivatives as controls only with the supporting electrolyte (1M, Tetrabutylammonium tetrafluoroborate, TBATFB). We ran these voltammograms from 0.35 V to 0.00 V (in order to be in regions where the Faradaic current is minimal).Then, we ran the pulse diffential voltammetries (PDV) or cyclic voltammetries (CV) at 0.5 V/sec, 0.1 V/sec, and 0.01 V/sec. Followed by PDVs and CVs in PBS 1X (1μM TBATFB), using 1μM Epi or Epi derivtives (we rinsed electrodes well between experiments using methanol and 0.1 M $HClO_4$ solution). Then, we ran PDVs for Gal and NaLAc (same conditions for Epi and Epi derivatives). Finally we rinsed the working electrode thoroughly and immersed it in

0.001 M octadecanethiol in EtOH for 30 min, removed the electrode from the solution and rinsed it thoroughly. (See supplementary data 6.8.6).

2.2.6.7 Catalase activity

BCAECs were exposed to 200 μM H_2O_2 after pre-treatment with 1 μM of **Epi**, Epi derivatives, and Gal and NaLAC as standards, for 48 h. After treatment, the BCAECs were washed three times with cold PBS (5 ml/well) then lysed in lysis buffer (1% Triton X-100, 20 mmol/l Tris, 140 mmol/l NaCl, 2 mmol/l EDTA, and 0.1% SDS), supplemented with protease and phosphatase inhibitor cocktails, 1 mmol/l PMSF, 2 mmol/l Na_3VO_4, and 1 mmol/l NaF. Homogenates were sonicated for 10 min at 4°C, and centrifuged (12,000x *g*) for 10 min to remove cell debris. Catalase activity was measured with a commercial colorimetric kit (Cayman Chemicals, intra-assay coefficient of variation of 3.8%), following the manufacturer's instructions. We added 100 μl of diluted Assay Buffer, 30 μl of methanol, and 20 μl of into a 96 well microtitre plates. We incubated the plate on a shaker for 20 min at room temperature. After incubation, 30 μl of Potassium Hydroxide were added to each well to terminate the reaction. Next, 30 μl of Catalase Purpald were added to each well, incubating the plates at room temperatura for 10 min. Finally, 10 μl of Catalase Potassium Periodate were added to each well, incubated for 5 min at room temperature with a shaker. Absorbance measurements were performed at 540 nm using a plate reader The results were expressed as nmol/min/mg of protein. The total protein concentration was measured in the supernatant with the Bradford assay (for Bradford assay see supplementary data), using bovine serum albumin as the standard.

2.2.7 Statistical analysis

Two types os statistical analysis were performed on the data: a) first, to examine whether there exists any discrepancy among each Epi derivative with respect to **Epi**, the control group (ctrl, untreated cells), H_2O_2 (cells only treated with

H_2O_2), galic acid (Gal) and ascorbic acid (NaLAC), and b) second, to examine whether there exists any discrepancy among different groups of compounds categorized by the effects displayed in previous analysis and their chemical structure. The first group of Epi-prop derivatives (Epi-prop deriv) which comprise **Epi-prop**, **Epi-4-prop** and **Epi-5**; the Standard group (std) which comprise galic acid (Gal) and ascorbic acid (NaLAC); and the **Epi** group which comprise only **Epi**, and **Epi-Ms,** with respect to two diferents groups: the control group (cntrl, untreated cells) and H_2O_2 (cells only treated with H_2O_2). Statistical comparisons were made using a one-factor analysis of variance (ANOVA) was conduted for each of group, with a confidence level of 95%. Significance level was set at $p < 0.05$. All data were expressed as a mean ± standard error of the mean (SEM). The mean values were calculated from data taken from different experiments performed in triplicates on separate days using freshly prepared reagents in all cases.

2.3 Design, synthesis and characterization of a column (EPI-COLUMN) with and Epi derivative for the isolation of Epi binding proteins

2.3.1 Reagents

Epi, protease inhibitor cocktail and dimethyl sulfoxide (DMSO), gallic acid (Gal), sodium ascobate (NaLAC), trypan blue solution and 0.2% trypan blue were purchased from Sigma Aldrich (St. Louis, MO, USA). Bovine Coronary Artery Endothelial Cells (BCAECs) were purchased from Cell Applications, Inc. (San Diego, CA, USA). Fetal bovine serum (FBS) and Dulbecco's Modified Eagle's Media (DMEM) with phenol red were from Life Technologies (Carlsbad, CA, USA). Bovine serum albumin (BSA) was from Tissue Culture Biologicals (Long Beach, CA, USA). Hank's Balanced Salt Solution (HBSS) phenol red free was from Mediatech Cellgro, Inc. (Herndon, VA, USA). The PVDF transfer membranes were from EMD Millipore (Bedford, MA, USA). Enhanced chemiluminescence (ECL) Plus Western Blot detection kit was from Amersham Biosciences (Piscataway, NJ, USA).

2.3.2 Cell culture

BCAECs were cultured in DMEM supplemented with fetal bovine serum (FBS), with 1% antibiotic and antimicotic solution and maintained at 37°C in an incubator with a humidified atmosphere of 5% CO_2. Six hours prior to experiments, BCAECs were washed with phenol red free Hank's salt solution and kept in phenol red free M-199 supplemented with 200 mmol/L of L-glutamine and 1% antibiotic mix. For eNOS activation and NO production assessment (-)-epicatechin derivatives solutions and G15 were added at 1 μM for 10 min. For antioxidant assessment (-)-epicatechin derivatives solutions and gallic acid (Gal) and sodium ascorbate (NaLAC) were added at 1 μM for previously to 200 μM H_2O_2 solution. As a positive control, 1 μM (-)-epicatechin was used in DMSO (5%, v/v).

2.3.3 Total protein extraction

BCAECs, they were washed three times with cold HBSS (5 ml/well), then we added 500 μl of lysis buffer (1% Triton X-100, 20 mmol/l Tris, 140 mmol/l NaCl, 2 mmol/l EDTA, and 0.1% SDS), that had been supplemented with protease and phosphatase inhibitor cocktails,1 mmol/l PMSF, 2 mmol/l Na_3VO_4, and 1 mmol/l NaF. The cell homogenates were sonicated for 10 min at 4°C, and centrifuged (12,000x *g*) for 10 min to remove cell debris, then we transfered the supernatant to a clean tube. The total protein concentration was measured in the supernatant using the Bradford assay (for the Bradford assay protocol see supplementary data).

2.3.4 EPI-COLUMN

2.3.4.1 Azide-Alkyne Click-Chemistry

Two hundred μL of a 50% suspension of Agarose-azide beads (1 Eq) was placed in a disposable vessel, allowed to settle for 30 min, and washed with deionized H_2O (1.3 mL), then pelleted by centrifugation and equilibrated with 3 column volumes of a 1:1 H_2O/*ter*-butanol mixture (2mL). 3-*O*-propargyl-(-)-

epicatechin [**Epi-prop**] (22 μmol, 5 Eq) or fluorescent dye (5 Eq) were dissolved in a 1:1 H_2O/*ter*-butanol mixture (1.8 mL), either of the previous solutions was mixed with 1 Eq of equilibrated agarose-azide beads (with a maximum of 20 μmol of azide groups per mL resin) followed by Copper(II) sulfate pentahydrate (1 Eq, in 100 μL of a 1:1 H_2O/*ter*-butanol mixture) and finally sodium ascorbate (7 mg, 2 Eq, prepared fresh with 100 μL of deionized H_2O).

The previous reaction mixtures were stirred at room temperature (RT) for 72 h. EDTA (0.1 M) was added to stop the reaction. Finally, the reaction mixture was loaded into a minicolumn (Thermo Scientific) and washed sequentially with approximately 5 column volumes of each of the following: a 1:1 H_2O/*ter*-butanol mixture, 0.1 M EDTA, CH_2Cl_2, Methanol, H_2O, and PBS 1X. As controls, we used beads treated by an identical procedure with the exception that no Epi-prop, or Copper (II) sulfate pentahydrate, or sodium ascorbate was added.

2.3.4.2 Zeta potential measurements

The Zeta (ξ) potential is the electrostatic potential that exists at the shear plane of a particle, which is related to both surface charge and the local environment of the particle. The Zeta potential of our samples was determined with a Zeta Potential Analyzer SZ-100 from Horiba. Measurements were recorded at 25°C suspended in HBSS buffer (ionic strength 40 mM, pH 7.4) with a carbon electrode using the Phase Analysis Light Scattering mode. Streaming potential measurements were carried out in the variable height parallel plate channel device described in de- tail by Werner *et al.* (8). This device allows adjustment of the distance between two 10 mm × 20 mm flat surfaces from over 50 μm down to 1 μm in perfect parallel position without having to remove the sample Plate parallelism along the *x* and *z* axes, was controlled via an optical microscope. A high-pressure N_2 gas reservoir is used to produce the pressure drop across the channel which is controlled electronically by a pressure transducer and electromagnetic valve. Measurements of the streaming potential and pressure drop were conducted at five different channel heights ranging from 66 μM to 3 μM for three streaming solutions:

HBSS buffer (ionic strength 40 mM, pH 7.4) and pure water. At each chan- nel height the measurements were conducted over a number of pressures ranging from 2.4 kPa to over 50 kPa (kPa: kilopascal). The height of the channel was determined by relating volume flow rate measurements of a high concentration solution, thus no double layer effects was assumed to be accurate to within ±0.2 μm.

2.3.4.3 Fluorescence Assay

A dilution series of **Epi-prop** and **BPY** solutions (0.01-0.5 mM) were prepared with 1:1 H_2O/*ter*-butanol mixture in a 96 well plate. For each data point, 10 μL of the appropriate compound solution was added into 600 μL of distilled water, to give a final compound concentration in the range 0.001-0.04 mM. The fluorescence emission intensity was measured within 1 min of adding Epi-prop or BPY to the distilled water well. Each measurement was repeated in triplicate and the mean and standard deviation were calculated. The fluorescence data were plotted as relative fluorescence intensity against flavonoid concentration. The H_2O/*ter*-butanol mixture diluted to 600 μL with distilled water was used as a blank. Samples were assayed in triplicate The fluorescence values of the sample eluted from the EPI-COLUM were extrapolated from the standard curve. For these experiments, a Perkin- Elmer LS55 Luminescence Spectrophotometer was used to determine emission spectra at an excitation wavelength of Ex_{280}/Em_{320}.

2.3.5 Protein isolation and elution

Two hundred μl of a BCAEC extract containing 0.8–1.0 mg protein was loaded into the Epi-Agarose column and incubated overnight at 4 °C with mild tumbling. The column was washed sequentially with 5 column volumes of each of the following: wash buffer (5 mM EDTA, 0.5% SDS, 250 mM NaCl in 1X PBS pH 7.5), 1X PBS (with 20 % wash buffer) and 1X PBS. The proteins that bounded to the column were then eluted 3 times with 100 μL of Elution buffer (8 M urea in 1X PBS). Finally, the column was washed with 10 column volumes of wash buffer and

1X PBS. The control columns were processed by an identical procedure.

2.3.6 SDS-PAGE analysis and Western Blot detection

Electrophoretic separation of proteins was carried out under denaturing conditions (i.e., in the presence of SDS) in a discontinuous gel system [Laemmli, 1970]. Electrophoresis was performed in Mini-PROTEAN® Systemvertical gel electrophoresis system. Bio-Rad's TGX (Tris/Glycine eXtended) Electrophoresis Gels were used in all experiments. Protein extracts prepared as described in the 2.2.5.1 were mixed with 1/5 volume of 6x sample buffer and heated at 95°C for 5 min prior the electrophoresis. A total of 40 µg of protein was loaded onto a 4–15% SDS-PAGE.

The electrophoresis was performed at the current of 25-30 mA for 2-3 h. Proteins separated in a SDS-polyacrylamide gel were transferred to a membrane to enable immunodetection. PVDF membranes (Immobilon P, from Millipore) were used in this work. Protein transfer was done using by semidry blotting. Prior to blotting, the membrane was immersed in methanol for 1 min, rinsed with distilled water and then equilibrated in transfer buffer for 15 min. The stacking gel was removed from the separating gel and discarded. The separating gel was also equilibrated in transfer buffer for 15 min. Then, the gel and membrane were placed between buffer-saturated blotting paper in the blotting apparatus. The PantherTM semidry electroblotter HEP-1 (PeqLab) was used in this work. Protein transfer required 2h. The membrane was stained with 1X Ponceau S solution for 5 min and destained in water for the next 2 min to visualize protein bands. Finally, Following the transfer of proteins from gel to membrane, the membrane was incubated in blocking buffer (5% nonfat dry milk [NFM] in TBS [tris-buffered saline solution] plus 0.1% Tween 20 [TBS-T]), at 4°C overnight. The membrane was washed briefly with washing buffer (TBS-T, 3 X 5 min) and incubated for 1 h with primary antibodies diluted in blocking buffer (Primary antibodies were typically diluted 1:1000 or 1:2000 in TBS-T plus 5% bovine serum albumin) Next, the membrane was washed three times with TBS-T and incubated 1h at room temperature in the

presence of HRP-conjugated secondary antibodies diluted 1:5,000 in blocking solution. The membrane was again washed three times with TBS-T and the immunoblots developed using the ECL detection kit. The band intensities were digitally quantified and phospho-proteins normalized against the total protein loaded.

2.3.7 Statistical analysis

Statistically significant differences between zeta potential values obtained before and after the click chemistry reaction, for **Epi-prop** and **BPY** were determined using a one-way ANOVA with 95% confidence limits ($p < 0.05$). The mean values were calculated from data taken from different experiments performed in triplicates on separate days using freshly prepared reagents in all cases. For fluorescence protocols, standard curves were performed using **Epi-prop** and **BPY** (0.001-0.04 mM) and analyzed using linear regression of the data and calculating the coefficient of correlation at a 95% confidence level. Statistical significance = $P \leq 0.05$. Fluorescence was determined for unknown samples by interpolation on the standard curve. The mean values were calculated from data taken from different experiments performed in triplicates on separate days using freshly prepared reagents in all cases.

CHAPTER 3

CHAPTER 3: RESULTS AND DISUSSION

3.1 Synthesis of (-)-epicatechin derivatives

Using benzyl bromide, mesyl chloride and propargyl bromide, esterification and alkylation reactions were carried out for selective modification of the **Epi** skeleton. For the synthesis of the compounds, native **Epi** was used as the starting material. Benzylation and propargylation reactions were carried out in order to protect the phenolic hydroxyl functionalities in the Epi structure before the modification of the C-3 aliphatic hydroxyl group, followed by a deprotection step (Figure 3.1).

To obtain 3-*O*-mesyl-(-)-epicatechin (**Epi-Ms)** the phenolic groups of **Epi** were benzylated according to the reaction proposed by Sharma *et al,* 2007, briefly Epi was treated with benzyl bromide and K_2CO_3 to obtain *5,7,3′,4′-tetra-O*-benzyl-(-)-epicatechin (**Epi-benzyl**) with a yield of 79%. Then we introduced a Mesylate group replacing the hydroxyl group at C-3 of the flavanal ring by treatment of **Epi-benzyl** with Mesyl chloride in the presence of triethylamine (TEA), yielding 5,7,3′,4′-tetra-O-benzyl-3-O-mesyl-(-)-epicatechin(**Epi-benzyl-Ms**). (Figure 3.2).

The propargyl derivatives were prepared via a similar Williamson ether reaction using propargyl bromide and NaH to obtain *5,7,3′,4′-tetra-O-propargyl-(-)-epicatechin* **(Epi-4-prop)** with 87% yield and *3,5,7,3′,4′-tetra-O-propargyl-(-)-epicatechin* **(Epi-5-prop)** with 81% yield.

For the synthesis of mono derivatives**, Epi-ms** and **Epi-prop,** first the phenolics groups of **Epi** were benzylated before modificate C-3 aliphatic hydroxyl group, to protect phenolic hydroxyl functionalities. The preparation of benzyl ethers from a phenol with a benzyl halide in the presence of a base is quite advantageous and multiple alternative protocols have been described in the literature [Tückmantel *et al.,* 1999; Sharma *et al*, 2007; Ranjan Banerjee *et al.,* 2014].

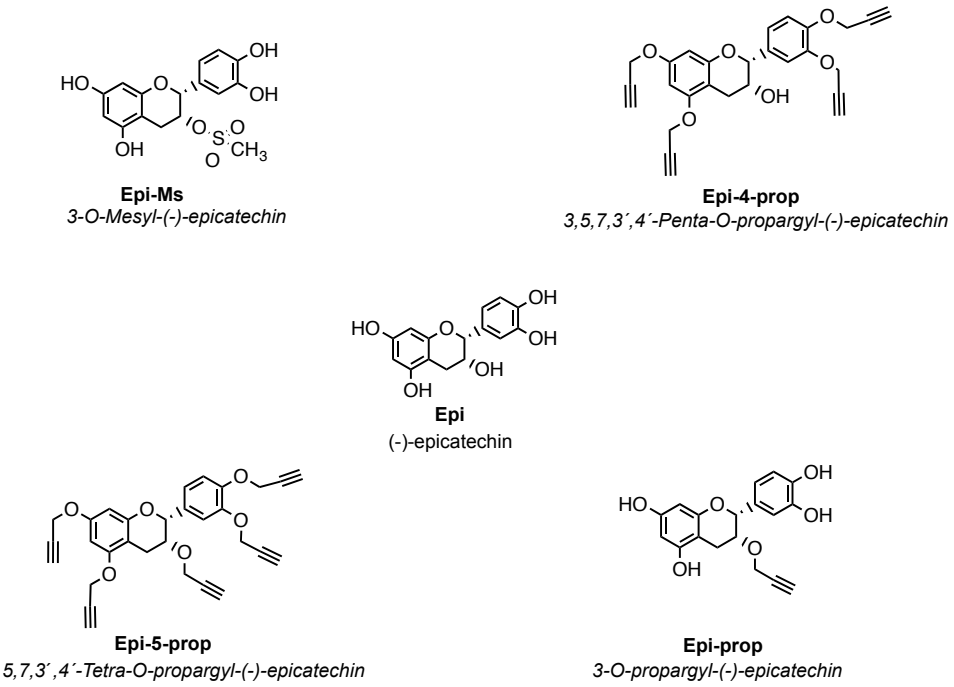

Figure 3.1. Design of Epi derivatives. Structure of the native compound Epi, intermediate derivatives Epi-5-prop and Epi-4-prop, as well as the final derivatives Epi-Ms and Epi-prop.

We carried out benzylation reactions according to the method of Sharma *et al* [2007], which was modified by using a high amount of base, to prepare **Epi-benzyl** with a high yield. Several methods for benzylation, which were attempted in our work, involved the use of various bases such as K_2CO_3, Et_3N, $NaHCO_3$, Na_2CO_3 dissolved in various solvents such as DMF, benzene, EtOAc, water, acetonitrile and EtOAc/THF at room temperature or moderate temperature (40-45°C). These experiments allowed us to increase yield however also C-benzylated compounds as major byproducts. The best conditions, which were eventually scaled up, involved the slow addition of BnBr to a suspension of **Epi** and >8 eq of K_2CO_3 in DMF at ~ 4ºC, under continuous stirring. Then the suspension was stirred at room temperature for an additional 18 to 24 h. The amount of base used in this method is higher than the amount reported by Sharma *et al*., [2007], they used 6 eq of base, while we used 8 eq of K_2CO_3, which allowed us to increase the yield

and decrease the byproducts in our protection reactions.

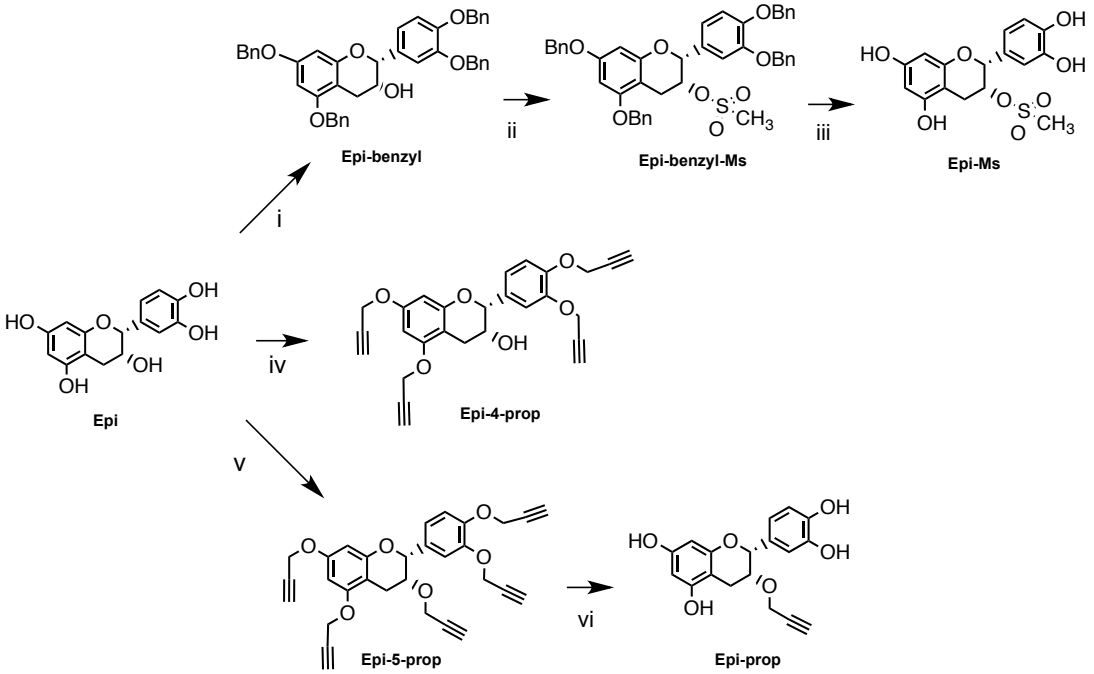

Figure 3.2. Synthesis of Epi derivatives. Reagents and conditions. (i) BnBr, K_2CO_3, DMF, 0 °C to RT 24 h; (ii) Mesyl chloride, TEA, dry CH_2Cl_2-DMF (1:1), 0 °C to RT, 24 h, under anhydrous conditions; (iii) 20% $Pd(OH)_2$-C, EtOAc-MetOH-H_2O (20:1:0.5), RT, 24 h; (iv) propargyl bromide, NaH (9 eq), DMF, 0 °C to RT, 24 h; (v) propargyl bromide, NaH (12 eq), DMF, 36 h; (vi) 20% $Pd(OH)_2$-C, EtOAc-MetOH (20:1), RT, 48 h

Once we had protected the phenolic groups, we focused on selective aliphatic C-3 transformations of **Epi-benzyl**. The stereoselective reduction at the C-3 position of catechins has been reported in the literature using L-selectride and LiBr at -78 °C in THF. In addition to the low temperature used for the reaction, the use of L-selectride and dry LiBr were identified as potential problems for our lab conditions.

Therefore, our initial efforts were focused at finding alternative reagents and conditions for the stereoselective reduction. First, we carried out an easy and selective reduction using mesyl chloride by an SN2 mechanism in anhydrous conditions (glove box). Thus, we introduced a mesylate group replacing the hydroxyl group at C-3 of the flavanal ring, by treatment of **Epi-benzyl** with mesyl

chloride to obtain **Epi-benzyl-ms**. Then, we wanted to apply our previously tested SN2 conditions reactions for the preparation of **Epi-benzyl-prop** (followed by a debenzylation step to produce **Epi-prop)** changing mesyl chloride, for propargyl bromide.

We found these conditions to be impractical as a mixture of products, and incomplete reaction products were observed. The rate of an SN2 reaction is significantly influenced by the solvent and humidity in the reaction. Moisture in SN2 reactions decreases the power of the nucleophile, because of strong hydrogen-bond interactions between “free” protons and the reactive lone pairs on the nucleophile. A less powerful nucleophile in turn means a slower SN2 reaction, which means that the reaction will proceed in anhydrous environments. Thus, SN2 conditions reactions to obtain **Epi-benzyl-prop** without a glove box proceded in low yield.

Because of the lack of practical alternatives to obtain **Epi-prop**, we decided to focus our efforts in the synthesis **Epi-4-prop** and **Epi-5-prop**. We used the Williamson ether reaction to synthetize the compounds. The Williamson ether synthesis is the most common method for the synthesis of dialkyl ethers by a SN2 type reaction between a haloalkane and an alkoxide ion. Thus, the derivatization of **Epi** was achieved by esterification of a phenol group by the Williamson ether synthesis. Using different eq of NaH in DMF we obtained **Epi-4-prop** and **Epi-5-prop** (9 eq and 12 eq, respectively) with a good yield (>80%).

Moreover, our initial synthetic plan to produce **Epi-prop** was not successful. At this point, we wondered whether the **Epi-5-prop** could yield the mono derivative **Epi-prop** by selective cleavage of the aromatic propargyl groups, leaving intact the aliphatic hydroxyl group (C-3). For this purpose, we relied on the reactions reported by Wang *et al*., They used an hydrogenation reaction with metallic palladium to promote the reductive hydrolysis of aromatic esters in an aqueous phase under mild conditions. Thus, increasing the reaction time and changing the solvent from the Wang *et al*. [2017] method, the aryl/propargyl ether bond was selectively cleaved from the **Epi-penta-prop** to give **Epi-prop** with a good yield (81%), along

with a modest amount of dipropargylated Epi (This by-product was detected by TLC, being generated by the partial depropargylation of **Epi-penta-prop**, with a moderate yield ≈19%). The alkyl/propargyl ether in C-3 was well tolerated during the course of the reaction (Figure 3.2).

We applied the same reactions conditions using **Epi-Benzyl-Ms** to obtain **Epi-Ms**. In contrast with **Epi-5-prop**, **Epi-Benzyl-Ms** was readily debenzylated to yield the corresponding phenol, **Epi-Ms**, in high yield (98%). Figure 3.2.

In chemical synthesis, esterification with aliphatic molecules (i.e. acetyl and alkyl groups) is a frequently used method to obtain flavonoid derivatives [Spencer *et al.,* 2001; Li *et al.* 2009, Moreno-Ulloa *et al.,* 2013].

It has been proposed that introducing acyl or alkyl groups to the native flavonoid skeleton, not only improves their physicochemical properties (i.e. stability) [Ishihara *et al.,* 2003], but also that novel or more potent bioactivities can be obtained [Nanjo *et al.,* 1999; Uesato *et al.,* 2003].

Alkine derivatives have been used in the past to change biological activity, an example is adenosine containing an alkyne dystal group showing antagonist activity for the adenosine-A_3 (3AR) receptor a G-protein coupled receptor (GPCR) [Tosh *et al.,* 2010]. Likewise, Sridha *et al.,* reported the synthesis of flavon propargyl derivatives showing increased selectivity and inhibitory potency on cytochrome P450 enzymes. In order to assess the potential contribution of propargyl sustitution to the Epi effects, we synthetized: **Epi-4-prop** and **Epi-5-prop** (Figure 3.1).

Moreover, since the flavonoid effects are assumed to be structure-dependent, thus one of the major contributing factors is the presence of hydroxyl groups [Vaya *et al.,* 2003; Garg *et al.,* 2001], we synthetized two types of Epi derivatives: **Epi-Ms** and **Epi-prop** which preserved four phenolic hydroxyl groups (Figure 3.1).

New methods for the protection and deprotection of functional groups are required to meet the emerging challenges in organic synthesis. Benzylation is used as the most common method to protect the phenolic functionalities of procyanidins and related molecules [Tückmantel *et al.,* 1999; Kozikowski *et al.,* 2000, Sharma *et al,* 2007]. Thus, several one-step deprotective methods have appeared, of which Pd-catalyzed deprotection was one of the most used [Tückmantel *et al.,* 1999; Kozikowski *et al.,* 2000]. Moreover, allyl and propargyl ethers are also of importance, as they are stable protective groups of alcohols [Weissman and Zewge, 2005]. The Propargyl group is attractive due to the presence of two orthogonal π-bonds, which may perhaps facilitate bond cleavage in the presence of transition metal complexes [Nandi *et al.,* 2000; Kandikere *et al.,* 2002].

However, a few examples are known in dealing with the cleavage of the C–O bond in aryl/propargyl ethers. These include the use of a low-valency titanium reagent [Ti(O-*i*-Pr)$_4$/TMSCl/Mg and Ti(O-*i*-Pr)$_4$/MgBr$_2$/Mg] [Ohkubo *et al.,* 2006], Pd(PPh$_3$)$_4$ (Pal *et al.,* 2002) or 10% Pd/C in water [Rambabu *et al.,* 2013]. Via palladium-catalyzed reactions, **Epi-Bn-Ms** and **Epi-penta-prop** were debenzylated and depropargylated to the parent alcohols via a C−O bond cleavage under mild reaction conditions.

The deprotection reactions were carried out in EtOAc-MetOH (20:1). The advantage in the use of EtOAc as solvent is its ability to solubilize the Epi derivatives which therefore facilitates the cleavage of the C-O bond. Moreover, MetOH solubilizes the deprotected Epi derivatives, a fact that facilitated their purification

The presence of H_2O and acid seemed to have a crucial role in the depropargylation reaction (the minimum amount of water and glacial acetic acid required for the successful depropargylation and debenzylation reactions was found to be EtOAc-MetOH:H_2O:glacial acetic acid [60:1:4]). Therefore further study of the influence of H_2O and acid on the rate of the reaction as well as product yield is in progress.

3.2 Biological effects of (-)-epicatechin and (-)-epicatechin derivatives

3.2.1 Molecular modeling, molecular dynamic (MD) simulations and molecular docking studies

As Protein-Ligand interactions play a key role in structure based drug design, so by using molecular docking, we screened the newly synthetized Epi derivatives and investigated their binding affinity against a G protein-coupled estrogen receptor (GPER). Molecular docking simulation was carried out using the graphic interface AutoDock Tools 4.2. The active site of the GPER used in the present molecular docking simulation is shown at 14 ns and 70ns in Fig 3.3, The interaction energy (ΔG) of **Epi-prop**, **Epi-4-prop, Epi-5-prop** and **Epi-Ms** at 14 ns was -8.05 kJ/mol, -8.68 kJ/mol, -9.2 kJ/mol and -7.74 kJ/mol respectively. Moreover the interaction energy (ΔG) of same derivatives at 70 ns was **Epi-prop=** -7-77 kJ/mol, **Epi-4-prop**=-8.27 kJ/mol, **Epi-5-prop=** -8.12 kJ/mol and **Epi-ms**=-7.27 kJ/mol. (See supplementary data Table 6.1)

MD simulations at 14 ns GPER conformer showed that interactions with **Epi** derivatives are hydrogen bonding and π-π interactions. **Epi-4-prop** (ΔG=-8.68) and **Epi-5-prop** (ΔG=-9.2) reached aminoacid residues Q138, M141, Y142, F208, Q215, E218 and E275, the same aminoacid residues as **Epi** (Moreno *et al.,* 2015)**.** Interestingly, **Epi-4-prop** and **Epi-5-prop** interact with more aminoacid residues. (See supplementary data Table 6.1)

The docking study on 14 ns GPER conformer also shows **Epi** and **Epi-Ms** (ΔG=-7.74) reached aminoacid residues L137, M141, Y142, F208; also, **Epi-Ms** interacts with A313, N316 and S317 via hydrogen bonding. **Epi-prop** (ΔG=-8.05) reach aminoacid residues H52, G58, L59, E275, F278, H282, P303, N310. Aditionally **Epi-prop** makes π-π interactions with Q53 and hydrogen bonds with Q54, G306 and V309 (Figure 6.2).

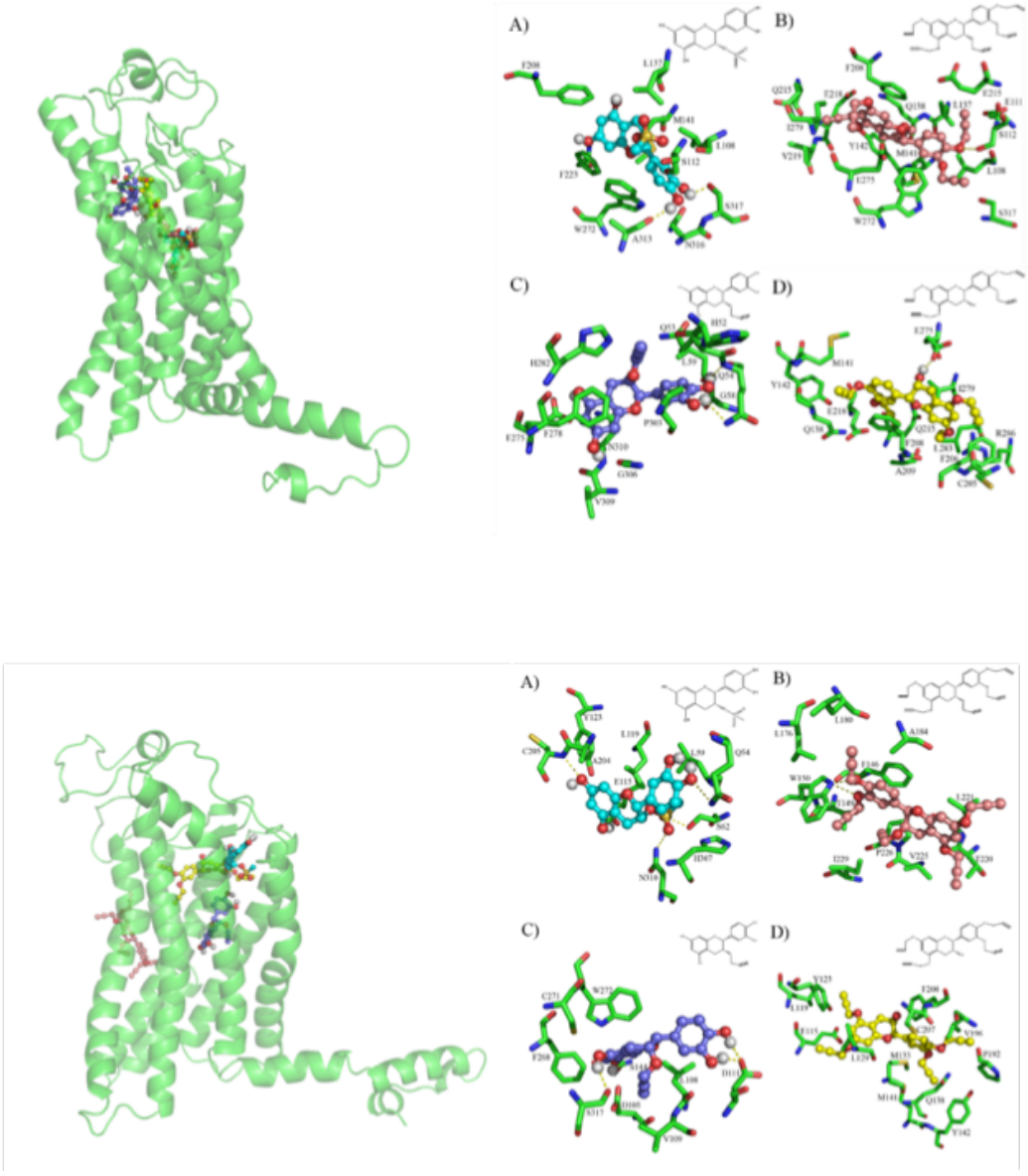

Figure 3.3 GPER 3D models with Epi derivatives at 14 and 70 ns. Upper left and right panel, GPER 3D model docked with Epi derivatives superimposed into the binding site at 14 ns with (A) Epi-Ms, (B) Epi-5-prop, (C) Epi-prop and (D) Epi-4-prop. Bottom left and right panel, GPER 3D model docked with Epi derivatives superimposed into the binding site at 70 ns. GPER 3D model docked with (A) Epi-Ms, (B) Epi-5-prop, (C) Epi-prop and (D) Epi-4-prop.

In contrast, the simulation with the 70 ns GPER conformer showed that Epi derivatives interacted with different aminoacid residues than **Epi** (Figure 3.3). **Epi-4-prop** reached aminoacid residues M133, G138, M141, V196 and F208, the same aminoacid residues as **Epi.**

Aditionally, **Epi-4-prop** establishes interactions with N118, E115, L119, Y123, L129, Y142, P192, C207. In contrast, **Epi-5-prop** interacts with T154, W150, L176, L180, A184, T220, L221, V225, P226, I229 and makes π-π interactions with F146. **Epi-Ms** reached aminoacid residues Q54, L59, S62, E115, L119, Y123, A204, H307 and hydrogen bonded with C205 and N103. Finally, **Epi-Ms** establishes interactions with Q54, L59, S62, E115, L119, Y123, A204, H307 and hydrogen bonded with C205 and N310.

In order to evaluate putative protein interactions of our previously synthetized compounds and based on *in silico* studies suggesting an energetically favorable interaction between native **Epi** and a G protein-coupled estrogen receptor (GPER) [Moreno-Ulloa *et al.,* 2015], Epi derivatives were docked into the active site of GPER using 14 and 70 ns conformers from molecular dynamics (MD) simulations. Thus, docking results at 14 and 70 ns GPER conformers suggest that the interactions between all Epi derivatives and GPER are energetically favorable.

Interactions of Epi derivatives with the 14 ns conformer are similar to **Epi**, in contrast, with the 70 ns GPER conformer results suggested diferent binding mode between Epi derivatives and **Epi** native. When using both the 14 and 70 ns conformers, **Epi-4-prop** and **Epi-5-prop** interacted with more aminoacid residues than **Epi-prop**, and even more than **Epi**. We suggest that the alkyne group, enables additional interactions with aminoacids and contributing to increase the free binding energy value of the native compound (**Epi**, ΔG=-7.9).

The docking studies with the 14 ns GPER conformer also shows **Epi** and **Epi-Ms** (ΔG=-7.74) reach similar aminoacid residues. For this analysis, the presence of the mesyl group in **Epi-Ms** contributed to establish interactions with more aminoacid residues**,** however, this does not lead to a significant change in the free energy value to the native compound.

3.3.2 eNOS activation and NO production

Once the derivatives were pre-validated *in silico*, we tested their *in vitro* efficacy using the GPER expressing bovine coronary artery endotelial cells (BCAEC). Our primary endpoint was to evaluate the capacity of derivatives to stimulate the eNOS/NO activation pathway (Figure 3.4). Cells were stimulated for 10 minutes with 1μM **Epi** (used as a positive control) or 1 μM Epi derivatives; nitrates/nitrites were measured as surrogates of NO synthesis (Figure 3.4A). For GPER blocking assays, cells were pre-incubated for 30 min with 1 μM G15, a GPER inhibitor**.**

Table 3.1. The effects of Epi and Epi derivatives. Values represent percenteges of NO production and eNOS activation (phosphorylation at Ser-1179) in endotelial cells (BCAEC) by Epi derivatives against Epi (100%). Epi, Epi-Ms, Epi-4-prop, Epi-5-prop, Epi-prop and preincubation with G15 were analysed (**).

Compound	NO production (%)	eNOSp activation (%)	NO production (%) **	eNOSp activation (%) **
Epi	100.0	100.0	60.0	55.6
Epi-Ms	54.5	64.8	41.8	53.0
Epi-5-prop	107.3	111.1	63.6	57.4
Epi-4-prop	101.8	92.6	60.0	54.8
Epi-prop	141.8	137.0	70.9	59.3

Results showed that **Epi-4-prop (**~58.6, nmol/mg prot, 111.11%), **Epi-5-prop** (~61 nmol/mg prot, 92.6%) and **Epi-prop** (80 nmol/mg prot, 137%) were able to stimulate eNOS activation compared to the positive control, **Epi** native (~54.5 nmol/mg prot, 100%). In contrast, eNOS activation in cells pre-incubated with **Epi-Ms** (~30 nmol/mg prot, 64.8%) was different to **Epi**. (Table 3.1).

All Epi derivatives and **Epi** native results were different to the control group (cntrl, untreated cells). Using the GPER inhibitor G15, results displayed that **Epi-4-prop (**~37 nmol/mg prot, 54.8%), **Epi-5-prop** (~34 nmol/mg prot, 57.4%), **Epi-prop** (~41 nmol/mg prot, 59.3%), **Epi** (~32 nmol/mg prot, 55.6%) and **Epi-Ms** (~24 nmol/mg prot, 53%) effects were decreased partially (Table 3.1).

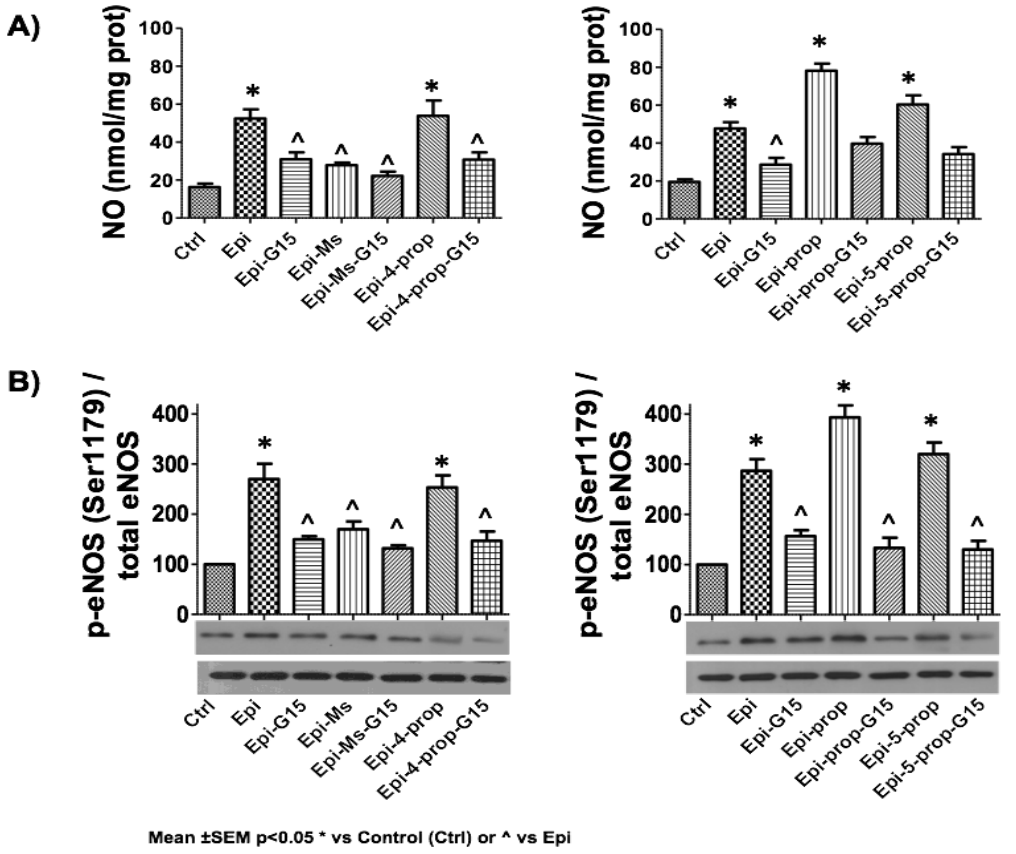

Figure 3.4. Biological effects of Epi and Epi derivatives. (A) Epi derivatives induced NO production in endotelial cells (BCAEC) and. (B) eNOS activation (phosphorylation at Ser-1179). Epi, Epi-Ms, Epi-4-prop, Epi-5-prop, Epi-prop and preincubation with G15 were analysed. Values are reported as the mean +/- SEM, p<0.05 * as compared vs control or ^ as compared vs Epi (n=5 per group).

Moreover NO production assessment showed **Epi-4-prop (**~107.3%), **Epi-5-prop** (~101.8%) and **Epi-prop** (~141.8%) were able to increase NO production compared to Epi native (100%). **Epi-Ms** (~54.5%) was different to **Epi**. (Table 3.1). All Epi derivatives and **Epi** native results were different to the control group (cntrl, untreated cells). Using the GPER inhibitor G15, results displayed that **Epi-4-prop**

(~60.0%), **Epi-5-prop** (~63.6%), **Epi-prop** (~70.9%), **Epi** (~60%) and **Epi-Ms** (~41.8%) effects were decreased partially (Table 3.1).

Results demonstrated that all derivatives were able to stimulate NO production (Figure 3.4 A left and right panels) through eNOS activation measured as Ser1179 phosphorylation (p-eNOS) (Figure 3.4 B left and right panels), meanwhile the GPER inhibitor G15 abrogated the **Epi** and Epi derivative effects (Table 3.1).

The compound **Epi-prop** induced a significant higher increased effect (i.e. NO production and eNOS activation) than **Epi-Ms**, **Epi-4-prop**, **Epi-5-prop** and **Epi**. Hydroxyl phenolic groups might be crucial for the optimal activity [Vaya *et al.,* 2003, Garg *et al.,* 2001], hence, the introduction of an alkyne group at the C-3 hydroxyl which increased hydrophobicity, in combination with free phenolic functionalities in **Epi-Prop**, likely enhanced its biological effects more than native **Epi** and all Epi derivatives.

The mesyl group provides a hydrofilic bulk group to **Epi-Ms**, we suggest that this increase in hydrophilicity affected its ability to interact with the cell membrane; therefore no significant differences in the biological effects were observed with respect to the control.

Interestingly, although **Epi-prop** also possesses a subtituent at the C-3 alcohol group, it displayed increased efficacy on the NO/eNOS activation pathway endpoints when compared to **Epi-Ms** and **Epi**. These results suggest that the modification of the C-3 alcohol group in the **Epi** molecule increases the efficacy of the flavanol to stimulate the eNOS pathway. It is also plausible, that the introduction of the hydrophilic mesylate group in the **Epi** molecule affects its ability to interact with the GPER present on the cell membrane, where it's localized [Moreno-Ulloa *et al.,* 2015]. Interestingly, **Epi-Ms** resulted with the lowest free binding energy in docking studies, suggesting a close relationship between *in silico* and *in vitro* data. In addition, all other derivatives showed higher free binding

energy values vs **Epi** that was also accompanied by a higher efficacy on the eNOS/NO activation endpoints shown by the Epi-derivatives.

In vitro and docking results indicate that GPER is capable of interacting and be activated by Epi and its derivatives. However, it´s likely that other receptors are also involved as G15 only partially inhibited eNOS activation and NO production.

3.3.3 Antioxidant activity

Elevated levels of ROS influx are implicated in abnormal endothelial activation, redox signaling, and cellular dysfunction [Birukov, 2009], and are involved in the pathogenesis of vascular disorders including inflammation and ischemia [Boueiz and Hassoun, 2009]. Flavonoids are powerful antioxidants *in vitro* by virtue of the reducing properties of their phenolic hydroxyl groups, definided by their redox potentials [Duthie *et al.,* 1997], in combination with the stability of the flavonoid aroxyl radicals [Jovanovic *et al.,* 1998]. Likewise, the cytoprotective effects of flavonoids have been attributed to their antioxidant properties either through their reducing capacities [Wang and Joseph, 1999] or through their influence on the intracellular redox status [Skaper *et al.,* 1997].

The antioxidant properties of flavonoids are structure-dependent and the major contributing factor is the presence in the B-ring. Thus, we assessed the potential contribution of several Epi derivatives to the protection of vascular endothelial cells against oxidative stress. We first assessed the potency of these compounds to protect from oxidative stress using BCAEC, subsequently, the *in vitro* radical scavenging activity and catalase levels were determined.

3.3.3.1 Cytoprotective effects of Epi and Epi derivatives (MTT assay, trypan blue exclusion method, crystal violet assay and resazurin assay)

Due to their possible shortcomings, using a single cell viability assay is associated with the risk of experimental erroneous interpretation [Putnam *et al.,*

2002], we used simultaneously several methods to assess the cytoprotective effects of **Epi** and **Epi** derivatives. The parameter of Cell viability was used for the estimation of cytoprotection displayed by the compounds. Gallic acid (Gal) and sodium ascorbate (NaLAC) were used as standards.

3.3.3.1.1 BCAEC sensitivity to H_2O_2-induced oxidative stress

To induce oxidative stress in BCAEC we have chosen H_2O_2, which is relatively stable and thus enabled us to impose a reproducible oxidative stress upon the cells. Also, H_2O_2 is a naturally occurring ROS which is constantly formed by endothelial cells through several enzymatic systems, e.g. via superoxide radicals formed by NAD(P)H oxidase (NOX) that dismutate to H_2O_2. Moreover, H_2O_2 activates a variety of redox-mediated signaling cascades by e.g. oxidation of critical thiol groups [Forman *et al.,* 2004]. In addition, H_2O_2 is able to amplify ROS production through enhanced intracellular iron uptake, and activation of radical production by mitochondria, NAD(P)H oxidase, xanthine oxidase and uncoupled eNOS [Cai, 2005; Li *et al.,* 2009]. Thus, we exposed BCAEC to H_2O_2 at 150, 200, 300, 400 and 600 mM to assess sensitivity to H_2O_2-induced oxidative stress. After incubation, the cell viability was determined using the MTT assay and the trypan blue exclusion method.

In our results, fo MTT assay, a gradual reduction in cell viability was observed. H_2O_2 at 200, 300, 400, and 600 μM significantly decreased cell viability to 55.2 ± 1.8%, 43.4 ± 1.5%, 16.3 ± 0.1%, and 7.5 ± 2.7% of the control (Ctrl, untreated cells: 100%), respectively. H_2O_2 at 150 μM decreased cell viability only to 73.1 ± 1.8% of the control (untreated cells) (Figure 3.5).

Trypan Blue dye method showed results showed that H_2O_2 at 200, 300, 400, and 600 μM significantly decreased cell viability (gradual increase in stained cells) 54.1 ± 1.8%, 43 ± 6.5%, 17.1 ± 5.9%, and 10.4 ± 5.7% of the control (Ctrl, untreated cells: 10%), respectively. H_2O_2 at 150 μM decreased cell viability to 40 ± 4.1% of the control (untreated cells).

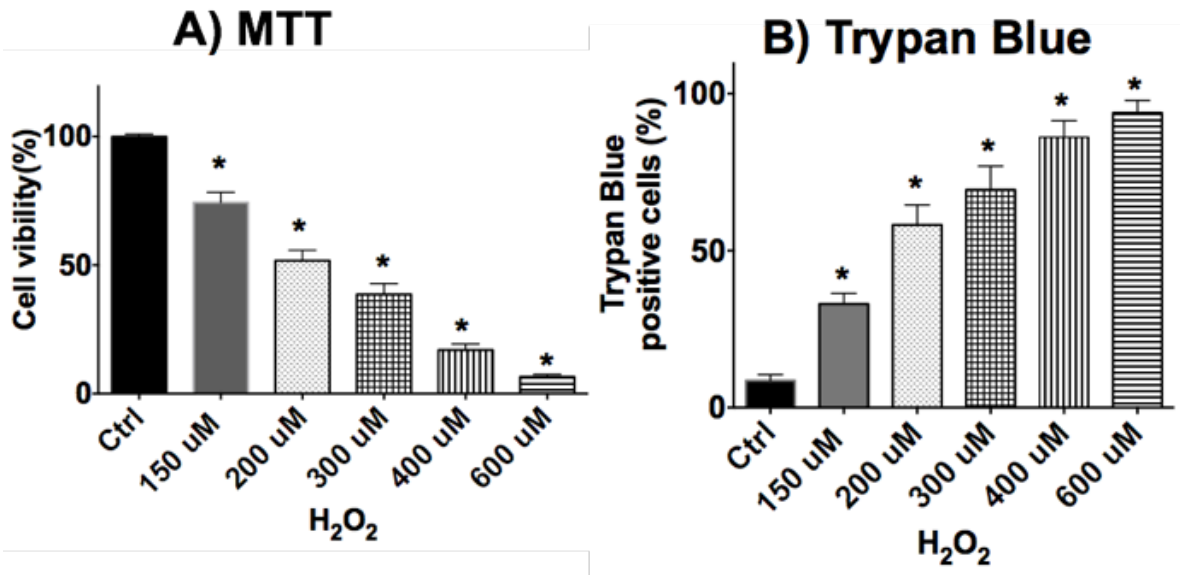

Figure 3.5. Assessment of H_2O_2-induced oxidative stress in living cells using the MTT assay and trypan blue. BCAECs were treated with H_2O_2 at 150, 200, 300, 400 and 600 uM. Cell viability was assessed using A) MTT assay and B) Trypan blue exclusion assay, and untreated cells as a control (Ctrl). The results are expressed as the mean ± SEM of three independent experiments. (*p <. 0 5 compared with Ctrl).

BCAEC were exposed to H_2O_2 at 50, 100, 150 and 200 µM. After incubation we used the *Crystal violet dye* to determine the number of viable BCAEC. As the H_2O_2 concentration increased, a gradual reduction of unstained cells was observed. H_2O_2 at 50 (92 ± 8%), and 100 (82 ± 5.8%) µM respectively, slightly decreased cell viability compared with the control (Ctrl, untreated cells). However, H_2O_2 at 150 and 200 µM significantly decreased cell viability to 57 ± 7.9% and 46 ± 3.8% of the control (untreated cells) respectively (Figure 3.6).

For *resazurin* assay, BCAEC were exposed to H_2O_2 at 50, 100, 150 and 200 µM. H_2O_2 at 50 (91 ± 3.3%), 100 (80 ± 4.6%) and 150 (76 ± 6.2%) µM only slightly to moderately decreased cell viability with respect to the control (Ctrl, untreated cells) respectively. In constrast, H_2O_2 at 200 µM significantly decreased cell viability to 55 ± 3.9% of the control (untreated cells) (Figure 3.6).

MTT is a colorimetric assay for assessing cytotoxicity and cell proliferation,

and is based on the capacity of living cells to reduce the yellow water-soluble substrate 3-(4,5-dimethylthiazol-2yl)-2,5-diphenyl tetrazolium bromide (MTT) into a dark blue/purple formazan product which is insoluble in water. The amount of formazan produced is directly proportional to the cell number in a range of cells lines [Mosmann, 1983; Gerlier and Thomasset, 1986]. Gradual reduction of cell viability was observed as the concentration of H_2O_2 increased, all concentrations of H_2O_2 showed significant difference as compared to the control group (cntrl, untreated cells), thus H_2O_2 produced a dose-dependent reduction in cell viability (Figure 3.5).

In contrast with the *MTT assay*, the *Trypan blue dye exclusión method* is based on the principle that live cells possess intact cell membranes that exclude certain dyes, such as trypan blue, whereas dead cells do not. In this test, a BCAEC suspension was simply mixed with dye and then visually examined to determine whether cells take up or exclude dye. After H_2O_2 incubation we used the dye exclusion test to determine the number of viable cells present in a BCAEC suspension. As the H_2O_2 concentration increased, a gradual reduction of stained cells was observed. All concentrations of H_2O_2 showed significant difference as compared to the control group (cntrl, untreated cells) as displayed in Figure 3.5.

The trypan blue results were similar to those from the MTT assay (Figure 3.5). Trypan Blue staining cannot be used to distinguish between the healthy cells and the cells that are alive but losing cell functions. This method also does not measure lysed cells. Moreover, adherent cells may perform less well in this method, as they first have to be physically or enzymatically removed from the growth surface. Thus, the most common method used with adherent cells has been the crystal violet assay [Sanford *et al.,* 1951].

Likewise, the MTT assay is also significantly influenced by compounds that modify cell metabolism by increasing the NADPH levels or the activity of LDH *(lactate dehydrogenase)* [Vistica *et al.,* 1991; Bruggisser *et al.,* 2002]. Maioli *et al.* [2009], showed that rottlerin, which uncouples the mitochondrial respiratory chain,

may enhance the production of formazan crystals, leading to false negative results in cell viability assays. Furthermore, the MTT tetrazolium salt may be reduced not only in the mitochondria but also within the cytoplasm, on the surface of cell, in the endosome or lysosome membranes, or even in the extracellular environment [Vistica *et al.,* 1991; Berridge *et al.,* 2005].

The Crystal violet assay lacks the limitations undermining the accuracy of the MTT and trypan blue assays, and other assays based on enzymatic reactions. The assay is based on the affinity between the dye and the external surface of the DNA double helix. The amount of dye absorbed depends on the total DNA content in the culture and permits the estimation of the number of viable cells in the culture [Saotome *et al.,* 1989; Chiba *et al.,* 1998].

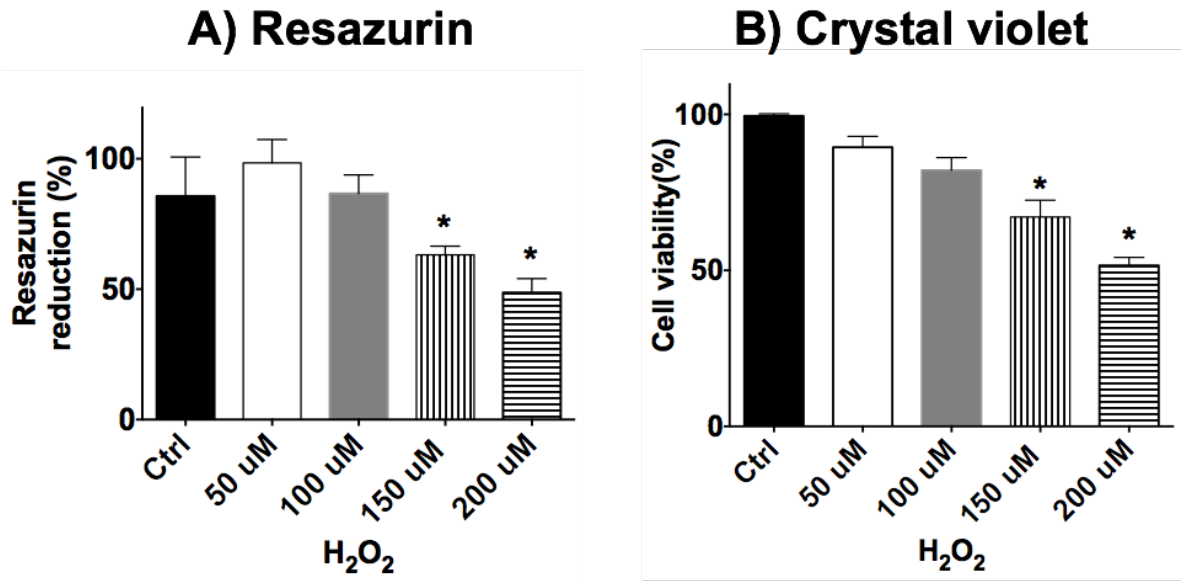

Figure 3.6 Assessment of H_2O_2-induced oxidative stress in living cells using the resazurin assay and the crystal violet assay. BCAECs were treated with H_2O_2 at 50, 100, 150 and 200 µM. Cell viability was assessed using A) resazurin assay and B) crystal violet exclusion assay, and untreated cells as a control (Ctrl). The results are expressed as the mean ± SEM of three independent experiments. (*$p < 0.05$ as compared with the Ctrl).

Thus, we used the crystal violet assay and the resazurin assay to determine the BCAEC sensitivity to H_2O_2-induced oxidative stress. Resazurin is a cell permeable redox indicator that can be used to monitor viable cell number with

protocols similar to those utilizing the tetrazolium compounds; however, the resazurin reduction assay is slightly more sensitive than the tetrazolium reduction assays [Shum *et al.,* 2008]. The *Resazurin assay* is based on the ability of viable, metabolically active cells to reduce resazurin to resorufin and dihydroresorufin. This conversion occurs intracellularly [O'Brien *et al.,* 2000], where the oxidized form of resazurin enters the cytosol first, and then is converted to the reduced form by mitochondrial enzyme activities that accept electrons from NADPH, FADH, FMNH, NADH as well as from numerous cytochromes [Al-Nasiry *et al.,* 2007]. The reduction related to growth causes the resazurin to be converted from the oxidized (or non-fluorescent) blue form, to the reduced (fluorescent) red form. Thus, we used lower H_2O_2 concentrations for the assays than previuos results using *MTT* and *trypan blue*.

Table 3.2. BCAEC viability measurements by several methods. After 2 hours of treatment with 200 μM H_2O_2, cell viability dropped to 50 ± 6.3% of the controls, as measured by the four methods. Differences between the results were not significant.

Method	% Cell viability, H_2O_2 at 200 μM
MTT assay	55.2 ± 1.8
Trypan blue	54.1 ± 1.8
Crystal violet	46 ± 3.8
Resazurin	55 ± 3.9

BCAEC were exposed to H_2O_2 at 50, 100, 150 and 200 μM. After incubation we used the *Crystal violet dye* and *resazurin* to determine the number of viable BCAEC. For *Crystal violet dye* H_2O_2 at 50 (92 ± 8%), and 100 (82 ± 5.8%) μM respectively, slightly decreased cell viability compared with the control (Ctrl, untreated cells). However, H_2O_2 at 150 and 200 μM significantly decreased cell viability to 57 ± 7.9% and 46 ± 3.8% of the control (untreated cells) respectively.

These results showed that H_2O_2 produced a dose-dependent reduction in cell viability. For *resazurin* assay, H_2O_2 at 50 (91 ± 3.3%), 100 (80 ± 4.6%) and 150 (76 ± 6.2%) μM only slightly to moderately decreased cell viability with respect to the control (Ctrl, untreated cells) respectively. In constrast, H_2O_2 at 200 μM significantly decreased cell viability to 55 ± 3.9% of the control (untreated cells).

Resazurin yielded higher values of cell viability than the crystal violet assay, especially at a concentration of 150 μM, however the differences between the results obtained using the *crystal violet assay* and *resazurin dye* were not significant.

In summary we noticed that after 2 hours of treatment with 200 μM of H_2O_2, cell viability dropped to 50 ± 6.3% of the controls, as measured by the four methods (*MTT*, *trypan blue assay*, *crystal violet assay* and *resazurin* dye). Differences between the results were not significant (Table 3.2). Thus, H_2O_2 was used in further experiments at a concentration of 200 μM since this induces ≈ 50 % cytotoxicity.

3.3.3.1.2 Antioxidant assesment of Epi and Epi derivatives

Once the optimal concentration of H_2O_2 was determined, BCAECs were exposed to 200 μM H_2O_2, after pretreatment with 1 μM of **Epi** or Epi derivatives, and Gal and NaLAC as standards for 24 h. After incubation, cell viability was determined using the MTT assay, crystal violet assay and the resazurin method. Cell viability was used to estimate cytoprotection by **Epi** and Epi derivatives.

In the first analysis, we examined whether any discrepancy exists between each Epi derivative with respect to **Epi** native, the control group (cntrl, untreated cells), H_2O_2 (cells only treated with H_2O_2), galic acid (Gal) and ascorbic acid (NaLAC), a one-factor analysis of variance (ANOVA) was conduted for each of group, with a confidence level of 95%. The significance level was set at $p < 0.05$. All data were expressed as the mean ± standard error of the mean (SEM). The

mean values were calculated from data taken from different experiments performed in triplicates on separate days using freshly prepared reagents in all cases.

In our results for the MTT assay, Gal (90 ± 0.7% $p < 0.0001$), NaLAC (96 ± 8.5%, $p < 0.0001$) **Epi (**88 ± 2.8%, $p < 0.0001$), **Epi-Ms (**77 ± 1.5%, p 0.0002) and **Epi-prop** (64 ± 4.2%, p 0.496) respectively, significantly increased cell viability in the H_2O_2 group. **Epi-4-prop** (51 ± 3.7%, p 0.9995) and **Epi-5-prop** (50 ± 2.4%, p 0.9987) had no significant difference with H_2O_2 (46 ± 6.4%) as shown in **Figure 2.6.** Moreover, **Epi-prop** (59 ± 4.2%, $p < 0.0001$), **Epi-4-prop** (40 ± 4.4%, $p < 0.0001$) and **Epi-5-prop** (49 ± 3.6%, $p < 0.0001$), **Epi (**81 ± 4.1%, p 0.0138), **Epi-Ms (**72 ± 3.9%, p 0.0116) and Gal (89 ± 3.5%, p 0.0496) respectively, showed significant differences as compared to the control group (cntrl, untreated cells, 100%). In contrast, the results with NaLAC (95 ± 1.6%, p 0.9460), showed no significant difference with the control group (cntrl).

Moreover, the results with the *Crystal violet dye* showed that Gal, NaLAC, **Epi** and **Epi-Ms** significantly increased cell viability to 89 ± 3.5% ($p < 0.0001$), 95 ± 1.6% (p 0.0012), 81 ± 4.1% ($p < 0.0001$), 72 ± 3.9% ($p < 0.0001$) respectively, of the H_2O_2 group. **Epi-prop** (59 ± 4.2%, p 0.884), **Epi-4-prop** (40 ± 4.4%, p 0.558) and **Epi-5-prop** (49 ± 3.6%, p 0.5035) showed no significant differences with H_2O_2 (55 ± 4.2%), as shown in **Figure 2.6.** With this assay **Epi-prop** (59 ± 4.2%, $p < 0.0001$), **Epi-4-prop** (40 ± 4.4%, $p < 0.0001$) and **Epi-5-prop** (49 ± 3.6%, $p < 0.0001$), **Epi (**81 ± 4.1%, p 0.0026), **Epi-Ms (**72 ± 3.9%, p 0.0001) and Gal (89 ± 3.5%, p 0.0106) showed significant differences when compared to the control group (cntrl, untreated cells, 100%). In contrast, the results with NaLAC (95 ± 1.6%, p 0.1211) showed no significant difference with the control group (cntrl).

In the *resazurin* assay, BCAEC were exposed to H_2O_2, after pretreatment with **Epi** (81 ± 6.5%, p 0.02), **Epi-Ms** (63 ± 3.1%, $p < 0.0001$), **Epi-4-prop** (55 ± 5.8%, $p < 0.0001$), **Epi-5-prop** (54 ± 7.9%, $p < 0.0001$) and **Epi-prop** (59 ± 1.9%, $p < 0.0001$), the results were significantly different with respect to the cntrl group

(100%). In contrast, Gal (93 ± 6.4%, *p* 0.4633), and NaLAC (86 ± 3.4%, *p* 0.0704), showed no significant difference with the cntrl group, as shown in **Figure 2.5**.
In the *resazurin assay,* **Epi** (81 ± 6.5%, $p < 0.0001$), **Epi-Ms** (63 ± 3.1%, $p < 0.0003$), **Epi-prop** (59 ± 1.9%, *p* 0.0322), Gal (93 ± 6.4%, $p < 0.0001$), and NaLAC (86 ± 3.4%, $p < 0.0001$) showed significant differences with the H_2O_2 group (47%). In contrast, **Epi-4-prop** (55 ± 5.8%, *p* 0.3365), **Epi-5-prop** (54 ± 7.9%, *p* 0.2266), showed no significant differences with respect to the H_2O_2 group.

In the three experiments that we carried out, pre-treatment with Epi, Epi-Ms, Gal and NaLAC at 1μM significantly increased cell viability in H_2O_2-treated cells as compared with H_2O_2 group. However, pre-treatment with Epi-5-prop, Epi-4-prop and Epi-prop, showed no increase in cell viability as compared with the H_2O_2-treated cells (Figure 3.7). The *Crystal violet* dye assay yielded slightly lower values of cell viability than the *MTT assay* and the *resazurin dye* assay; however, the differences found in the results between the three methods were not significant.

Likewise, we performed a second analysis to examine whether any discrepancy exists among the Epi compounds, when we categorize them by their chemical structure. Compounds were grouped as follows: Epi-prop derivatives (Epi-prop deriv) which comprised **Epi-prop**, **Epi-4-prop** and **Epi-5**; the standard group (std) which comprised galic acid (Gal) and ascorbic acid (NaLAC); and the **Epi** group which comprised **Epi** and **Epi-Ms**, which were compared with two diferents groups: the control group (cntrl, untreated cells) and the H_2O_2 (cells only treated with H_2O_2).

With the *MTT assay,* the results showed that the Epi group (*p* 0.0082), the Epi-Ms group (*p* 0.0002) and the Epi-prop deriv group ($p < 0.0001$), had significant differences with respect to the cntrl group. The Std group (*p* 0.28) had no significant differences with the cntrl group. We also compared the previous groups with the H_2O_2 group, and the results showed again that the Epi group ($p < 0.0001$), the Epi-Ms group (*p* 0.0001), and the Std group ($p < 0.0001$) had significant

differences with respect to the H_2O_2 group, in contrast, the Epi-prop deriv group (*p* 0.367) showed no significant difference.

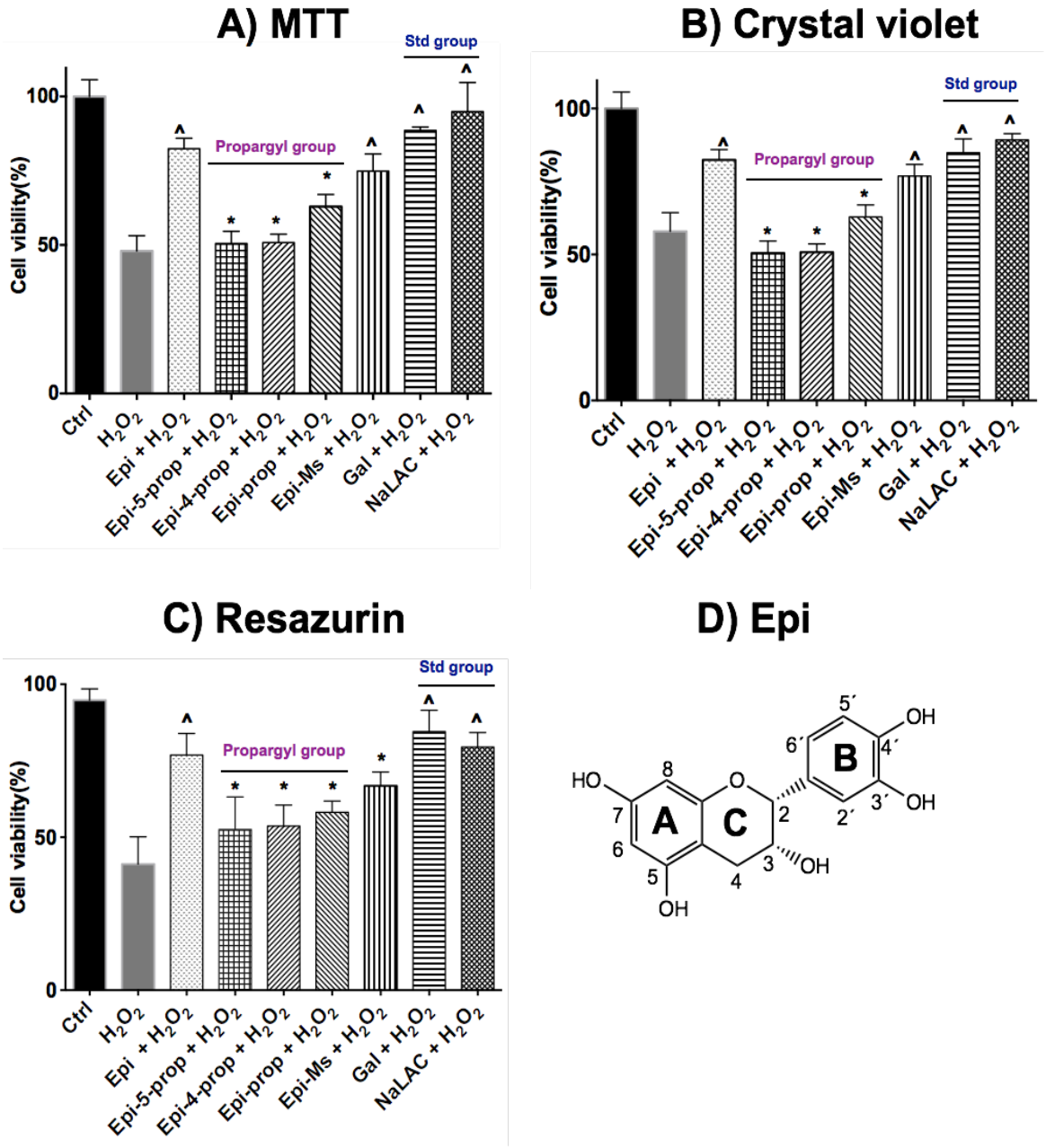

Figure 3.7 Cytoprotective effects of Epi and Epi derivatives. BCAECs were pre-treated with 1μM of the compounds for 24 h, before the addition of H_2O_2 (200 μM). Cellular damage was assessed by the A) MTT assay, B) trypan blue method and C) Resazurin method. Gallic acid (Gal) and sodium ascorbate (NaLAC) were used as standards. Data are means of three separate experiments, each performed in triplicate. $p<0.05$ as compared vs ^ control or * as compared vs H_2O_2 treated cells. D) Structure of Epi.

Likewise, with the *crystal violet assay* the results showed that the Epi group (*p* 0.0011), the Epi-Ms group (*p* < 0.0001), the Std group (p 0.0488) and the Epi-prop deriv group (p < 0.0001), had significant differences when compared to the cntrl group. Then, we compared the previous groups with the H_2O_2 group, the results showed that the Epi group (*p* 0.0001), the Epi-Ms group (*p* 0.0049), and the Std group (*p* < 0.0001), had significant differences as compared to the H_2O_2 group, in contrast, the results for the Epi-prop deriv group (*p* 0.295) showed no significant differences.

Finally, with the *resazurin* assay, the results of the analysis showed that the Epi group (*p* 0.001), the Epi-Ms group (*p* 0.0004), the Std group (*p* 0.0288), and the Epi-prop deriv group (*p* < 0.0001), had significant differences as compared to the cntrl group. We also compared the previous groups with the H_2O_2 group, the results indicated that the Epi group (*p* < 0.0001), the Epi-Ms group (*p* 0.0002), the Epi-prop deriv group (*p* 0.0399), and the Std group (*p* < 0.0001), had significant differences when compared to the H_2O_2 group.

In the three experiments we carried out, pre-treatment with compounds of the Epi group, the Epi-Ms group and the Std group, significantly increased cell viability in the H_2O_2-treated cells as compared with H_2O_2 group. However, pre-treatment with compounds in the Epi-prop deriv group, did not increased cell viability as compared with H_2O_2-treated cells.

Since in the *resazurin dye* method and in the *MTT* method, these compunds are converted to the reduced form by mitochondrial enzyme activities that accept electrons from NADPH, FADH, FMNH, NADH, as well as from numerous cytochromes [Al-Nasiry *et al.,* 2007] (the MTT tetrazolium salt may also be reduced within the cytoplasm, on the cell surface, in endosome or lysosome membranes, or even in the extracellular environment) [Vistica *et al.,* 1991; Berridge *et al.,* 2005], we used these methods for measuring mitochondrial activity. In the

first analysis, the results showed that **Epi** and **Epi-Ms** are able to decrease oxidative damage induced by H_2O_2, and such activity appears to be mediated by a protective effect on mitochondria. Interestingly, we noticed that propragyl derivatives (**Epi-prop**, **Epi-4-prop** and **Epi-5-prop)** displayed lower antioxidant activity than **Epi** and **Epi-Ms**. We hypothesize that the protection against oxidative stress might be decreased by the presence of the propargyl group in the **Epi** skeleton. Based upon the previous results; we performed a second statistical analysis to study the impact of the propargyl group in the antioxidant activity of **Epi**.

Our results showed that the group of the propargyl derivatives (Epi-prop deriv) had lower antioxidant activity when compared with the Epi group, the Epi-Ms and the Std group. The highest antioxidant activity was displayed by the Std group, followed by the Epi group and the Epi-Ms group.

In summary, our results strongly suggest that **Epi** protects BCAEC from oxidative damage (induced by H_2O_2) by helping cells to maintain their mitochondrial functions. The presence of the mesyl group in the **Epi** structure, only slightly decreased **Epi** activity; however differences between **Epi** and **Epi-ms** were not significant. Thus, the mesyl substitution has no significant effect on **Epi** antioxidant activity, conversely, the mono, tetra or penta propargyl substitution, had a significant effect, suggesting that the presence of the propargyl group decreases the antioxidant activity of Epi**.** Therefore, further studies on the influence of the propargyl substitution in Epi native as well as the structure-activity relationships, are necessary.

3.3.2 The TEAC-ABTS assay

Once the derivatives were assessed in cell assays, we tested their scavenging ability on the $ABTS^{\bullet+}$ radical cation, with the aim to further understand their structure-activity relationship. The TEAC-ABTS assay is used to assess the ability of an antioxidant to scavenge the $ABTS^{\bullet+}$ radical cation. Potassium

persulphate at pH 7.4, were used to generate the $ABTS^{\bullet+}$ radical cation. The activities of the samples were compared to that of Trolox, a water-soluble vitamin E analog.

The radical scavenging actitvity of **Epi-Ms** was lower than **Epi** native, but higher than **Epi-5-prop** (0.90), **Epi-4-prop** (0.82) and **Epi-prop** (0.981). The highest scavenging activity was shown by the standard compounds, Gal and NaLAC, 6.60 and 4.7, respectively **(**Table 3.3).

The mechanism by which phenolic compounds are able to scavenge free radicals is yet to be exactly established. In any case, it's clear that the basic structure of the compounds and other structural features are very important in the scavenging mechanism [Choi *et al.,* 2002; Sadeghipour *et al.,* 2005]. As reported by Heijne *et al.* [2002] the aromatic OH groups are the reactive centers, primarily the 3′,4′-dihydroxy catechol group, and their activity can be enhanced by the electron donating effects of other substituents.

In regards to the antioxidant activity of **Epi**, it has been suggested that the A ring does not function as an advantageous structure for radical scavenging, and so, the presence of hydroxyl groups in the B ring is the important structural feature for its radical scavenging ability [Heim *et al.,* 2002] (Figure 3.8).

Therefore, the decreased scavenging activity of **Epi-4-prop** and **Epi-5-prop** can be explained by the propargyl substitution at the hydroxyl groups, mainly of the catechol moiety, thus reducing the scavenging activity of the derivatives. The scavenging effects of **Epi-prop** were reduced drastically by the specific propragylation at C3-OH whereas there was hardly any decrease in effectiveness with the specific modification at C3-OH using a mesyl (Methylsulfonyl) group (Table 3.3).

There has been much discussion in the literature on the role of the C3-OH group. Whereas most authors agree on the importance of this substituent, especially in compounds with a C2-C3 double bond, derivatization of this group

was described to be masking the antioxidant activity, or having no effect.

Nanjo *et al.,* [1996] reported that the galloyl moiety attached to flavan-3-ols at C3-OH has a strong scavenging ability on the DPPH radical, and that specific acylation of same position causes no significant changes in their scavenging activities. In contrast, Burda and Oleszek [2001] compared the antioxidant activity of flavonol glycosides and methyl derivatives, and showed that the blockage of the C3-OH resulted in a total loss of antioxidant activity, suggesting that the C3-OH was responsible for the high inhibition of *β*-carotene oxidation, since glycosylation or methylation of other flavonol hydroxyls did not produce such effect.

Table 3.3. Antioxidant acitvity of Epi, Epi derivatives, galic acid (Gal) and sodium ascorbate (NaLAC), expressed as Trolox equivalents.

Compound	TEAC Trolox equivalent antioxidant capacity (μM)
Epi	4.019
Epi-5-prop	0.909
Epi-4-prop	0.820
Epi-prop	0.981
Epi-Ms	3.179
Gal	6.6
NaLAC	4.792

Conversely, according to kinetic studies of flavonoids, one of the structural requirements for high antioxidant activity of a flavonoid is the presence of both C3- and C5-OH groups, which enable the formation of stable quinonic structures upon flavonoid oxidation [Firuzi *et al.,* 2005]. Performing substitutions at the C3-OH results in an increased tortion angle and loss of coplanarity, which subsequently

reduces the antioxidant activity [Seeram and Nair, 2002].

Thus, the chemical properties of the derivatization compounds may either improve or decrease its antioxidant activity. Whereas aryl sustitutions increase scavenging ability, the presence of alkyne or alkyl group might decrease such effect.

Therefore, the decreased scavenging activity of **Epi-prop** and **Epi-mesyl** can be explained by the substitution at C3. However **Epi-Ms** antioxidant effects were slightly decreased. *In vitro* studies seem to suggest that the methylsulfonyl group reduces oxidative stress and inflammation by a mechanism that appears to involve supression of mitochondrial generation of superoxide, hydrogen peroxide, and hypochlorous acid [Beilke *et al.,*1987]. Thus, we attribute the **Epi-Ms** effects to its methylsulfonyl group instead of free phenols.

The TEAC values Epi alkyne derivatives (relative to Trolox) were lower than **Epi**, indicating that the H-donating ability is greatly reduced on derivatization of the hydroxyl groups. Thus, Epi native has a more effective scavenging activity than Epi derivatives (Table 3.3).

3.3.3 Antioxidant activity assessment of Epi and Epi derivatives by electrochemical methods.

To examine results obtained from TEAC-ABTS assay on the structure-activity relationship of Epi. We performed a second analys by electrochemical approach. Thus cyclic voltametries and differential pulse vltametries were carry out. Cyclic voltammetry analysis of **Epi** showed at pH 7.4, two oxidation peaks associated with oxidation of cathecol +0.015 V, confirmed in the second scan by inverting the potential scan just before peak 2, and an irreversible peak 2 at +0.46 V to the oxidation of the C ring. For **Ep-Ms** cyclic voltammograms showed one wide peak around +0.15 V which corresponds to oxidation of cathecol. Cyclic voltammograms of **Epi-5-prop** and **Epi-4-prop** peaks were not observed in this study (Figure 3.8). The potential range of **Epi-prop** was +0.05 to +0.5 V. In

contrast, the tested oxidation potentials of **Epi** and **Epi-Ms** spanned in a wide potential range of more than +0.9 V.

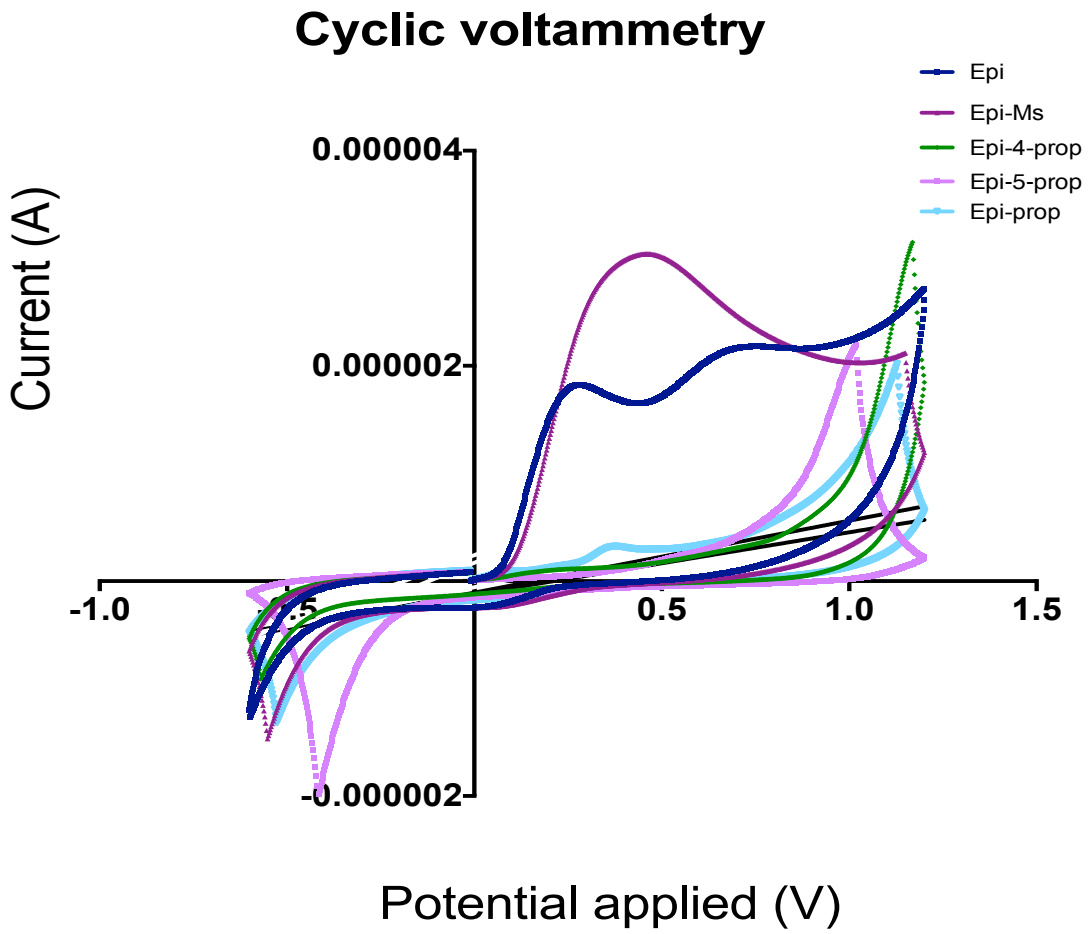

Figure 3.8. Cyclic voltammograms of Epi and Epi derivatives. Cyclic voltammograms of 1mM Epi and Epi derivatives in PBS (1X, pH 7.4). The scan rate is 50 mV/s.

We also performed differential pulse voltammetry of **Epi**, **Epi-prop** and **Epi-Ms**, using Gal and NaLAC as controls, at pH 7.4. As shown in **Figure 3.9, Epi** had the lowest oxidation potential (*E*) at +0.01 V. For NaLAC +0.10 V and **Epi-Ms** +0.11 V, there was a slight differrence in the oxidation potential. **Epi-prop** displayed the highest oxidation potential at +0.35 V followed by Gal at +0.18 V (Figure 3.9).

The oxidation of flavonoids is of great interest because of their action as

antioxidants with the ability to scavenge radicals generated by electron transfer processes. Spectrophotometric methods are mainly used in the analysis of antioxidant properties. However, these methods are dependent on many parameters, such as temperature, time of the analysis, character of a compound or mixture of compounds (extracts), concentration of antioxidants and pro-oxidants and many other substances [Rop *et al.,* 2010; Sochor *et al.,* 2010; Pohnka *et al.,* 2012].

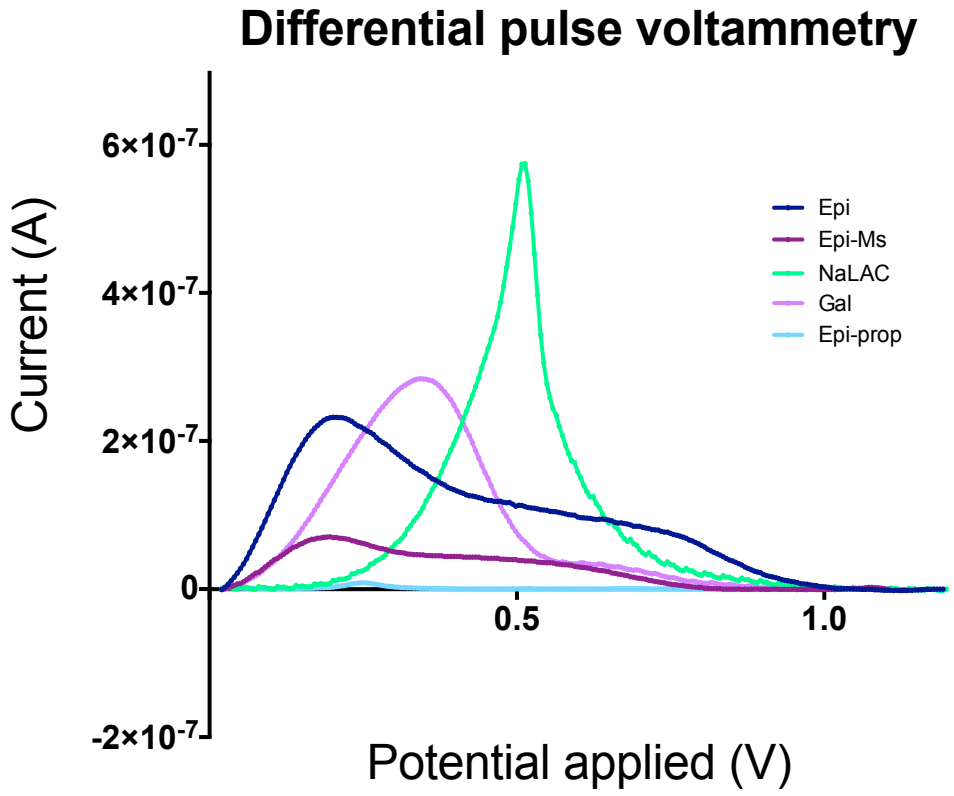

Figure 3.9. Differential pulse voltammograms of 1mM Epi, Epi-Ms, Epi-prop, Gal and NaLAC. 1X PBS (pH 7.4) was used as the supporting electrolyte at the scan rate of 5 mV/s.

Electrochemical methods used for the determination of antioxidant capacity are still in development. Voltammetry methods are the most commonly used techniques for the characterization of redox systems. They can provide information about the number of redox states as well as qualitative information about the

stability of these oxidation states and the electron transfer kinetics [Jelen *et al.,* 2009; Wang, 2000].

Table 3.4 Measurements of the oxidation potential (*E*) by voltammetric methods. Oxidation potential of Epi, Epi derivatives, Gal and NaLAC by Cyclic voltammetry and Differential pulse voltammetry at pH 7.4, room temperarure, E (V/Ag/AgCl). * peaks were not observed. (…) Not assessed.

Compound	Cyclic voltammetry E_{pa} (V)	Differential pulse voltammetry E_{pa} (V)
Epi	+0.015	+0.01
Epi-5-prop	*	(…)
Epi-4-prop	*	(…)
Epi-prop	+0.41	+0.35
Epi-Ms	+0.15	+0.15
Gal	(...)	+0.18
NaLAC	(…)	+0.10

Voltammetry involves scanning the voltage of a working electrode while recording the anodic current produced by the low molecular mass antioxidants in the solution, which are oxidized on the surface of the working electrode [Hynek *et al.,* 2012]. The current generated is proportional to the combined concentration of the antioxidants [Kilmartin *et al.,* 2012; Mittal *et al.,* 2010]. Antioxidant compounds can act as reduction agents and, in solution, they tend to be easily oxidized on the inert electrodes. Based on this fact, the relationship between electrochemical behavior of compounds with antioxidant activity and their resulting “antioxidant power” (capacity) is very interesting, because a “low oxidation potential” corresponds to a “high antioxidant power”. Thus, we investigated the electrochemical oxidation of the flavonoid **Epi** and its derivatives. In voltammetric

methods the measured oxidation potential (*E*) is inversely proportional to the free radical scavenging capability of the investigated compounds. Results showed appreciable diferences in the *E* value of the **Epi** and Epi derivatives. The *E* values were found to depend greatly on the structures, as shown in Table 3.4.

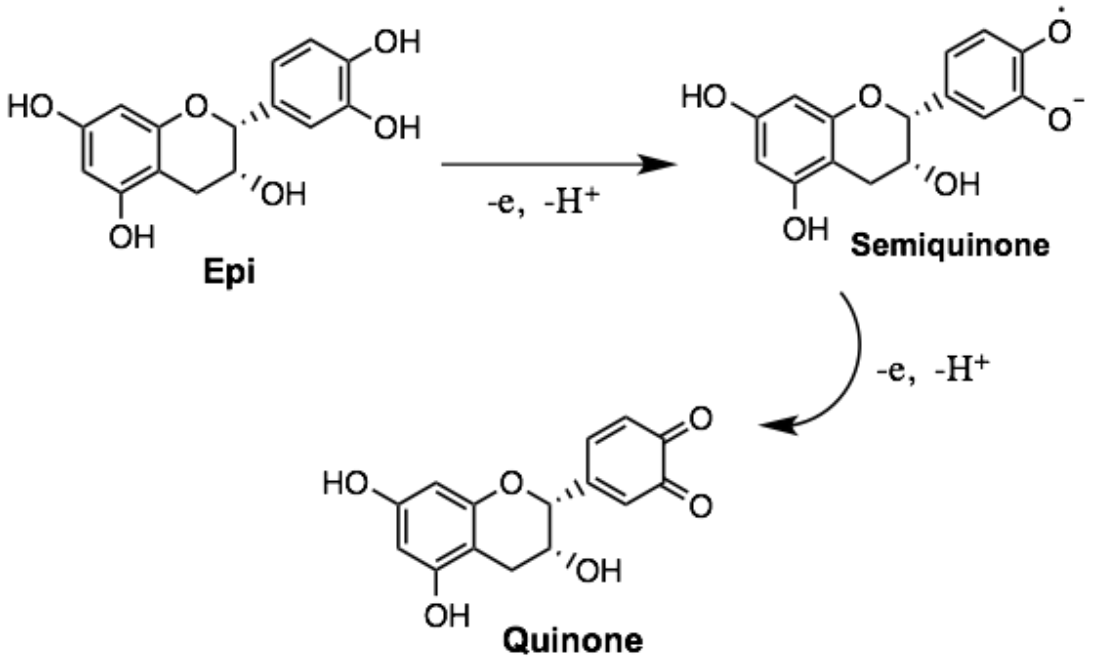

Figure 3.10**.** Mechanism of oxidation of Epi. [Janeiro and Oliveira-Brett, 2004].

The catechol-containing flavonoid structures are powerful well known H-donating antioxidants (Figure 3.10). Thus **Epi** and **Epi-Ms**, which reserved free ring B, displayed low values of *E*. Interestingly **Epi-prop** whose OH groups in B ring were free, displayed high *E* value than **Epi** and **Epi-Ms**. **Epi-prop** results were consistent with Bors *et al.,* who suggested that the C3-OH determines the fate of the flavonoid aroxyl radical. A lack of the C3-OH influences electron de-localization in **Epi**, which might result in a decrease of its antioxidant activity as observed in **Epi-prop**. Moroever, **Epi-Ms** lacked the C3-OH and showed a lower *E* value than **Epi-prop**. These results may be attributed to the presence of the methylsulfonyl (Mesyl) group that might increase the aroxyl radical stability contributing to decrease of the *E* value. Propargylation of the B ring and A ring, as in **Epi-4-prop** and **Epi-5 prop**, greatly increases the *E* value*,* thus derivatization of the B and A ring decrease antioxidant capacity of **Epi**.

The low oxidation potentials of **Epi** and **Epi-Ms** are an indication of their high antioxidant capacity, and the high oxidation potential of the propargyl derivatives describes their low antioxidant capacity. **Epi** showed the lowest *E* value, and therefore the highest antioxidant activity. These results were consistent with our previous results for the TEAC-ABTS and Cell assays. The TEAC assay gave the same relative order of antioxidant capacities of investigated compounds as shown by cyclic voltammetry, the lower half-wave potential value *E* of the first oxidation wave, also points to the higher antioxidant capacity, in which **Epi** had the highest activity followed by **Epi-Ms**, and propargyl derivatives.

2.3.4 Catalase activity

Catalase activity was determined spectrophotometrically according to Aebi, [1970]. BCAEC were pre-incubated during 48 h with **Epi** and Epi derivatives before treatment with 200 μM H_2O_2. We used Gal and NaLAC as controls. Results showed catalase acitvity of **Epi (**~0.27 nmol/min/mg prot) and **Epi-Ms** (~0.25 nmol/min/mg prot) was increased compared to the H_2O_2 group (~0.15 nmol/min/mg prot) similar to the control group (~0.24 nmol/min/mg prot). In contrast, catalase activity in cells pre-incubated with **Epi-5-prop** (~0.16 nmol/min/mg prot), **Epi-4-prop** (~0.15 nmol/min/mg prot), **Epi-prop** (~0.18 nmol/min/mg prot), Gal (~0.16 nmol/min/mg prot) and NaLAC (~0.18 nmol/min/mg prot) was diferent to the control group. (Figure 3.11).

The vascular endothelium constitutes a primary target for oxidants released during inflammatory events [Birukok, 2009]. ROS produced by activated leukocytes and endothelial cells have been implicated in endothelial contraction and loss of barrier integrity. The susceptibility of a tissue to oxidative injuries depends mainly on their antioxidant defense mechanisms. Lack of antioxidant enzymes makes a tissue more susceptible to oxidative damages. The antioxidant enzyme activity of cells is determined by inherent characteristics of the cells, their metabolic specialization, and environmental factors to which the cells are exposed such as

the level of oxygenation and the presence of metabolites [Marklund *et al.,* 1982]. Superoxide dismutase, catalase, and glutathione peroxidase (Figure 3.12) are considered to be the most important enzymes in protecting oxidatively challenged tissues [Marklund *et al.,* 1982].

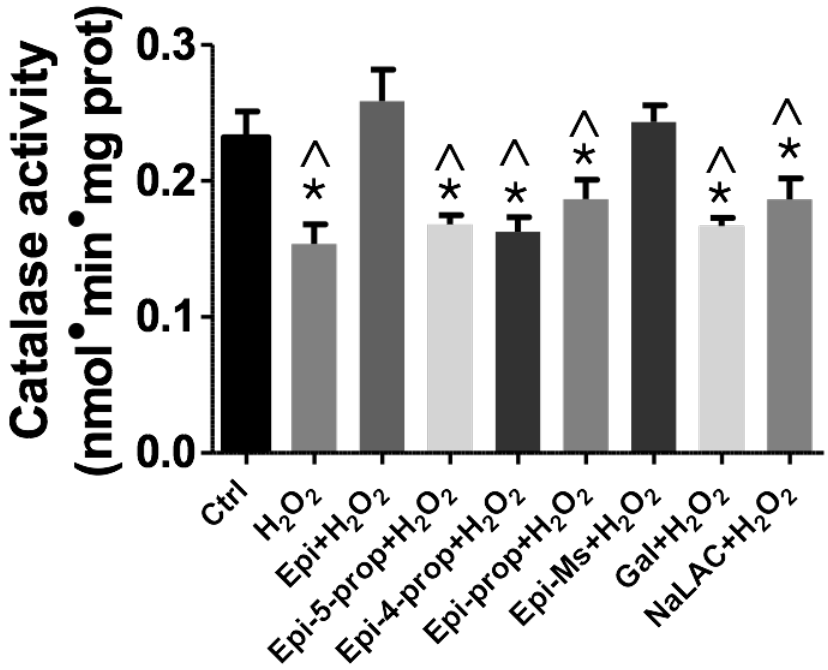

Figure 3.11. Catalase activity measurements. BCAEC were pre-incubated for 48 h with Epi, Epi-prop, Epi-5-prop, Epi-4-prop and Epi-Ms before the treatment with 200 μM H_2O_2. Gallic acid (Gal) and sodium ascorbate (NaLAC) were used as controls. Data represent the means of three separate experiments, each performed in triplicate. $p<0.05$ as compared vs ^ control or * as compared vs H_2O_2 treated cells.

Catalase is a potent antioxidant enzyme that dismutates H_2O_2 into H_2O and oxygen (Figure 3.12). Cells treated with H_2O_2 showed reduced catalase activity. In contrast, catalase activity was significantly increased vs control, in cells pretreated with **Epi** and **Epi-Ms**. The **Epi** propargyl derivatives were not able to prevent a decrease in catalase activity induced by H_2O_2. (Figure 3.12).

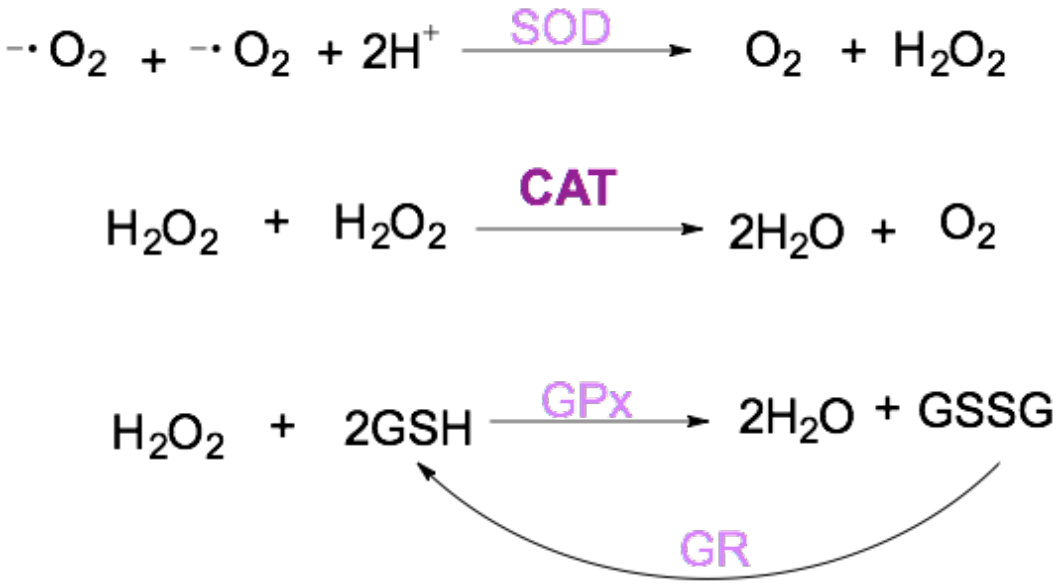

Figure 3.12. Main enzymatic antioxidant defense system *in vivo* and their reactions on scavenging free radicals and hydrogen oxide. SOD, superoxide dismutase; CAT, catalase; GPx, glutathione peroxidase; and GR, glutathione reductase.

These results were consistent with our previous results in cell assay (*Crystal violet*, *MTT* and *resazurin*) which **Epi** had the highest activity followed by **Epi-Ms**, and the propargyl derivatives had no significant activity. Since *MTT* and *resazurin* were used to assess protection against damage induced by H_2O_2 and increased catalase activity, we could assume that **Epi** and **Epi-Ms** exert their protective effects in mitochondria. However studies using other mitochondrial enzymes as well as an assessment of mitochondrial transcriptional factors are necessary.

3.3 Design, synthesis and characterization of a column (EPI-COLUMN) with an Epi derivative for the isolation of EPI binding proteins

3.3.1 EPI-COLUMN. Affinity chromatography

To elucidate the molecular mechanisms underlying the action of **Epi**, identification of its binding targets is essential. Affinity chromatography is one of the most important techniques in the characterization of specific interactions between biomolecules, and is based on the immobilization of a molecule of interest to a

solid support. For selective immobilization, the molecule must contain a functional group for attachment. For a small molecule, such as **Epi**, current affinity-based target identification techniques are limited by the necessity to modify the molecule and its bioactivity must be unaffected by the derivatization.

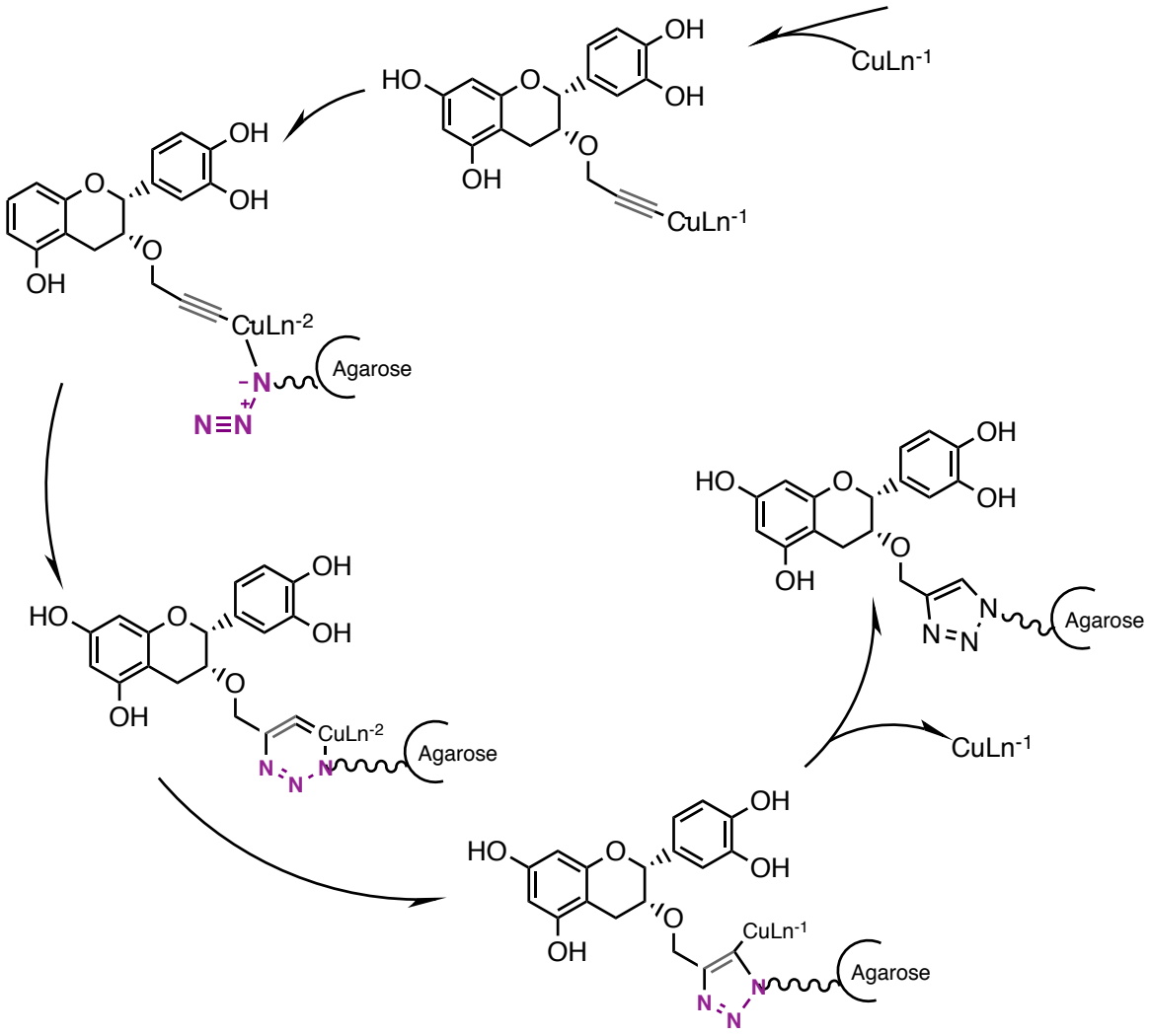

Figure 3.13. Scheme for Click chemistry coupling (proposed reaction mechanism) of Epi-prop to agarose azide. First Cu(I) catalyst is reduced from Cu(II) sulfate pentahydrate by sodium ascorbate (reducing agent), followed Cu(I) coordinates the alkyne group, then a σ-bound copper acetylide bearing to π-bound copper coordinates the azide. Then, an unusual six-membered copper metallacycle is formed. The 2nd copper atom acts as a stabilizing donor ligand. Ring contraction to triazolyl-copper derivative is followed by protonolysis that delivers the triazole product and closes the catalytic cycle.

To capture and isolate potential targets of **Epi**, we developed an affinity chromatography method (EPI-COLUMN) using the compound **Epi-prop** immobilized onto agarose-azide beads which were able to display its unaffectated bioactivity in cultured cells (with even higher effects than with **Epi** native) and an energetically favorable interaction with GPER, similar to **Epi** native. In this case, the alkyne motif in **EPI-prop** reacts selectively with organic azides, such as the ones found in the agarose azide beads, while the hydroxyl phenolic groups are unreactive for Click chemistry (Figure 3.13).

Click chemistry reactions are highly efficient and specific, with modularity, and easy work up, and is an attractive strategy to functionalize biomaterials (Nwe and Brechbiel, 2009; Kristi and Harm-Anton, 2016).

To develop the EPI-COLUMN, **Epi-prop** was covanlently immobilized by Click chemistry to commercially available agarose azide beads using Copper (II) sulfate as pentahydrate as catalyst and sodium ascorbate as reducing agent, which were then packed into a minicolumn (Figure 3.13). The reaction performs best in aqueous systems, briefly the proposed mechanism: Cu(I) catalyst is first reduced from (reducing agent). The reaction begins with the reduction of Cu(II) sulfate pentahydrate to Cu(I) by sodium ascorbate, followed alkyne (Epi-prop) is converted to the acetylide by the coordination of the acetylene to the Cu (I), displacing one of the water ligands (solvent). In the next step the azide replaces one of the ligands and binds to the copper atom via the nitrogen proximal to carbon, forming intermediate agarose-Epi-prop. After that, the distal nitrogen of the azide in the agarose attacks the C-2 carbon of the acetylide in Epi-prop, forming the unusual six-membered copper(III) metallacycle. A 2nd copper atom acts as a stabilizing donor ligand and give the triazolyl-copper derivative. Protonolysis releases the triazole product, thereby completing the catalytic cycle [Himo *et al*., 2004; Hein and Fokin, 2010]. (Figure 3.13)

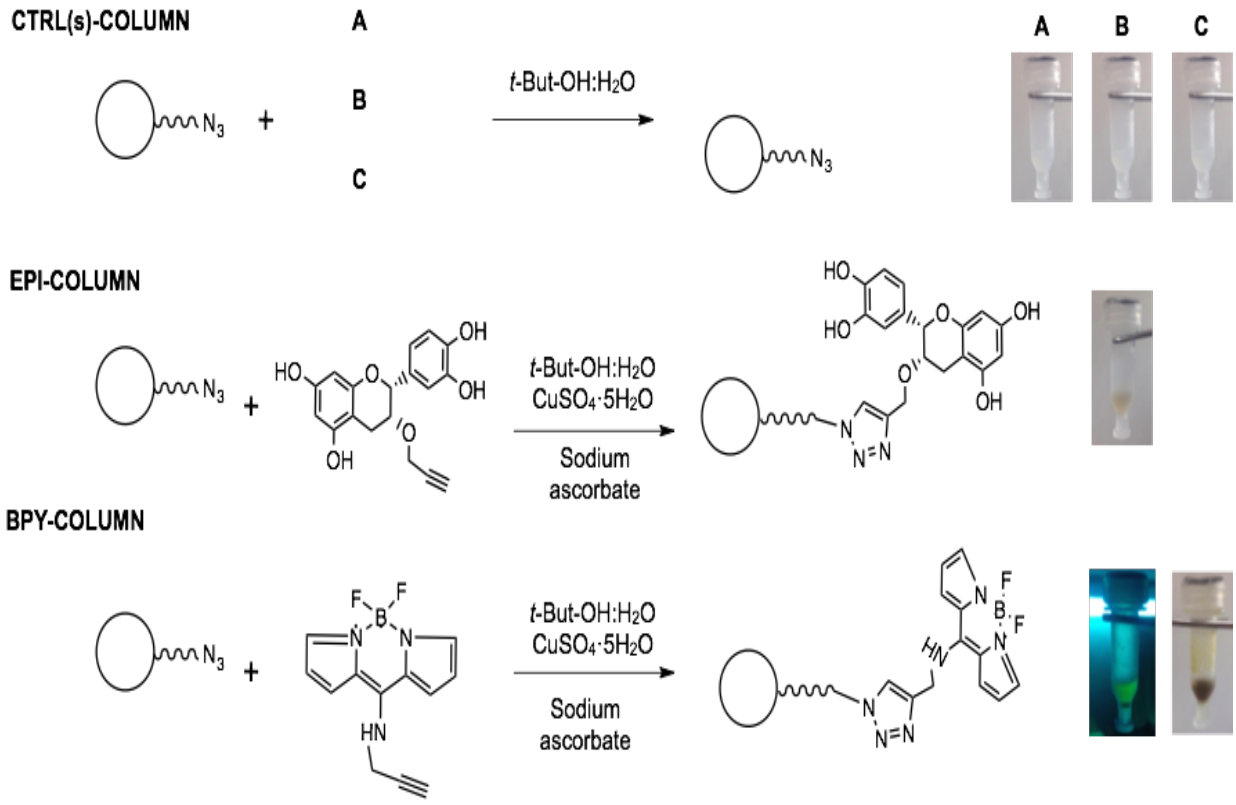

Figure 3.14 Click chemistry coupling conditions for the controls, **Epi-prop** and **BPY**. CTRL(s)-COLUMN. The control columns were prepared by the same procedure, but with the sequential omission of the following components (**A**) **Epi-prop,** (**B**) Copper (II) sulfate pentahydrate and Sodium ascorbate and (**C**) **Epi-prop**, Copper(II) sulfate pentahydrate and Sodium ascorbate. EPI-COLUMN and BPY-COLUMN; Coupling conditions for the preparation of the **Epi-prop** and BPY columns are described in Experimental Procedures. As the last step, all of the columns were washed extensively with 0.1 M EDTA to remove copper ions and non-specific reaction reagents adsorbed to the surface of the agarose-azide beads.

For the reaction we added a slight excess of sodium ascorbate to prevent the formation of oxidative homocoupling products. Non-specific adsorption of reaction reagents on the column surface was removed by exhaustive washing with EDTA to remove the Copper catalyst in excess. We used as controls, agarose-azide beads treated with the identical procedure, except that no **Epi-prop** or Copper (II) sulfate pentahydrate, or sodium ascorbate was added (CTRL(s)-COLUMN) Figure 3.2.

3.3.2 Assessment of the immobilization procedure yield

3.3.2.1 Fluorescence determination

Once that the click reaction was performed we investigated the presence of the **Epi-prop** at the ends of the agarose-azide beads by quantitation of the **Epi-prop** recovered using concentration dependent fluorescence experiments with the free **Epi-prop** in solution serving as a control. The results showed that 86.6% of the **Epi-prop** attached to the agarosa-azide beads (Figure 3.15).

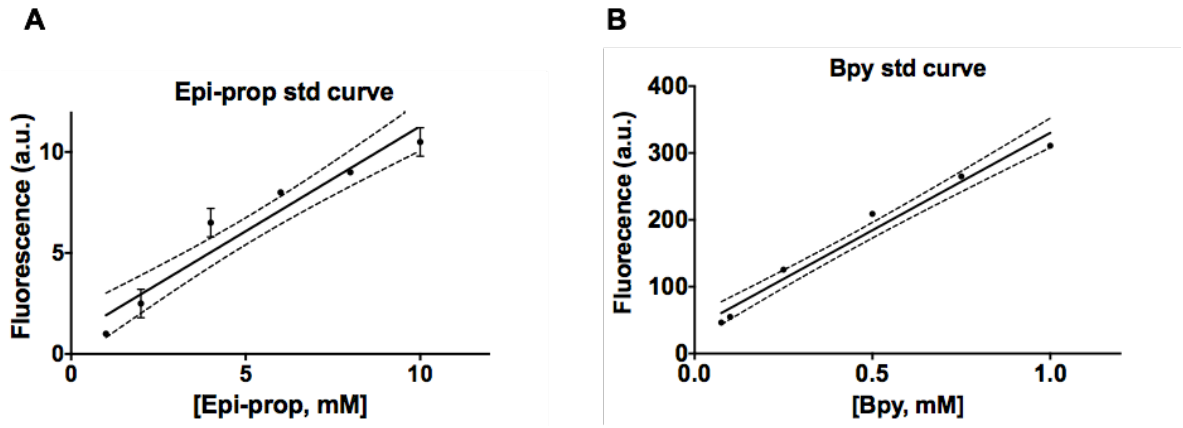

Figure 3.15. Fluorescence standards curve of Epi-prop and BPY. Standard curves were derived from serial dilutions of the compounds. (A) Standard curve of **Epi-prop**. (B) Standard curve of **BPY**.

However, to test the feasibility of resin attachment by the Click chemistry reaction, agarose-azide beads were treated with an alkyne-fluorescein (**BPY**) under the same Click chemistry conditions in the presence of the Copper catalyst. The **BPY** was successfully attached (80% yield), as indicated by permanent fluorescence in the resulting beads under ultraviolet light (Figure 3.2) and the quantitation of the free **BPY** recovered (Figure 3.15).

3.3.2.2 Electrochemical assessment

To ascertain la presence of the compound in the agarose beads, we carried out a second analysis. We expect that the overall surface charge of the agarose

beads will change after the click chemistry procedure. We've tested this hypothesis by quantifying the net charge of the agarose beads before and after the click chemistry procedure by performing zeta potential measurements.

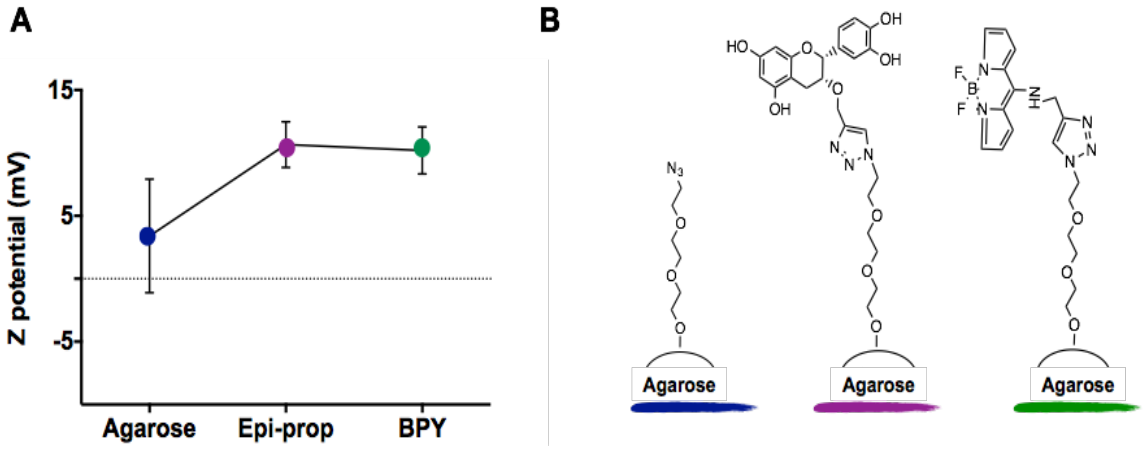

Figure 3.16. Electochemical assessments. (A) Zeta potential measumerents of the agarose beads before the click chemistry procedure (agarose), and after the click chemistry reaction with **Epi-prop** and **BPY**. (B) Molecular models of the agarose with the compounds

For the agarose beads, the initial zeta potential value was 3.1 ± 1.4 mV; after click chemistry with **Epi-prop**, the potential increased to 11.4 ± 2.1 mV and the after the reaction with **BPY**, the potential increased to 10.9 ± 1.9 mV. We attribute this increase in the zeta potential to the presence of the **Epi-prop** and **BPY** on the surface of the agarose beads (Figure 3.16).

3.3.3 Epi-column elution and protein detection

Once we had the certainty of the coupling of the derivative to the surface of the agarose beads, cell lysates from BCAEC were subjected to affinity chromatography using the EPI-COLUMN (Figure 3.17 A). We first established experimental conditions to obtain a reproducible pattern of bands by SDS-PAGE electrophoresis; gels were stained with Coomassie-Blue. A consistent set of protein bands with apparent molecular weights of 50-kDa, 42-kDa and 37-kDa respectively were identified in the elution fractions from the EPI-COLUMN. The elution fractions from the control columns were analyzed in parallel experiments

under the same conditions, no protein bands were observed in these elution fractions (Figure 3.7 B).

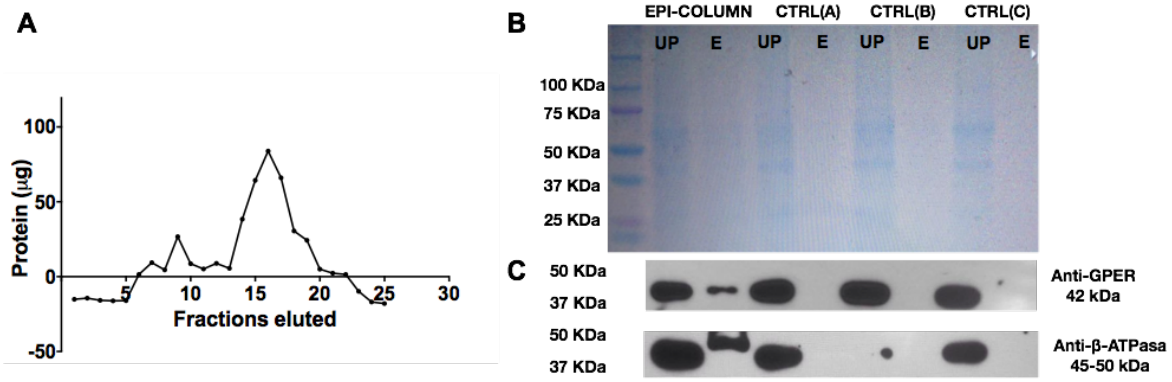

Figure 3.17. Isolation, separation and identification of potential target proteins that bound to the EPI-COLUMN. Total protein lysates from endothelial cells (BCAEC) were applied to the EPI-COLUMN and the control columns. (A) Affinity chromatography elution fractions of proteins with 8M Urea. (B) SDS-PAGE analysis of the elution fractions, gel stained with Coomassie-Blue. (C) Western blot analysis using monoclonal GPER and β-ATPase antibodies. UP: Unbound proteins fraction, E: Elution fraction.

Elution fractions containing potential target proteins were separated by SDS-PAGE, and then transferred onto PVDF membranes. Western blot analysis revealed the presence of a 42-kDa protein that was reactive with the GPER antibody and a band of ~50-kDa that was reactive with β-ATPase antibody (Figure 3.17 C).

CHAPTER 4

CHAPTER 4: CONCLUSION

4.1 Synthesis of (-)-epicatechin derivatives

Epi is a flavanol found in natural products such as cocoa seeds that has exhibited antioxidant and vascular benefits as well as many health promoting effects [Schroeter *et al.* 2005, Ottaviani *et al.* 2011; Heim *et al.,* 2002; Martin *et al.,* 2010; Monagas *et al.,* 2009; Steffen *et al.,* 2008]. Due to the biological relevance of this flavanol, the purpose of this work was to prepare and characterize four Epi derivatives and therefore change the chemical and physical properties of the Epi native in order to elucidate its vascular effects.

Considering that the flavonoid effects are assumed to be structure-dependent and the major contributing factor is the presence of the hydroxyl groups (Vaya *et al.,* 2003, Garg *et al.,* 2001). We synthetized two types of **Epi** derivatives: **Epi-Ms** and **Epi-prop** which retained four phenolic hydroxyl groups. Moreover, in order to assess the potential contribution of the hydroxyl groups to the elicited effects, we synthesized **Epi-4-prop** and **Epi-5-prop.**

Using the Williamson ether synthesis and a method reported by Sharma *et al*. [2007], alkyl and benzyl substituents were added to the **Epi** skeleton, allowing us to obtain Epi derivatives tetra and penta substituted (**Epi-Benzyl**, **Epi-4-prop** and **Epi-5-prop**) with a good yield. Using mesyl chloride, we achieved the stereoselective reduction of the C-3 position of **Epi-Benzyl** to produce **Epi-Benzyl-Ms** with a good yield as previously reported.

Moreover, by using of palladium-catalyzed reactions, previously reported by Wang *et al*., **Epi-Benzyl-Ms** and **Epi-penta-prop** were selectively debenzylated and depropargylated to the parent alcohols via a phenolic C−O bond cleavage under mild reaction conditions to obtain the Epi mono-derivatives: **Epi-Ms** and **Epi-prop**.

The depropargylation and debenzylation reactions were achieved using 20%

$Pd(OH)_2/C$ as the catalyst in EtOAc-MetOH (20:1). Cleavage of benzyl ethers is a quite advantageous method and multiple alternative protocols have been described. [Tückmantel *et al.,*1999; Sharma *et al.*, 2007; Ranjan Banerjee *et al.,* 2014]. Notably, a few examples are known dealing with the selective cleavage of the C–O bond employing aryl halides as substrates and Pd/C as catalyst. Here, we describe an improved synthetic route previously reported by Wang *et al*., for the selective cleavage of C–O in propargyl ethers at room temperature, in the presence of hydrogen and catalytic amounts of Pd/C. A remarkable feature of this reaction is that the aromatic C-O bonds (benzyl-O and propargyl-O) were cleaved, rather than the weaker aliphatic C-O bond (C-3).

All Epi derivatives were synthesized and characterized by NMR and Mass spectroscopy.

In summary, four new Epi derivatives were synthetized by improving methods previously reported. Esterification reactions using alkynes proved to be a successful and potentially advantageous route to generate Epi derivatives. Modification of the C-3 by a SN2 reaction was difficult, since humidity affected the reaction; we sorted this out by changing our synthetic route. This synthesis was strengthened, by our continued efforts to elucidate a selective modification of the phenolic hydroxyl groups of **Epi**. However, further optimization of the methods is required to achieve full selectivity of the flavanol modification.

In this work we report the partial or total chemical modificaton of the hydroxyl groups of **Epi** to obtain derivatives that may be optimal to elucidate **Epi's** vascular effects.

4.2 Biological effects of (-)-epicatechin and (-)-epicatechin derivatives

Epi has a wide array of biological actions in vascular cells related directly to its chemical structure, although the mechanisms by which such effects are mediated have not been fully elucidated. There is indirect evidence that its biological actions involve the activation of several membrane receptors such as G-

protein-coupled receptors (GPCRs) (Panneerselvam *et al.,* 2010, Moreno-Ulloa, 2015). Thus, we assessed the effects of novel and recently synthetized Epi derivatives (**Chapter 1**), in an effort to elucidate the mechanics of **Epi's** actions on vascular cells as well as the impact of alkyne derivatization in such effects. For this purpose, we developed three different approaches. First, *in silico* analysis to evaluate putative protein interactions of our previously synthetized compounds with the active site of GPER using the 14 and 70 ns conformers from molecular dynamics (MD) simulations. Then, we assessed the contribution of the alkyne group to improve NO production by eNOS activation using GPER expressing bovine coronary artery endotelial cells (BCAEC), in order to examine the potential role of GPER on these effects. Finally, in an effort to further understand the structure-activity relationships involved in **Epi**'s biological effects. We examined the impact of its derivatization on antioxidant activity. Since the antioxidant activity of flavonoids depend on a combination of several factors, we assessed: a) the protective effects against oxidative stress, b) the ability to scavenge free radicals, c) electrochemical oxidation and d) the effects of the compounds on catalase activity.

For the first aim, novel **Epi** derivatives were docked into the active site of GPER using the 14 and 70 ns conformers derived from a MD analysis performed in a previous study [Méndez-Luna *et al.,* 2015]. In this study, molecular docking revealed that the binding interaction between all Epi derivatives and GPER conformers is energetically favorable. Based in these results we suggested that the Epi derivatives could be potential ligands for GPER.

Once the derivatives were pre-validated *in silico*, we tested their *in vitro* efficacy using the GPER expressing bovine coronary artery endotelial cells (BCAEC). We evaluated the capacity of Epi-derivatives to stimulate the eNOS/NO activation pathway. Nitrates/nitrites levels in the supernatant and immunodetection of phosphorylated (at Ser1179) eNOS (p-eNOS by Western blots) were measured as a surrogate of NO synthesis and eNOS activation, respectively. To explore the participation of GPER the antagosist G15 was used. Cells were pre-incubated with

G15, a GPER inhibitor**.** The results demonstrate that as predicted by *in silico* modeling, the derivatives were able to stimulate to different degrees NO production via eNOS activation and that effects were notably attenuated by the GPER antagonist G15.

Using the *MTT assay*, the *crystal violet assay* and the *resazurin method* we assessed the protective effects of Epi derivatives against oxidative stress. BCAECs were exposed to 200 μM H_2O_2, after pretreatment compounds for 24 h. After incubation, cell viability was determined using the MTT assay, crystal violet assay and the resazurin method. Mesyl substitution had no significant effects in **Epi** antioxidant activity, conversely propargyl substitution, had significant effect, suggesting that the presence of propargyl group decrease antioxidant acitvity of **Epi.**

The TEAC-ABTS assay was used to assess the ability of **Epi** and Epi derivatives to scavenge the ABTS radical cation. The results were expressed as Trolox equivalents (TEAC). The TEAC values of **Epi** native had a more effective scavenging activity than Epi alkyne derivatives suggesting that the H-donating ability is greatly reduced on derivatization of the hydroxyl groups.

Moreover, using cyclic and differential pulse voltammetry we examined the structure-activity relationships of **Ep**i, by performing the electrochemical oxidation of the **Epi** and **Epi** derivatives. This study showed that the electrochemical oxidation of **Epi** and **Epi-Ms** on a glassy carbon electrode, which corresponds to oxidation of the 3',4'-dihydroxy substituent on the B-ring (the first oxidation peak), includes the transfer of two electrons and two protons and that the oxidation products are strongly adsorbed on the electrode surface. The structural differences of the investigated compounds were shown to be related to the values of their oxidation potential (*E*), the highest values were displayed by the propargyl derivatives, meanwhile Epi displayed the lowest value, hence the highest antioxidant capacity.

Catalase activity was determined spectrophotometrically according to Aebi, [1970]. BCAEC were pre-incubated for 48 h with the compounds before treatment with 200 μM H_2O_2. Propargyl derivatives had no significant effect on catalase activity, meanwhile **Epi** and **Epi-Ms** contributed to the enhancement of catalase activity.

The antioxidant activity of the standards Gal and NaLAC was in accordance with previous reports in terms of overall order and magnitude, a fact that validated our results. Some discrepancies with NaLAC, may be due to the differences in the reaction conditions, such as the initial reagent concentration and analysis run time, and also because of the normalization of the values employed in our the studies.

In summary, we assessed four Epi derivatives, previously synthetized, in an effort to elucidate **Epi's** vascular effects. Our *in vitro* and docking results indicated that GPER could interact and was activated by Epi and its derivatives. However, other receptors are also likely to be involved as G15 only partially inhibited eNOS activation and NO production (In cultured cells). Moreover, **Epi** and **Epi-Ms** were able to decrease the oxidative damage induced by H_2O_2 and such activity appears to be mediated by a protective effect on mitochondria (Since the *MTT* and *resazurin* methods were used for assess cell viability and catalase activity was increased). Studies using other mitochondrial enzymes, as well as an assessment of mitochondrial transcriptional factors will be necessary. Our limited structure-activity relationship study suggests that the propargyl substitution at the 3,*5,7,3',4'* phenols or at the C-3 alcohol on Epi decreased its ability to scavenge free radicals as well as its antioxidant effects in cultured cells. The antioxidant activity sequence of the investigated, structurally different, Epi derivatives was: **Epi** > **Epi-Ms** > **Epi-prop**> **Epi-4-prop** > **Epi-5-prop**. Therefore, further studies on the influence of the propargyl substitution in Epi native, as well as on the structure-activity relationships, are necessary.

4.3 Design, synthesis and characterization of a column (EPI-COLUMN) with an Epi derivative for the isolatION of Epi binding proteins

Elucidation of the molecular targets of **Epi** at the cellular level is essential for the improvement of the specificity of human studies and for an understanding of their mode of action. Our previos *in vitro* and docking results displayed that GPER is capable to interact and be activated by Epi and its derivatives. However, other receptors are also likely involved as G15 only partially inhibited eNOS activation and NO production. In order to explore this possibility, we implemented an affinity chromatography protocol to isolate and identify potentials molecular targets of Epi.

Affinity chromatography is potentially the most selective method for protein purification [Labrou, 2003]. This approach is based on the immobilization of the molecule of interest to a solid support as a means to isolate and eventually characterize specific binding proteins, including receptors. However, the immobilization of ligands to a solid support may alter the biological properties of the free ligand. Hence it is the design and synthesis of appropriate ligands which is often the rate limiting step in introducing affinity-based purification protocols, we designed and selected the compound **Epi-prop** which displayed unaffectated bioactivity in cultured cells, and has an alkyne motif for Click chemistry suitable to develop an affinity column (EPI-COLUMN).

We therefore developed an affinity column (EPI-COLUMN) using **Epi-prop** that was covalently immobilized by the use of Click chemistry to commercially available agarose-azide beads. To achieve this goal, we took advantage of the propargyl substituent at the C-3 alcohol group in **Epi-prop** that reacts selectively with organic azide groups such as those present on agarose-azide beads, leaving the **Epi** phenol groups unchanged. To use as controls, we generated three different agarose columns, and demonstrated there's no non-specific protein binding to the column matrix. We tested the covalent binding of **Epi-prop** onto agarose beads by zeta potential measurements. And also, the covalent binding of **BPY** to agarose beads under same click conditions, yielding yellow beads that were strongly fluorescent under ultraviolet light. We isolated several potential target proteins of **Epi** from total protein lysates of BCAEC by using the EPI-COLUMN.

Finally, we analized by SDS-PAGE the elution fractions from the EPI-COLUMN an identified potential target proteins of **Epi** by immunodetection. In this work we have described the development of an affinity column (EPI-COLUMN) that was used to isolate potential target proteins of **Epi**. By using this EPI-COLUMN we identified GPER and β-ATPase, as molecular targets of **Epi**.

REFERENCES

Aebi, H. Oxydasen und reductasen. In: BERGEMEYER H.V., ed. Methoden der Enzymatishen. *Analys Berlin Acad Verl*, **1970**, 6, 34.

Al-Nasiry, S.; Geusens, N.; Hanssens, M.; Luyten, C. *Pijnenborg R Hum Reprod*. **2007**, 22, 13, 04.

Allan J.; and Robinson, R. Accessible derivative of chromonol. *J Chem Soc*. **1924**, 21, 92.

Arts, I.C.; van de Putte, B.; Hollman. P.C. Agric Food Chem. **2000**, 48, 1746.

Bach, S. et al. *J Biol Chem.* **2005***,* 280, 31208.

Beckman, K.B.; Ames B N *Physiol. Rev*. **1998**, 78, 547.

Beilke, M.A.; Collins-Lech, C.; Sohnle, P.G. *J Lab Clin Med*. **1987**, 110, 91.

Berridge, M.V.; Herst, P.M.; Tan, A.S. *Biotechnol Annu Rev*. **2005**, 11, 127.

Beugelmans, R.; Bourdet, S.; Bigot, A.; Zhu, J. Tetrahedron Lett. **1994**, 35, 4349.

Birben, E.; Sahiner, U. M.; Sackesen, C.; Erzurum, S.; Kalayci, O. *The World Allergy Organization Journal*. **2012**, *5*, 9.

Birukov, K.G. *Antioxid Redox Signal*. **2009**, 11, 1651.

Bois-Choussy, M.; Neuville, L.; Beugelmans, R.; Zhu, J. *J Org Chem*. **1996**, 61, 9309.

Boss, R.; Scheffold, R. Angew. *Chem Int Ed*. **1976**, 15, 558.

Boueiz, A.; Hassoun, P.M. *Microvasc Res*. **2009**, 77, 26.

Bruggisser, R.; von Daeniken, K.; Jundt, G.; Schaffner, W.; Tullberg-Reinert, H. *Planta Med*. **2002**, 68, 445.

Buijsse, B.; Feskens, E.J.; Kok, F.J.; Kromhout, D. Arch Intern Med. **2006**, *66*, 411.

Buijsse, B.; Weikert, C.; Drogan, D.; Bergmann M.; Boeing H. Eur. Heart J. **2010**, *31*, 1616.

Burda, S.; Wieslaw, J. Agric. Food Chem. **2001**, 49, 2774.

Cai H. Cardiovasc. Res. **2005**, 68, 26.

Chandrasekhar, S.; Raji, R. C.; Jagadeeshwar, R. *Tetrahedron* **2001**, 57, 3435.

Chiba, K.; Kawakami, K.; Tohyama, K. *Toxicol in Vitro*. **1998**, 2, 251.

Choi,J.S.; Chung, H.Y.; Kang, S.S.; Jung, M.J.; Kim, J.W.; No, J.K.; Jung,H.A.

Phytother Res. **2000**, 16, 232.

Corti, R.; Flammer, A.J.; Hollenberg, N.K.; Luscher, T.F. *Circulation*. **2009**, 119, 1433.

Crawford, D.L.; Sinnhuber, R.O.; Aft, *H J Food Sci.* **1961**, 26, 139.

Cuatrecasas, P.; Wilchek, M.; Anfinsen, C.B. *Proc Natl Acad Sci USA. **1968,*** 61, 636.

Deb Ranjan Banerjee, Debajyoti Dutta, Baisakhee Saha, Sudipta Bhattacharyya, Kalyan Senapati, Amit K. Das Amit Basak. *Org Biomol Chem*. **2014**, 12, 73.

Dessolin, M.; Guillerez, M. G.; Thieriet, N.; Guibe, F.; Loffet, A. *Tetrahedron Lett*. **1995**, 36, 5741.

Dudzinski, D. and Michel, T. *Cardiovascular research*. **2007**, *75*, 247.

Eicher, T.; Ott, M.; Speicher, A. *Synthesis* **1996**, 7, 55.

Ellinger, S; Reusch, A.; Stehle, P.; Helfrich, H.P. *Am. J Clin Nutr*. **2012**, 95, 1365.

Firuzi, O.; Lacanna, A.; Petrucci, R.; Marrosu, G.; Saso, L. *Biochim Biophys*. Acta **2005,** 1721, 174.

Four, P.; Guibe, F. *Tetrahedron Lett*. **1982**, 23, 1825.

Fraga, C.G.; Oteiza P.I. *Free Radical Biol Med*. **2011**, 51, 813.

Franco, D.; Panyella, D.; Rocamora, M.; Gomez, M.; Clinet, J.C.; Muller, G.; Dunach, E. *Tetrahedron Lett*. **1999**, 40, 5685.

Fujimura, Y.; Umeda, D.; Yamada, K.; Tachibana, H. *Arch Biochem Biophys*. **2008**, 476, 133.

Galleano, M.; Oteiza, P.I.; Fraga, C.G.J. *Cardiovasc Pharmacol*. **2009**, 54, 483.

Garg, R.; Kurup, A.; Hansch, C. *Rev Toxicol*. **2001**, 31, 223.

Gerlier, D. and Thomasset, N. *J Immunol Methods*.**1986**, 94, 57.

Green, T.W. and Wuts, P.M.G. Protective Groups in Organic Synthesis; 3rd ed. Wiley: New York, **1999**.

Harding, M.W.; Galat, A.; Uehling, D.E.; Schreiber, S.L. *Nature*. **1989**, 341, 758.

Heijnen, C.G.M.; Haenen, G.R.M.M.; Vekemans, J.A.J.M.; Bast, A. *Environ Toxicol Pharmacol*. **2001**, 10, 199.

Heim, K.E.; Tagliaferro, A.R.; Bobilya, D.J. *J Nutr Biochem*. **2002,** 13, 572.

Heiss, C.; Keen C.L.; Kelm M. *Eur Heart J*. **2010**, 31, 2583.

Hercouet, A.; LeCorre, M. *Synthesis*.**1982**, 5, 97.

Honda, M.; Morita, H.; Nagakura, I. *J Org Chem*. **1997**, 62, 8932.

Hynek, D.; Krejcova, L.; Sochor, J.; Cernei, N.; Kynicky, J.; Adam, V.; Trnkova, L.; Hubalek, J.; Vrba R.; Kizek, R. *Int J Electrochem Sci*. **2012**, 7, 1802.

Iinuma, M.; Iwashima, K., Matsura, S. *Chem. Pharm. Bull*. **1984**, 32, 4935.

Ishihara, K. and Nakajima, *N. J Mol Catal*. B. Enzym. **2003**, *23*, 411.

Janeiro, P. and Oliveira-Brett, A.M. *Anal* Chim Acta. **2004**, 518, 109.

Jelen, F.; Kourilova, A.; Hason, S.; Kizek R.; Trnkova, L. *Electroanalysis*. **2009**, 21, 439.

Johnston, K.A. *PharmaGenomics*. **2001**,13, 28.

Jones, C.; Patel, A.; Griffin, S.; Martin, J.; Young, P.; O'Donnell, K.; Silverman, C.; Porter, T.; Chaike, I. *J Chromatogr A*. **1995**, 707, 3.

Kandikere, R. P.; Naduthambi, D.; Chandrasekaran, S. *Synlett*. **2002**, 17, 62.

Park, K. D.; Lee,S.G.; Kim, S.U.; Kim, S.H.; Sun, W.S.; Cho S.J.; Jeong, D.J. *Bioorg Med Chem*. Lett. **2004**, 14, 5189

Kilmartin, P. A.; Zou H. L.; Waterhouse, A. L. *Am J Enol Vitic*. **2002**, 53, 294.

Kristi, S. A.; Harm-Anton, K. *Biomacromolecules.* **2016** 17, 1.

Kuhnle, G.; Spencer, J.P.E.; Schroeter, H.; Shenoy, B.; Debnam, E.S.; Srai, S.K.; Rice-Evans, C.; Hahn, O. *Biochem Biophys Res Commun*. **2000,** *227*, 507.

Lamb J, *et al. Science.* **2006,** 313, 1929.

Lappano, R.; Santolla, M.F.; Pupo, M.; Sinicropi, M.S.; Caruso, A.; Rosano, C.; Maggiolini, M. *Breast Cancer Res*. **2012**, 14, 12.

Li, N.G.; Shi Z.H.; Tang Y.P.; Yang J.P,; Duan J.A. Beilstein J Org Chem. **2009**, 5, 60.

Liu, S.; Premont, R.T.; Rockey, D.C. *J Biol Chem.* **2014**, *289*, 18, 163.

Loke, W.M.; Hodgson, J.M.; Proudfoot, J.M.; McKinley, A.J.; Puddey, I.B.; Croft, K.D. *Am J Clin Nutr*. **2008**, *88*, 1018.

Lyddiatt et al. *Curr Opin Biotechnol*. **2002,** 13, 95.

Mahal, H.S. and Venkataraman, K. *Curr Sc*. **1933**, 4, 214.

Manach, C.; Williamson, G.; Morand, C.; Scalbert, A.; Rémésy, C. *Am J Clin Nutr*. **2005**, 81, 230.

Manning, B.D.and Cantley, L.C. *Cell*. **2007**, *129*, 1261.

Marklund, S. L.; Westman, G.; Lundgren, E.; Roos, G. *Cancer Res*. **1982**, 42, 1955.

Martin, M.A.; Serrano, A.B.; Ramos, S.; Pulido, M.I.; Bravo, L.; Goya, L. *Biochem*. **2010**, 21, 196.

Mendez-Luna, D.; Martinez-Archundia, M.; Maroun, R.C.; Ceballos-Reyes, G.; Fragoso-Vazquez, M.J.; Gonzalez-Juarez, D.E.; Correa-Basurto, J.J. *Biomol Struct Dyn*. **2015**, 33, 2161.

Middleton, E. Jr.; Kandaswami, C.; Theoharides, T.C. *Pharmacol Rev*. **2000**, 52, 673.

Min-Hsiung, P.; Ching-Shu, L.; Chi-Tang, H. *Food Funct.* **2010**, 1, 15.

Mittal, A.; Goke, F.; Flint, R.; Loveday, B. P. T.; Thompson, N.; Delahunt, B.; Kilmartin, P. A.; Cooper, G. J. S.; MacDonald, J.; Hickey, A.; Windsor J. A.; Phillips, A. R. J. Shock. **2010**, 33, 460.

Monagas, M.; Khan, N.; Andres-Lacueva, C.; Casas, R.; Urpi-Sarda, M.; Llorach, R.; Lamuela-Raventos, R.M.; *Am J Clin Nutr*., **2009**, 90, 1144.

Moreno-Ulloa, A.; Cid, A.; Rubio-Gayosso, I.; Ceballos, G.; Villarreal, F.; Ramirez-Sanchez I. *Bioorg Med Chem Lett*. **2013**, 23, 4441.

Moreno-Ulloa, A.; Mendez-Luna, D.; Beltran-Partida, E.; Castillo, C.; Guevara, G.; Ramírez-Sánchez, I.; Correa-Basurto, J.; Ceballos, G.; Villarreal, F. *Pharmacol Res*. **2015**, 100, 309.

Moreno-Ulloa, A.; Romero-Perez, D.; Villarreal, F.; Ceballos, G.; Ramírez-Sánchez, I. *Bioorg Med Chem*. **2014**, 24, 2749.

Mosmann, J.P. *J Immunol Methods*.**1983**, 65, 55.

Mostofsky, E.; Levitan, E.B.; Wolk, A.; Mittleman, M.A. *Circulation Heart failure.* **2010**, *3*, 612.

Nakayama, T.; Ishii, T.; Uekusa, Y.; Kato, K.; Kumazawa, S. *J. Food Drug Anal*. **2012**, 20, 305.

Nandi, B.; Das, K.; Kundu, N. G. *Tetrahedron Lett*. **2000**, 41, 7259.

Nanjo, F.; Goto, K.; Seto, R.; Suzuki, M.; Sakai, M.; Hara, Y. *Free Radical Biol. Med*. **1996**, 21, 895.

Nwe, K.; Brechbiel, M.W. *Cancer Biother Radiopharm*. **2009**, 24, 289.

O'Brien, J.; Wilson, I.; Orton, T.; Pognan, F. *Eur J Biochem*. **2000**, 267, 5421.

Panneerselvam, M.; Tsutsumi, Y.M.; Bonds, J.A.; Horikawa, Y.T.; Saldana, M.; Dalton, N.D.; Head, B.P.; Patel, P.M.; Roth, D.M.; Patel, H.H. *Am J Physiol Heart Circ Physiol.* **2010**, *299*, 1604.

Park, K.D.; Lee, S.G.; Kim, S.U.; Kim, S,H.; Sun, W.S.; Cho, S.J.; Jeong, D.H. *Bioorg Med Chem Lett*. **2004**, 14, 5189.

Patra, S,K.; Rizzi, F.; Silva, A.; Rugina, D.O.; Bettuzzi, S. *J Physiol Pharmacol.* **2008**, 59, 217.

Pohanka, M.; Sochor, J.; Ruttkay-Nedecky, B.; Cernei, N.; Adam, V.; Hubalek, J.; Stiborova, M.; Eckschlager T.; Kizek, R. *J Appl Biomed*. **2012**,10,155.

Putnam, K.P.; Bombick, D.W.; Doolittle, D.J. *Toxicol In Vitro*. **2002**, 16, 599.

Ramirez-Sanchez, I.; Maya, L.; Ceballos, G.; Villarreal, F. *Hypertension*. **2010**, *55*, 1398.

Rop, O.; Jurikova, T.; Sochor, J.; Mlcek, J.; Kramarova, D. *J Food Qual*. **2011**, 34, 187.

Sadeghipour, M.; Terreux, R.; Phipps, J. *Toxicol In Vitro*. **2005**, 19, 155.

Saotome, K.; Morita, H.; Umeda, M. *Toxicol In Vitro*. **1989**, 3, 317.

Sato, Y.; Sato, K.; Suzuki, Y. *Arch Biochem Biophys*. **1999**, 366, 61-69.

Schieber, M.; Chandel, N.S. *Current biology*. **2014**, 24, 453.

Schroeter, H.; C. Heiss, C.; Balzer, J.; Kleinbongard, P.; Keen,C.L.; Hollenberg, N.K.; Sies, H.; Kwik-Uribe, C.; Schmitz, H.H.; Kelm, M. *Proc Natl Acad Sci*. 103, **2006**, 1024.

Schroeter, H.; Heiss, C.; Balzer, J.; Kleinbongard, P.; Keen C.L.; Hollenberg, N.K.; Sies, H.; Kwik-Uribe, C.; Schmitz, H.H.; Kelm, M. *PNAS*. **2005**, 103, 1024.

Seeram, N.P.; Nair, M.G. *J Agric Food Chem*. **2002,** 50, 5308.

Sharma, P.K.; Kolchinski, A.; Shea, H.A.; Nair, J.J,; Gou, Y.; Romanczyk, L.J.Jr.; Schmitz, H.H. *Org Process Res Dev*. **2007**, 11, 422.

Shum, D.; Radu, C.; Kim, E.; Cajuste, M.; Shao, Y.; Seshan, V.E.; Djaballah, H. *J Enz Inhib Med Chem*. **2008**, 23, 931.

Sochor, O.; Zitka, O.; Skutkova, H.; Pavlik, D.; Babula, P.; Krska, B.; Horna, A.; Adam, V.; Provaznik I.; Kizek, R. *Molecules***. 2010**, 15, 6285.

Sofer, G.; J Chromatogr A. **1995**, 70, 723.

Spencer, J.P.; Schroeter, H.; Kuhnle, G.; Srai, S.K.; Tyrrell, R.M.; Hahn, U.; Rice-Evans, C. *Biochem J*. **2001**, 354, 493.

Spencer, J.P.E.; Chowrimootoo, G.; Choudhury, R.; Debnam, E.S.; Srai, S.K.; Rice-Evans, C. *FEBS Lett*. **1999**, 458, 224.

Sridhar, J.; Ellis, J.; Dupart, P.; Liu, J.; Stevens, C.L.; Foroozesh, M. *Drug metabol Lett.* **2012**, *6*, 275.

Steffen, Y.; Gruber, C.; Schewe, T.; Sies, H. *Arch Biochem Biophys*. **2008**, 469, 209.

Strausberg, R.L.; Schreiber, S.L. *Science*. **2003**, 300, 294.

Tosh, D.K.; Yoo, L.S.; Chinn, M.; Hong, K.; Kilbey, S.M.; Barrett, M.O.; Fricks, I.P.; Harden, T.K.; Gao, Z.G.; Jacobson, K.A. *Bioconjug Chem.* **2010**, 21, 372.

Tuckmantel, W.; Kozikowski, A. P.; Romanczyk, L. J., Jr. *J Am Chem Soc*. **1999**, 121, 12073.

Tückmantel, W.; Kozikowski, A. P.; Romanczyk, L. J., Jr. *J. Am Chem Soc.* **1999**, *121*, 12073.

Tuñón, M.J.; García-Mediavilla, M.V.; Sánchez-Campos, S.; González-Gallego, *J Curr Drug Metab*. **2009**, 10, 256.

Uesato, S.; Taniuchi, K.; Kumagai, A.; Nagaoka, Y.; Seto, R.; Hara, Y.; Tokuda, H.; Nishino, H. *Chem Pharm Bull*. **2003**, 51,1448.

Uzunoglu, S.: Karaca, B.; Atmaca, H.; Kisim, A.; Sezgin, C.; Karabulut, B. *Toxicol Mech Methods*. **2010**, 20, 482.

van Acker SA, van den Berg DJ, Tromp MN, Griffioen DH, van Bennekom WP, van der Vijgh WJ, Bast A.. *Free Radic Biol Med*. **1996**, 20, 331.

Vaya, J.; Mahmood, S.; Goldblum, A.; Aviram, M.; Volkova, N.; Shaalan, A.; Musa, R.; Tamir, S. *Phytochem*. **2003**, *62*, 89.

Vistica, D.T.; Skehan, P.; Scudiero, D.; Monks, A.; Pittman, A.; Boyd, M.R. *Cancer Res.* **1991**,1, 2515.

Wang, J. *Analytical electrochemistry*, Wiley-VCH, New York, 2000.

Weinges, K.; Seiler, D.; Liebigs, D. *Ann Chem*. **1968**, 714, 193.

Weissman, S.A. and Zewge, D. *Tetrahedron*. **2005**, 61, 7833.

Wheeler T.S. “Organic Syntheses,” Collective By N. Rabojohn, John Wiley & Sons. (**1967**) 2nd ed.

Williams, D.A.; Lemke, T.L.; Foye's principles of medicinal chemistry. Philadelphia: Lippincott Williams & Wilkins. (**2002**). 6a Ed.

Yoshikawa, T. and Naito, Y. *Jpn Med Assoc J*. **2002**, 45, 271.

Zhang, J. and Zhang, Y. *Bioinformatics*. **2010**, 26, 3004.

Zubaida, F.; Valentine, Y.N.: Suparana, D.; Ather, A.; David, L.K. *Am J Clin Nutr.* **2008**, 88, 58.

SUPPLEMETARY DATA

6.1 Spectroscopic and spectrometric Data

6.1.1 NMR and HRMS spectra for *5,7,3',4'-tetra-O-benzyl-(-)-epicatechin* (Epi-benzyl).

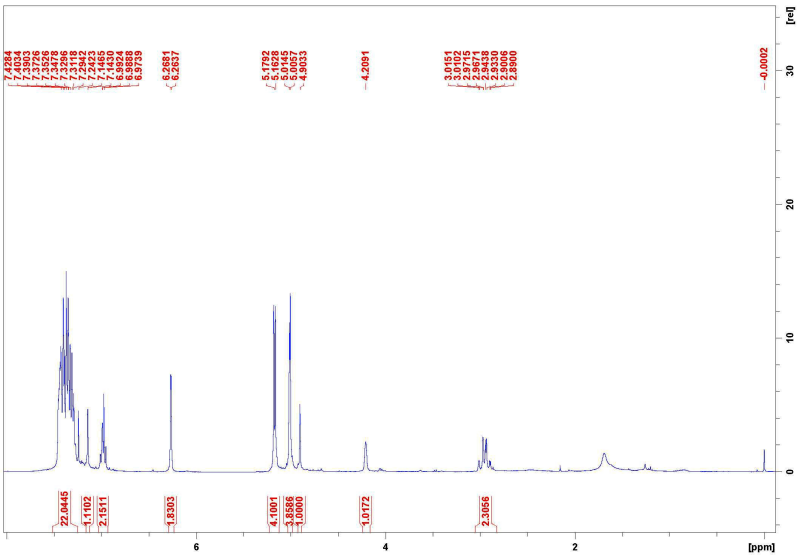

Figure 6.1. ^{1}H NMR spectrum (400 MHz, $CDCl_3$) of **Epi-benzyl**.

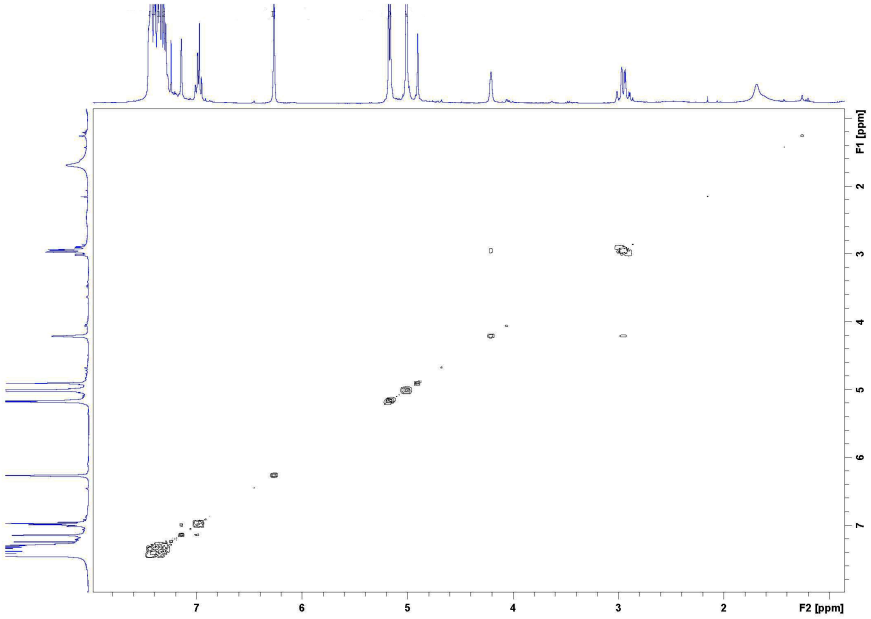

Figure 6.2. ^{1}H-^{1}H COSY NMR spectrum (100 MHz, $CDCl_3$) of **Epi-benzyl**.

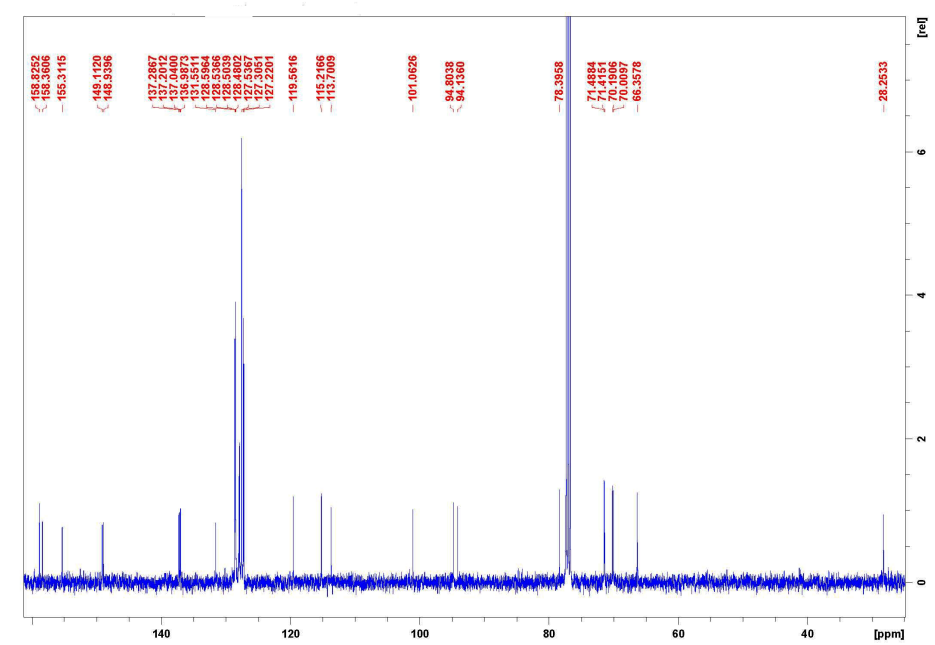

Figure 6.3. ^{13}C NMR spectrum (100 MHz, $CDCl_3$) of **Epi-benzyl**.

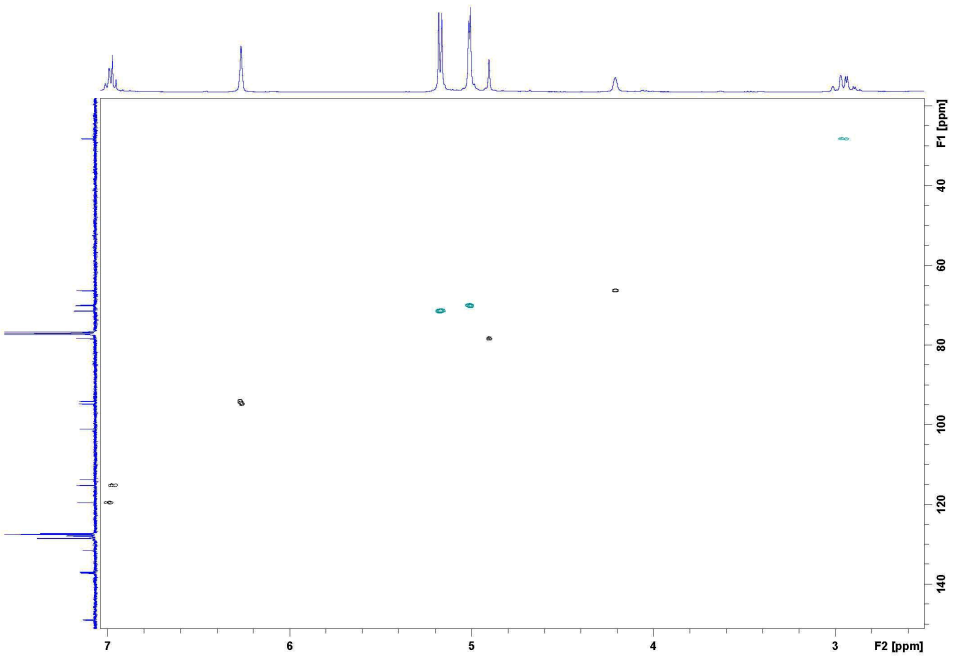

Figure 6.4. ^{1}H-^{13}C gHSQC spectrum ($CDCl_3$) of **Epi-benzyl**.

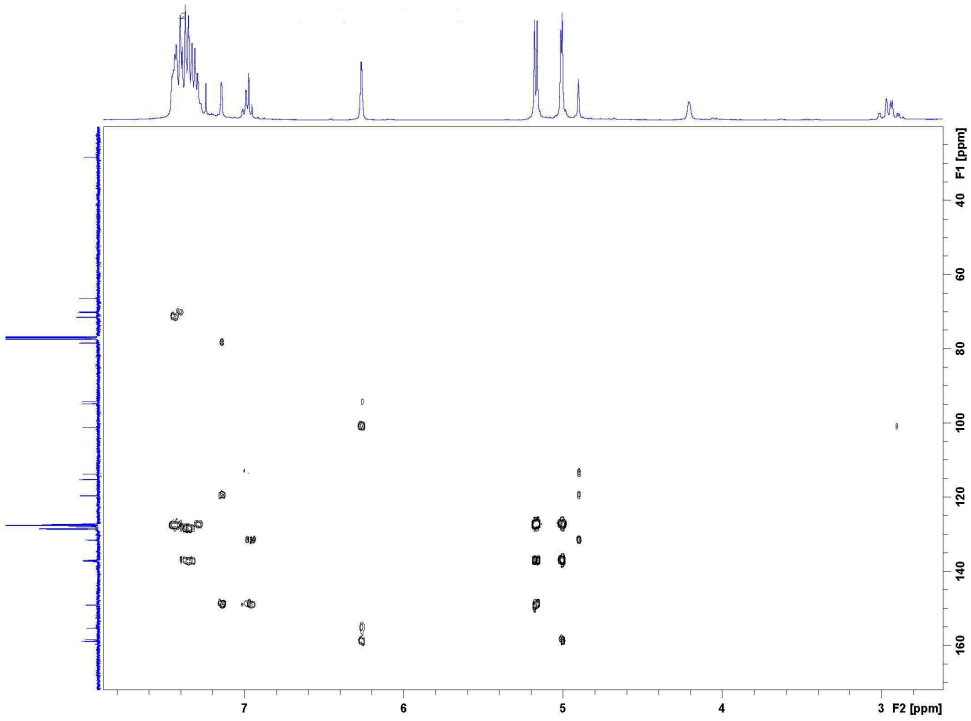

Figure 6.5. ^{1}H-^{13}C gHMBC spectrum ($CDCl_3$) of **Epi-benzyl**.

6.1.2 NMR and HRMS spectra for *5,7,3',4'-tetra-O-benzyl-3-O-mesyl-(-)-epicatechin (*Epi-benzyl-Ms).

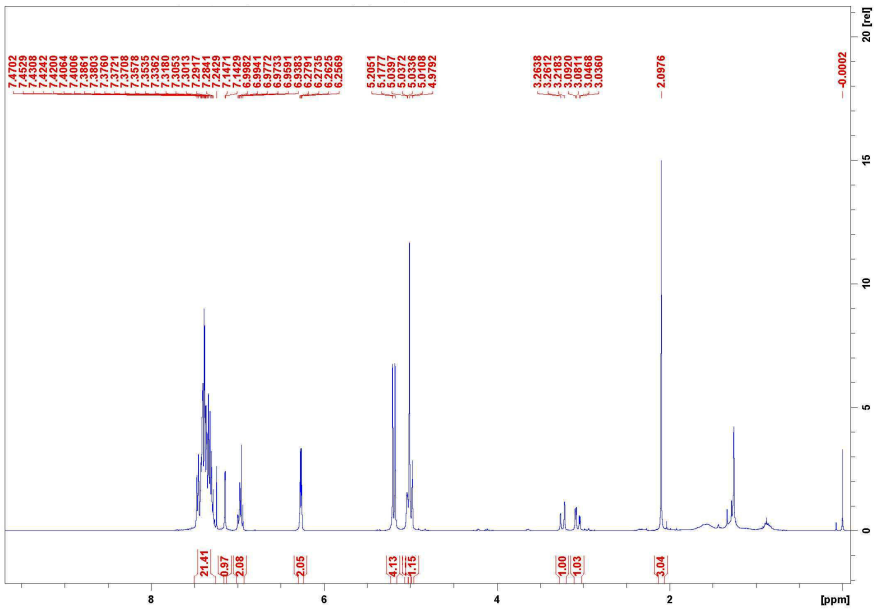

Figure 6.6. ^{1}H NMR spectrum (400 MHz, $CDCl_3$) of **Epi-benzyl-Ms**.

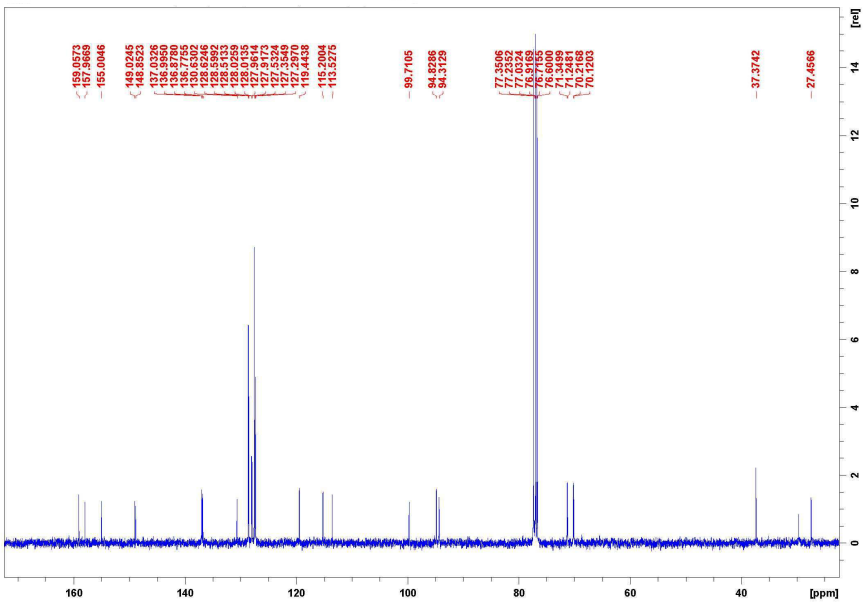

Figure 6.7. ^{13}C NMR spectrum (100 MHz, $CDCl_3$) of **Epi-benzyl-ms**.

6.1.3 NMR and HRMS spectra for *5,7,3',4'-tetra-O-propargyl-(-)-epicatechin* (Epi-4-prop)

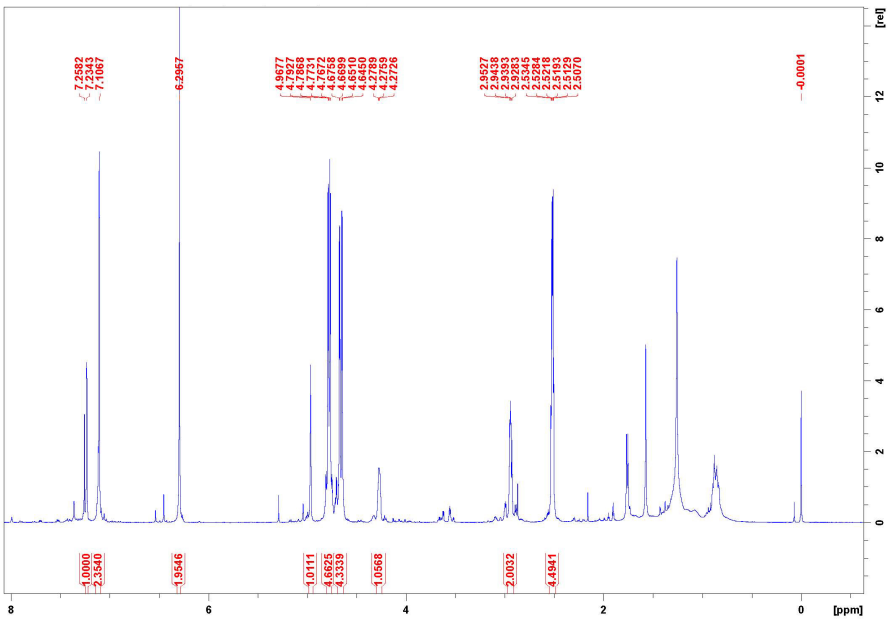

Figure 6.8. ^{1}H NMR spectrum (400 MHz, $CDCl_3$) of **Epi-4-prop**.

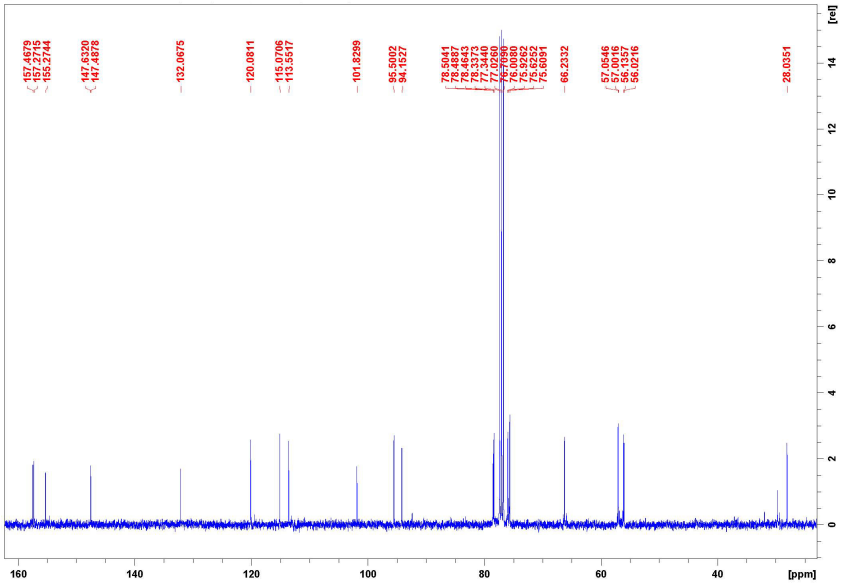

Figure 6.9. ^{13}C NMR spectrum (100 MHz, $CDCl_3$) of **Epi-4-prop**.

6.1.4. NMR and HRMS spectra for *3,5,7,3',4'-Penta-O-propargyl-(-)-epicatechin* (Epi-5-prop).

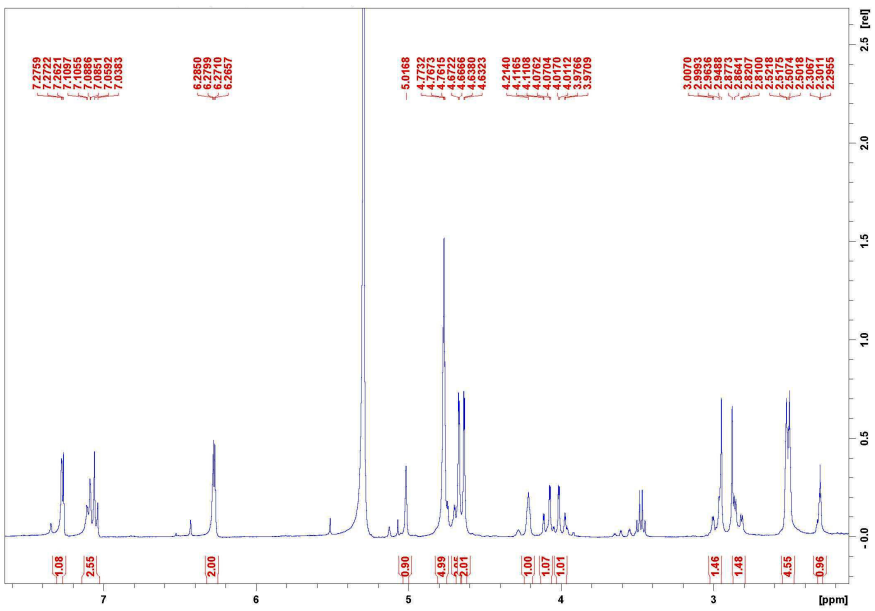

Figure 6.10. ^{1}H NMR spectrum (400 MHz, $CDCl_3$) of **Epi-5-prop**.

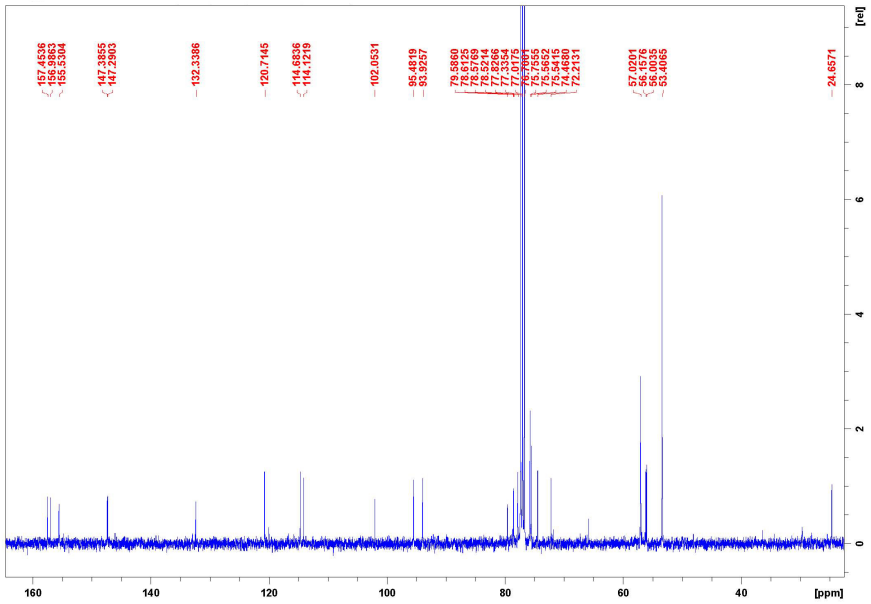

Figure 6.11. ^{13}C NMR spectrum (100 MHz, $CDCl_3$) of **Epi-5-prop**.

6.1.5 NMR and HRMS spectra for *3-O-Mesyl-(-)-epicatechin* (Epi-Ms).

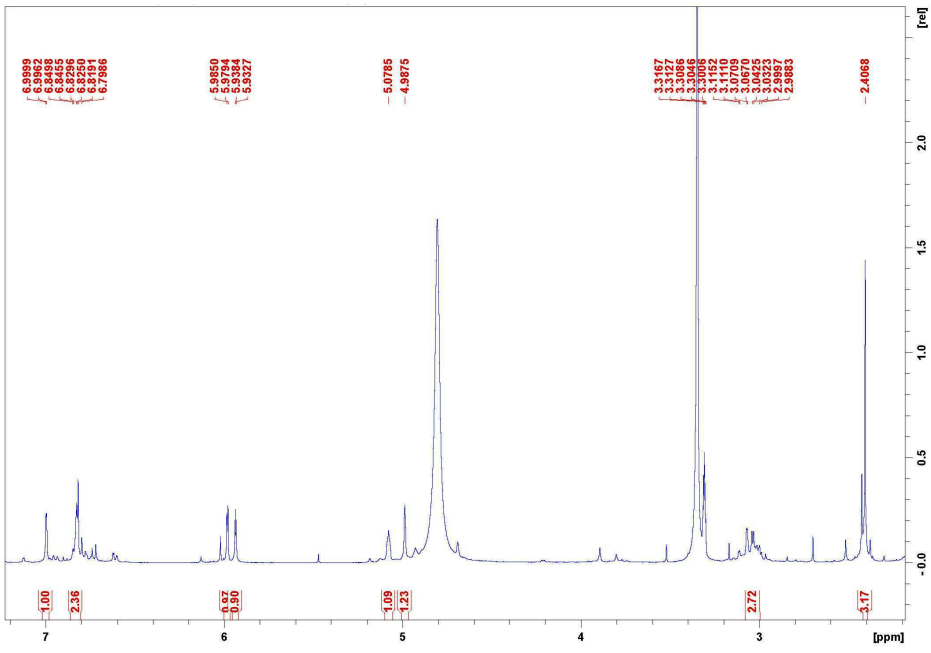

Figure 6.11. ^{1}H NMR spectrum (400 MHz, $CDCl_3$) of **Epi-Ms**.

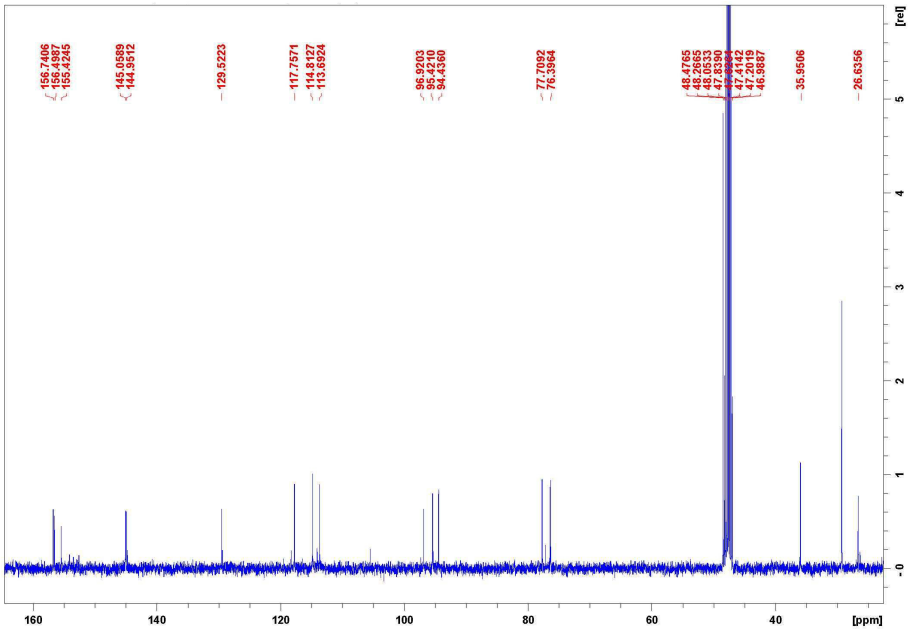

Figure 6.12. ^{13}C NMR spectrum (100 MHz, $CDCl_3$) of **Epi- Ms**.

6.1.6. NMR and HRMS spectra for *3-O-propargyl-(-)-epicatechin* (Epi-prop).

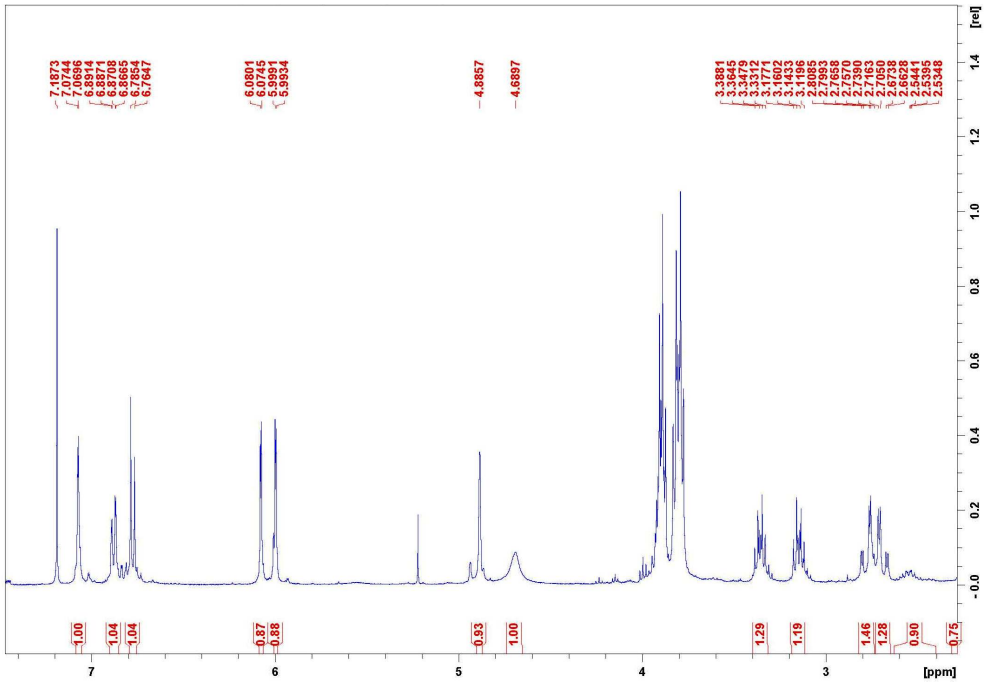

Figure 6.13. ^{1}H NMR spectrum (400 MHz, $CDCl_3$) of **Epi- prop**.

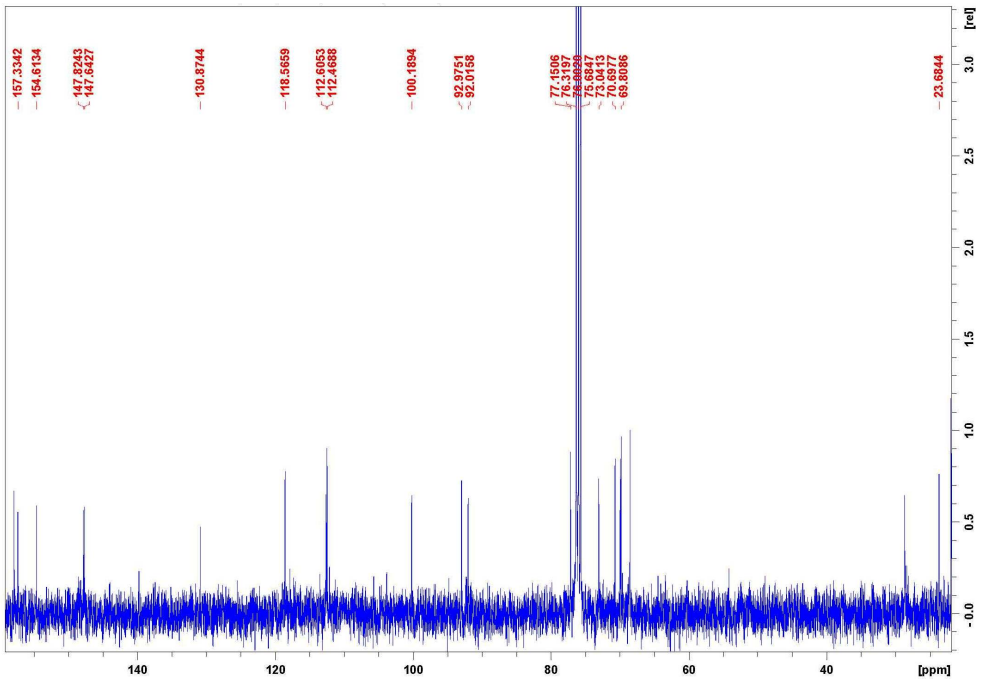

Figure 6.14. ^{13}C NMR spectrum (100 MHz, $CDCl_3$) of **Epi- prop.**

6.7 Tables

Table 6.1. Binding affinity energies of Epi derivatives using a GPER 3D model at 14 ns. Binding affinity energies of Epi derivatives docked in a GPER 3D model at 14 ns with the corresponding interacting residues. * hydrogen bond and * π-π interactions.

Ligand	Chemical structure	Binding affinity energy (ΔG)	Interacting residues
Epi-Ms	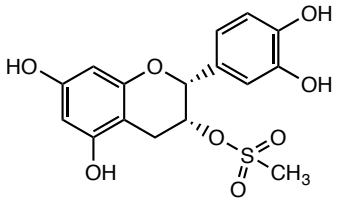	-7.74	L108, S112, L137, M141, F208, F223, W272, A313*, N316, S317*
Epi-prop	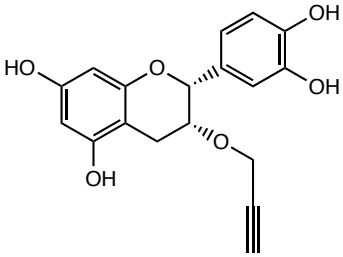	-8.05	H52, Q53, **Q54*, G58, L59, E275*, F278, H282, P303, G306*, V309, N310
Epi-4-prop	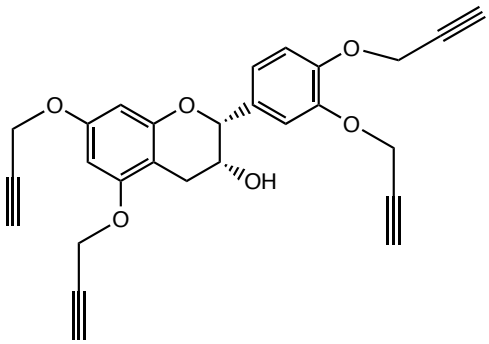	-8.68	Q138, M141, Y142, C205, F206, F208, A209, Q215, E218, E275*, I279, L283, R286
Epi-5-prop	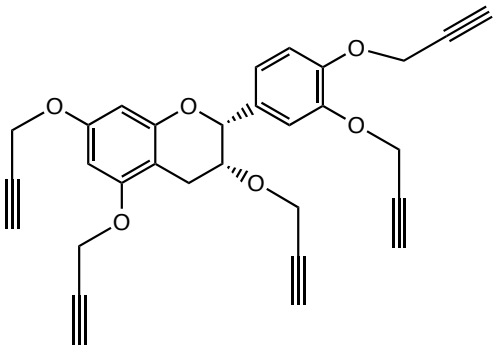	-9.2	H52, Q53, **Q54*, G58, L59, E275*, F278, H282, P303, G306*, V309, N310

Table 6.2. Binding affinity energies of Epi derivatives using a GPER 3D model at 70 ns. Binding affinity energies of Epi derivatives docked in a GPER 3D model at 70 ns with the corresponding interacting residues. * hydrogen bond and * π-π interactions.

Ligand	Chemical structure	Binding affinity energy (ΔG)	Interacting residues
Epi-Ms	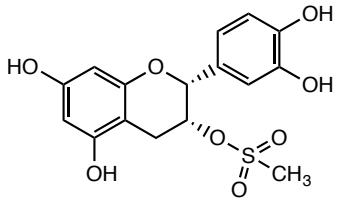	-7.27	Q54*, L59, S62*, E115, L119, Y123, A204, C205*, H307, N310*
Epi-prop	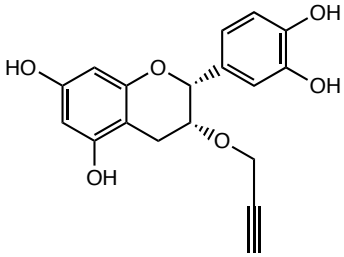	-7.77	D105, L108, V109, *D111*, S144*, F268, C271*, W272, S317*
Epi-4-prop	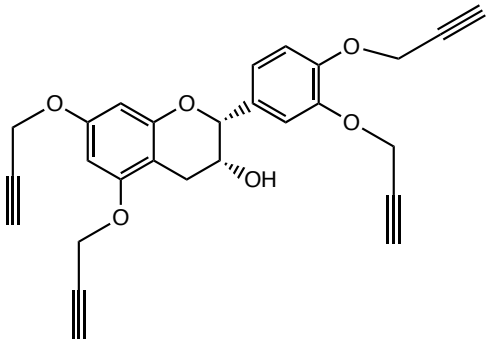	-8.25	N118, E115, L119, Y123, L129, M133, G138, M141, Y142, P192, V196, C207, F208
Epi-5-prop	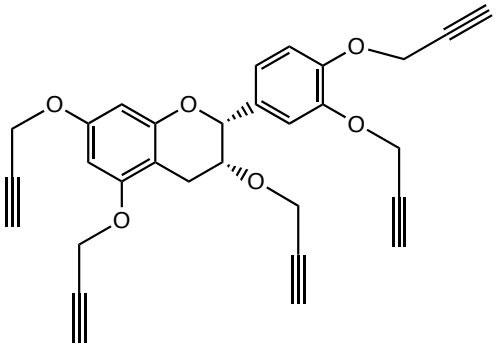	-8.12	F146**, T149, *W150*, L176, L180, I180, A184, T220, L221, V225, P226, I229

6.8 Protocols

6.8.1 Bradford standard assay procedure (for sample with 5-100 µg/ml protein)

1. Prepare five to eight dilutions of BSA (standard solution) with a range of 5 to 100 µg protein.
2. Dilute unknown protein samples to obtain 5-100 µg protein/30 µl.
3. Add 30 µl each of standard solution or unknown protein sample to an appropriately labeled test tube.
4. Set two blank tubes. For the standard curve, add 30 µl H_2O instead of the standard solution. For the unknown protein samples, add 30 µl protein preparation buffer instead. Protein solutions are assayed in triplicate.
5. Add 1.5 ml of Bradford reagent to each tube and mix well.
6. Incubate at room temperature (RT) for at least 5 min. Absorbance will increase over time; samples should incubate at RT for no more than 1 h.
7. Measure absorbance at 595 nm.

6.8.2 MTT assay

1. Seed cells in a 96 well plate. Ensure that the volumen of the culture medium is ≥100 µL/well. Incubate the cells f overnight at 37ºC to enable adhesion of cells to wells. Include three control wells of medium alone to provide the blanks for absorbance readings.
2. Aspirate the medium from the wells, and add ≥100µL/well of fresh medium supplemented with Epi derivatives (1 uM final concentration). Treat cells in triplicate wells for each derivative. Incubate cells for 24 h.
3. Aspirate the medium, and wash the cells twice with PBS. After washing, invert the plate on filter paper and tap the plate gently to remove any remaining liquid.
4. Add 100 uL of H_2O_2 for 2 h at 37ºC. Aspirate the solution, and wash the cells twice with PBS buffer. After washing, invert the plate on filter paper and

tap the plate

5. Add 10o µL of MTT Reagent (5 mg/mL in clear medium without phenol red) to each well, including controls. Return plate to cell culture incubator for 4 h.
6. When the purple precipitate is clearly visible under the microscope add 100 µL of DMSO to all wells, including controls. Swirl gently, do not shake. Leave plate in the dark for 4 h or overnight at 37ºC.
7. Measure the absorbance at 570 nm (OD_{570}) in a microtiter plate reader. If the readings are low return the plate to the dark for longer incubation.

6.8.3 Trypan blue method

1. Seed cells in a 96 well plate. To three Wells, add medium without cells. Ensure that the volumen of the culture medium is ≥100 µL/well. Incubate the cells for overnight at 37ºC to enable adhesion of cells to wells.
2. Aspirate the medium from the wells, and add ≥100µL/well of fresh médium supplemented with Epi derivatives (1 uM final concentration). Treat cells in triplicate wells for each derivative. Incubate cells for 24 h.
3. Aspirate the medium, and wash the cells twice with PBS buffer. After washing, invert the plate on filter paper and tap the plate gently to remove any remaining liquid.
4. Add 100 uL of H_2O_2 for 2 h at 37ºC. Aspirate the solution, and wash the cells twice with PBS buffer.
5. Trypsinize cells in 100 uL (0.025% trypsin-EDTA). Transfer 10 µl of the cell suspension into a test tuve.
6. Add 10 uL of 0.4% Trypan Blue solution (w/v) to a test tube. Mix thoroughly and allow to stand 5 to 15 minutes.
7. With the cover-slip in place, use a pipette to transfer 10 uL of Trypan Blue-cell suspension mixture to both chambers of the hemocytometer. Carefully touch the edge of the cover-slip with the pipette tip and allow each chamber to fill by capillary action. Do not overfill or underfill the chambers.
8. Starting with chamber 1 of the hemocytometer, count all the cells in the 1

mm center square and four 1 mm corner squares

9. **CELLS PER ml** = the average count per square X dilution factor X 10^4 (count 10 squares)
10. **TOTAL CELLS** = cells per ml X the original volume of fluid from which cell sample was removed.
11. **CELL VIABILITY (%)** = total viable cells (unstained)) ÷ total cells (stained and unstained) X 100.

6.8.4 Crystal violet assay

1. Seed cells in a 96 well plate. To three Wells, add medium without cells. Ensure that the volumen of the culture medium is ≥100 µL/well. Incubate the cells for 18–24 h (overnight) at 37ºC to enable adhesion of cells to wells.
2. Aspirate the médium from the wells, and add ≥100µL/well of fresh médium supplemented with Epi derivatives (1 uM final concentration). Treat cells in triplicate wells for each derivative. Incubate cells for 24 h.
3. Aspirate the medium, and wash the cells twice with PBS. After washing, invert the plate on filter paper and tap the plate gently to remove any remaining liquid.
4. Add 100 uL of H_2O_2 for 2 h at 37ºC. Aspirate the solution, and wash the cells twice with PBS buffer. After washing, invert the plate on filter paper and tap the plate.
5. Add 50 µL of 0.5% crystal violet staining solution (20% methanol) to each well, and incubate for 30 min at 37ºC. Aspirate the medium, and wash the cells four times with water. After the wells have filled with water, immediately aspirate the water from the wells. After washing, invert the plate on filter paper and tap the plate gently to remove any remaining liquid.
6. Add 200 µL of methanol to each well, and incubate the plate with its lid on for 30 min at room temperature on a bench rocker.
7. Measure the optical density of each well at 570 nm (OD_{570}) with a plate reader.

6.8.5 Resazurin assay

1. Thaw out Resazurin solution (if kept frozen) and warm it to 37°C to ensure all components are completely in solution.
2. Plate cells in 96-well plate. Ensure that the volumen of the culture medium is ≥100 µL/well. Incubate the cells for 18–24 h (overnight) at 37ºC to enable adhesion of cells to wells.
3. Aspirate the medium from the wells, and add ≥100µL/well of fresh médium supplemented with Epi derivatives (1 uM final concentration). Treat cells in triplicate wells for each derivative. Incubate cells for 24 h.
4. Aspirate the medium, and wash the cells twice with PBS buffer. After washing, invert the plate on filter paper and tap the plate gently to remove any remaining liquid.
5. Add 100 uL of H_2O_2 for 2 h at 37ºC. Aspirate the solution, and wash the cells twice with PBS buffer.
6. Add Resazurin solution to plate (10% of the initial volume in the well). For example, for plates containing 100 µl medium/well, add 10 µl resazurin solution to each well.
7. Incubate the plate for 1–6 hr in standard culture conditions.
8. Measure the relative fluorescent units (RFU) using a plate reader. Ex = 530–570 nm, Em = 590–620 nm.

H_2O_2 solutions

The Molarity of 30% H2O2 (Weight / Weight) solution (Or 33.30 % H2O2 solution (Weight / Volume) is 9.79.

50 mM H_2O_2

255 uL H_2O_2 (9,79 M)

50 mL water

200 uM H_2O_2

40 uL 50 mM H_2O_2 → 100 uL/well

10 mL HBS

6.8.6 Cyclic and pulse differential voltammetry

a. The first step is cleaning of the electrode in an effort to ensure that we will have good electron transfer. Place the glassy carbon electrode (WE), the Ag/AgCl reference electrode (RE), and the platinum wire counter electrode (CE) in a solution of 0.1 M $HClO_4$. (Make sure that you connect the reference electrode to the green clip, working to black, and counter to red, see the Figure 2.12)

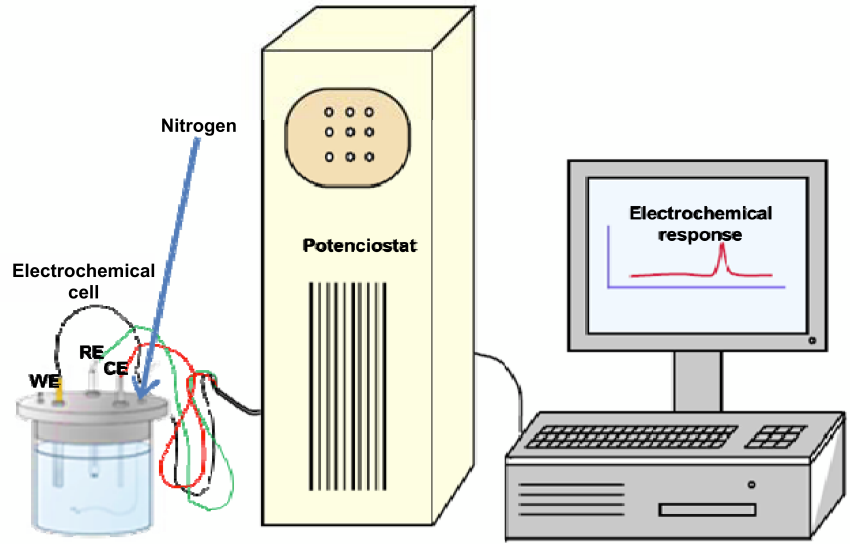

Figure 5.16. Scheme of a 3-electrode cell used in voltammetry techniques, where gas inlet used for bubbling electrolyte solution with an inert gas (Nitrgen) at room temperature.

b. Cycle the electrode between 0.2 and 1.5 V for 10 minutes at 20 mV/sec. Stop the cyclic voltammograms after ten minutes. Steps 1 and 2 should give you a clean electrode.
c. First, run a voltammogram in PBS 1X without adding Epi or Epi derivatives. Run this voltammogram from 0.35 V to 0.00 V so that your are in regions where there is minimal Faradaic current. Run the

PDV's or CV's at 0.5 V/sec, 0.1 V/sec, and 0.01 V/sec. Note how capacitive current varies with scan rate.

d. Then, run the voltammogram in PBS 1X, 1uM Epi or Epi derivtives. Run a voltammogram for Gal and NaLAc. Make sure that you rinse electrodes very well between experiments. Run the CV from 0.5 to -0.1 V. Do the CV at three different scan rates to see how peak currents and peak splitting vary with scan rate.
e. Rinse the electrode thoroughly and immerse it in 0.001 M octadecanethiol in EtOH for 30 minutes. Remove the electrode from the solution and rinse it thoroughly.